

Aus der Arbeitsgruppe Prädiktive Diagnostik  
(Leiter: PD Dr. Michael Schlosser)  
des Instituts für Medizinische Biochemie und Molekularbiologie  
(Direktor: Univ.-Prof. Dr. Reinhard Walther)  
der Universitätsmedizin der Ernst-Moritz-Arndt-Universität Greifswald

Thema: Differenzierte Untersuchung der lokalen und systemischen  
Entzündungsreaktionen nach Implantation von Niedertemperatur-  
Plasmapolymer-modifizierten Titanplättchen im Tiermodell Ratte

Inaugural-Dissertation

zur

Erlangung des akademischen

Grades

Doktor der Wissenschaften in der Medizin  
(Dr. rer. med.)

der

Universitätsmedizin

der

Ernst-Moritz-Arndt-Universität

Greifswald

2013

vorgelegt von:  
Uwe Walschus  
geboren am: 2. März 1975  
in: Wolgast

Dekan: Prof. Dr. Reiner Biffar

1. Gutachter: PD Dr. Michael Schlosser (Ernst-Moritz-Arndt-Universität Greifswald)

2. Gutachter: Prof. Dr. Barbara Bröker (Ernst-Moritz-Arndt-Universität Greifswald)

3. Gutachter: Prof. Dr. Thomas Groth (Martin-Luther-Universität Halle-Wittenberg)

Ort, Raum: Universitätsklinikum Greifswald, Ferdinand-Sauerbruch-Str., Hörsaal Nord

Tag der Disputation: 17. Juni 2014

# Inhaltsverzeichnis

|          |  |    |
|----------|--|----|
| <b>1</b> | <b>Einleitung</b>  | 5  |
| 1.1      | Biomaterialien und Biokompatibilität   | 5  |
| 1.2      | Biomaterial-bedingte Entzündungsreaktionen   | 7  |
| 1.3      | Titan als Biomaterial und dessen Funktionalisierung durch<br>Niedertemperaturplasmen   | 9  |
| 1.4      | Zielstellung   | 11 |
| <b>2</b> | <b>Experimentelle Arbeiten</b>   | 12 |
| 2.1      | Quantitative immunhistochemische Untersuchung der lokalen Gewebs-<br>reaktionen nach Implantation von Biomaterialien         | 12 |
| 2.2      | Chronische lokale Entzündungsreaktionen gegen Titan-Implantate mit<br>unterschiedlich geladenen Plasmapolymer-Beschichtungen | 14 |
| 2.3      | Akute und chronische lokale Entzündungsreaktionen gegen Titan-Implantate<br>mit plasma-polymerisiertem Allylamin             | 15 |
| 2.4      | Serumprofil pro- und anti-inflammatoryischer Zytokine nach Implantation<br>von Plasmapolymer-beschichteten Titan-Implantaten | 18 |
| <b>3</b> | <b>Zusammenfassung</b>   | 22 |
| <b>4</b> | <b>Referenzen</b>  | 24 |
| <b>5</b> | <b>Anhang</b>  | 29 |
| 5.1      | Eidesstattliche Erklärung  | 29 |
| 5.2      | Lebenslauf   | 30 |
| 5.3      | Publikationsliste  | 31 |
| 5.4      | Danksagung   | 33 |
| 5.5      | Beigefügte Veröffentlichungen  | 34 |

# Verzeichnis der verwendeten Abkürzungen

|              |   |
|--------------|---|
| APAAP        | Alkalische Phosphatase Anti-Alkalische Phosphatase  |
| DC           | Duty cycle, Verhältnis aus Pulsdauer und gesamter Pulswiederholzeit                                     |
| ED1          | Monoklonaler Maus Anti-Ratte CD68 Antikörper zur Markierung von Monozyten und Makrophagen               |
| ED2          | Monoklonaler Maus Anti-Ratte CD163 Antikörper zur Markierung von Gewebsmakrophagen                      |
| ELISA        | Enzyme-linked Immunosorbent Assay   |
| HE-Färbung   | Hämalaun-Eosin-Färbung  |
| IL           | Interleukin   |
| IFN $\gamma$ | Interferon gamma  |
| MHC          | Major Histocompatibility Complex  |
| NK-Zellen    | Natürliche Killerzellen   |
| OX6          | Monoklonaler Maus Anti-Ratte MHC Klasse II Antikörper zur Markierung von antigen-präsentierenden Zellen |
| PPAAc        | Plasma-polymerisierte Acrylsäure (Plasma polymerized Acrylic Acid)                                      |
| PPAAm        | Plasma-polymerisiertes Allylamin (Plasma polymerized Allylamine)  |
| R73          | Monoklonaler Maus Anti-Ratte TCR $\alpha/\beta$ Antikörper zur Markierung von T-Lymphozyten             |

# Einleitung

## 1.1 Biomaterialien und Biokompatibilität

Erste Anwendungen medizinischer Implantate sind historisch bereits vor etwa 2.000 Jahren dokumentiert, die Verwendung von chirurgischen Nahtmaterialien sogar vor rund 32.000 Jahren [RATNER & BRYANT 2004]. Gegenwärtig sind Implantate, die dauerhaft oder vorübergehend in den Körper eingesetzt werden, in verschiedenen Bereichen der Medizin wie der Gefäßchirurgie, der Orthopädie, der Unfallchirurgie, der Zahnheilkunde und der plastischen Chirurgie von wesentlicher Bedeutung. Die zur Herstellung solcher Implantate verwendeten Werkstoffe werden zusammenfassend als Biomaterialien bezeichnet. Seit Anfang der 1970er Jahre kam es in der Biomaterialforschung zu einer bis in die Gegenwart anhaltenden Ausweitung der Forschungs- und Entwicklungsaktivitäten. Dies findet unter anderem Ausdruck in mehr als 100.000 Veröffentlichungen in wissenschaftlichen Zeitschriften und einer jährlichen Zunahme um derzeit mehr als 8.000 Publikationen [MEDSUM 2013]. Die wirtschaftliche Bedeutung wird durch ein weltweites Marktvolumen für Medizinprodukte auf der Basis von Biomaterialien von rund 115 Milliarden US-Dollar im Jahr 2008, mit einer voraussichtlichen Steigerung auf rund 250 Milliarden US-Dollar im Jahr 2014, verdeutlicht [BIOMARKET GROUP 2009].

Das wissenschaftliche Verständnis des Begriffs Biomaterial ergibt sich unmittelbar aus der medizinischen Anwendung dieser Materialien und den daraus resultierenden Anforderungen an ihre Eigenschaften. Eine 1987 während einer Konferenz der Europäischen Gesellschaft für Biomaterialien formulierte erste Definition beschrieb Biomaterialien als „in einem Medizinprodukt verwendete nicht lebende Materialien, die mit biologischen Systemen interagieren sollen“ [WILLIAMS 1987]. Basierend auf den Ergebnissen der Biomaterialforschung entwickelte sich jedoch in der Folgezeit ein zunehmend umfassenderes und komplexeres Konzept dieses Begriffs. So wurde einige Jahre später zunächst die Einschränkung auf „nicht lebende Materialien“ aus der Definition entfernt, wodurch dem Einsatz von Materialien biologischer Herkunft Rechnung getragen wurde. In einer 1999 veröffentlichten Definition erfolgte eine Präzisierung der Funktionen von Biomaterialien, indem diese als „Materialien, die mit biologischen Systemen interagieren sollen, um Gewebe, Organe oder Körperfunktionen zu untersuchen, zu behandeln, zu erweitern oder zu ersetzen“ beschrieben wurden [WILLIAMS 1999]. Einem zehn Jahre später veröffentlichtem Vorschlag für eine erweiterte Definition zufolge ist ein Biomaterial „eine Substanz, deren Eigenschaften dahingehend gestaltet wurden, dass sie allein oder als Teil eines komplexen Systems, durch

Steuerung von Interaktionen mit Komponenten von lebenden Systemen, den Verlauf einer therapeutischen oder diagnostischen Maßnahme in der Human- oder Veterinärmedizin lenkt“ [WILLIAMS 2009]. Wesentliche Neuerung dieses Vorschlags ist die Betonung der Interaktionen zwischen lebenden Systemen und Biomaterialien als entscheidendem Teil von deren Biofunktionalität.

Aus diesem im Laufe der Zeit entstandenem Verständnis von Biomaterialien ergibt sich, dass ihre wichtigste Eigenschaft in Abgrenzung zu anderen Materialien ihre Fähigkeit ist, „in Kontakt mit Körpergewebe zu existieren, ohne den Körper in einem nicht akzeptablen Maß zu schädigen“ [WILLIAMS 2008]. Die Auswahl der ersten klinisch eingesetzten Biomaterialien zwischen 1940 und 1980 richtete sich insbesondere nach ihrer biologischen Sicherheit. Sie orientierte sich damit vor allem am Ziel möglichst wenig negativer Auswirkungen auf den Körper. Es zeigte sich jedoch bald, dass die Reaktionen des Körpers auf ein bestimmtes Material je nach Implantationsort variieren können und damit nicht allein von den Eigenschaften des Materials abhängen. Darüber hinaus ergaben sich zunehmend Anwendungen, bei denen spezifische Interaktionen von bioaktiven Materialien mit dem umgebenden Gewebe für die Funktion erwünscht waren. Demgegenüber stehen die als bioinert bezeichneten und durch ein Minimum an Wechselwirkungen mit dem biologischen Umfeld charakterisierten Materialien. Für bestimmte Zwecke sind außerdem biodegradierbare Materialien, die nach der Implantation im Körper abgebaut werden, besser geeignet.

Die vorrangige Fokussierung der Auswahl von Biomaterialien auf ihre biologische Sicherheit erwies sich somit als unzureichend, woraus ab 1970 das weiter gefasste Konzept der Biokompatibilität entstand [RATNER 2011]. Seitdem nimmt das Forschungsinteresse in diesem Bereich stetig zu, wie rund 14.000 wissenschaftliche Veröffentlichungen mit einem jährlichen Anstieg um derzeit über 1.000 Publikationen belegen [MEDSUM 2013]. Auch der Begriff Biokompatibilität wurde 1987 erstmals definiert als „die Fähigkeit eines Materials, in einer spezifischen Situation mit einer angemessenen Körperantwort zu funktionieren“ [WILLIAMS 1987]. Diese Definition betont die Abhängigkeit der Biokompatibilität von der konkreten Anwendung sowie die Bedeutung der Biofunktionalität des Materials anstelle seines reinen Vorhandenseins im Körper. Trotzdem ist sie sehr allgemein formuliert und trägt damit wenig zum Verständnis der zugrunde liegenden Prozesse bei. Auf klinischen Erfahrungen sowie Forschungsergebnissen zu den physikochemischen und biochemisch-physiologischen Grundlagen der Wechselwirkungen zwischen Biomaterialien und dem Empfängerorganismus basiert deshalb eine 2008 vorgeschlagene Definition, welche die biologische Reaktion des Organismus berücksichtigt. Diese beschreibt die Biokompatibilität als „die Fähigkeit eines Biomaterials, seine vorgesehene Funktion im Hinblick auf eine medizinische Therapie zu erfüllen, ohne unerwünschte lokale oder systemische Effekte im Empfänger zu verursachen,

und dabei aber die geeignete Zell- oder Gewebsantwort in dieser spezifischen Situation hervorzurufen sowie die klinisch relevante Durchführung der Therapie zu optimieren“ [WILLIAMS 2008]. Während die Definition von 1987 keine konkreten Anhaltspunkte zur Untersuchung oder Beeinflussung der Biokompatibilität eines Materials enthält [RATNER 2011], nennt diese Formulierung diesbezüglich unerwünschte lokale oder systemische Effekte sowie die durch das Biomaterial hervorgerufene Zell- oder Gewebsantwort.

Die Biokompatibilität unterliegt vielfältigen Einflussfaktoren, die in komplexer Weise miteinander interagieren. Dies betrifft zum einen den Empfängerorganismus und dessen Alter und Gesundheitszustand, seinen immunologischen und pharmakologischen Status sowie die individuelle Situation am Implantationsort. Zum anderen wird die Körperantwort durch Materialeigenschaften wie zum Beispiel die Größe und Form des Implantats, die Makro-, Mikro- und Nanostruktur der Oberfläche, den Kristallaufbau und die Porosität, die Festigkeit und die Elastizität, die Hydrophilie beziehungsweise Hydrophobie sowie das elektro-chemische Verhalten und die Korrosionsbeständigkeit beeinflusst. Weitere Einflussfaktoren sind unter anderem Veränderungen durch die Sterilisation, die produktionsprozessbedingte Heterogenität und die Zugabe von Additiven. Die von diesen Parametern beeinflussten Körperreaktionen umfassen je nach Material unter anderem die Adsorption und Desorption von Proteinen, die Ansammlung und Aktivierung von verschiedenen Zellen, die Bildung von spezifischen Antikörpern, die Aktivierung des Komplementsystems sowie die Vaskularisierung und Fibrosierung des Gewebes. Die Körperantwort ist dabei durch eine charakteristische Abfolge von Prozessen gekennzeichnet, die durch die implantationsbedingte Verletzung von Geweben oder Organen und die daraus resultierende Wundheilung sowie durch das Implantat als Fremdkörper und seine Eigenschaften bestimmt werden [ANDERSON 2001].

## 1.2 Biomaterial-bedingte Entzündungsreaktionen

Die auf die Implantation eines Biomaterials folgende Reaktionskaskade beginnt mit Interaktionen zwischen dem Material und Blutbestandteilen, die aus der Verletzung von durchblutetem Bindegewebe resultieren. Dies umfasst, bereits wenige Sekunden nach Implantation, die Adsorption von Proteinen wie Albumin, Fibrinogen und  $\gamma$ -Globulin an der Materialoberfläche [ANDERSON et al. 2008]. Darüber hinaus kommt es zur Entstehung von Thromben, in deren Folge die Blutgerinnung, das Komplementsystem und die Fibrinolyse aktiviert werden [ANDERSON 2001]. Innerhalb weniger Minuten bis Stunden nach Implantation resultiert aus diesen Prozessen die Bildung einer sogenannten provisorischen Matrix, die vorwiegend aus Fibrin besteht. Über weitere Bestandteile, insbesondere Fibronectin und Thrombospondin, vermittelt sie die Adhäsion von Zellen und den Beginn der implantationsbedingten Entzündungsreaktionen [ANDERSON 2001].

Zweck einer Entzündung, definiert als Reaktion von durchblutetem Gewebe auf eine lokale Verletzung, ist vorrangig die Begrenzung, die Neutralisierung, der Abbau oder die Abschirmung der auslösenden Ursache. Darüber hinaus initiiert die Entzündung Prozesse zur Heilung oder Wiederherstellung der verletzten Gewebsbereiche. Die dominierenden Entzündungszellen, die an den Ort einer Implantation einwandern, sind in den ersten 24 bis 48 Stunden vorwiegend neutrophile Granulozyten [ANDERSON 2001]. Außerdem wurde die Beteiligung von Mastzellen in der akuten Entzündungsphase beschrieben [TANG et al. 1998]. Im weiteren Verlauf sind vorrangig Monozyten und Makrophagen präsent [ANDERSON 2001]. Die Einwanderung dieser Zellen, die vor allem durch Adhäsion, Opsonisierung, Phagozytose und die Freisetzung von Zytokinen reguliert wird, ist das Charakteristikum dieser Entzündungsphase, in deren Folge es zum Abbau der provisorischen Matrix und unter Beteiligung von Fibroblasten zur Bildung von Granulationsgewebe kommt.

Neben der zentralen Bedeutung von Makrophagen wurde auch für T-Lymphozyten eine Rolle bei der Entzündung nach Implantation von Biomaterialien nachgewiesen [DAVIS et al. 2003; ANDERSON & MCNALLY 2011], die bisher jedoch noch nicht im Detail geklärt ist [GOODMAN 2007; RODRIGUEZ et al. 2008]. Möglich sind diesbezüglich beispielsweise Interaktionen zwischen T-Lymphozyten sowie Makrophagen und B-Lymphozyten in ihrer Rolle als antigen-präsentierende Zellen und damit in Abhängigkeit von den Materialeigenschaften auch spezifische Immunreaktionen. Hierzu zählt beispielsweise eine durch B-Lymphozyten vermittelte Bildung von spezifischen Antikörpern gegen die Matrix [SCHLOSSER et al. 2002] oder die Beschichtung [SCHLOSSER et al. 2005] von Implantaten, durch die lokale Entzündungsreaktionen beeinflusst werden [ZIPPEL et al. 2008]. Neuere Untersuchungen erbrachten darüber hinaus auch für natürliche Killerzellen (NK-Zellen) Hinweise auf eine Beteiligung [HUSS et al. 2010; ALMEIDA et al. 2012]. Entscheidend für die gegenseitige Regulation dieser verschiedenen Zellen und ihre Interaktionen, und damit für den Verlauf einer Entzündung, ist die Freisetzung von pro- und anti-inflammatorisch wirkenden Zytokinen [ANDERSON & MCNALLY 2011]. So ist zum Beispiel das durch NK-Zellen und T-Lymphozyten produzierte IFN $\gamma$  von grundlegender Bedeutung für die Aktivierung von Makrophagen und deren Differenzierung zu einem pro-inflammatorischen Phänotyp [MARTINEZ et al. 2009]. Demgegenüber lenkt IL-10, welches die humorale Immunantwort aktiviert und zelluläre Immunreaktionen inhibiert, die Aktivität von Makrophagen in Richtung Wundheilung [KOU & BABENSEE 2011].

Die letzte Phase der durch die Implantation eines Biomaterials ausgelösten Entzündung, und damit das spezifische Charakteristikum Implantat-bedingter Wundheilungsprozesse im Gegensatz zur normalen Gewebsregeneration nach einer Verletzung, ist der Ersatz des Granulationsgewebes durch eine 50 bis 200  $\mu\text{m}$  dicke fibröse Kapsel und die Fremdkörper-

reaktion im unmittelbaren Material-Gewebe-Kontaktbereich [RATNER & BRYANT 2004]. Sie ist vor allem gekennzeichnet durch das Vorhandensein von mehrkernigen Fremdkörperriesenzellen, die durch Fusion von Makrophagen entstehen, und besteht in der Regel für die gesamte Verweildauer des Implantats im Körper. Die Bildung der Fremdkörperriesenzellen aus Makrophagen wird dabei vor allem durch Mannose-Rezeptoren vermittelt, deren Expression durch die Zytokine IL-4 und IL-13 induziert wird [ANDERSON 2001]. Im Rahmen eines als frustrierte Phagozytose bezeichneten Prozesses setzen die Fremdkörperriesenzellen und Makrophagen Mediatoren wie reaktive Sauerstoff- und Stickstoffspezies und proteolytische Enzyme in den Material-Gewebe-Kontaktbereich frei [XIA & TRIFFITT 2006; KOU & BABENSEE 2011]. Diese können bei bestimmten Materialien wie zum Beispiel Polymeren zu einer Biodegradation des Implantats führen.

Die akuten und chronischen Entzündungsprozesse nach Implantation beeinflussen sowohl durch Modulation der Wundheilung das Einwachsen des Implantats in das Gewebe als auch durch Biodegradation dessen Langzeitstabilität. Dies zeigen unter anderem Untersuchungen zur Rolle von Makrophagen bei der Osteolyse von Gelenkprothesen [INGHAM & FISHER 2005; REVELL 2008] oder bei der Degradation von Calciumphosphat [HEYMANN et al. 1999]. Auch mechanische Materialabnutzung kann die Entzündungsantwort beeinflussen und durch daraus resultierende Gewebskomplikationen zum Implantatversagen führen [GRAMMATOPOULOS et al. 2013]. Diese Beispiele verdeutlichen die zentrale Bedeutung von Entzündungsprozessen für die Implantatfunktionalität. In-vivo-Untersuchungen der Entzündungsreaktionen im zeitlichen Verlauf spielen demzufolge eine wichtige Rolle für die Bewertung der Biokompatibilität von neuen oder modifizierten Implantatmaterialien [ANDERSON 2001].

### **1.3 Titan als Biomaterial und dessen Funktionalisierung durch Niedertemperaturplasmen**

Die Auswahl an Materialien für medizinische Implantate orientierte sich anfangs, wie bereits dargestellt, vor allem empirisch an Sicherheitsaspekten. Sie folgte dabei der Beobachtung, dass Materialien mit geringer chemischer Reaktivität von Vorteil waren [WILLIAMS 2008]. Je nach Anwendung handelte es sich diesbezüglich neben keramischen Werkstoffen zum einen um Kunststoffe wie Polytetrafluorethylen (Teflon®) und Polyethylenterephthalat (Dacron®) für gefäßchirurgische Implantate, Polypropylen (Prolene®) für Herniennetze, Silikon im Bereich der plastischen Chirurgie und Polymethylmethacrylat als Knochenersatzmaterial. Zum anderen betraf dies metallische Materialien wie rostfreie Stahlvarianten sowie Titan (Ti) und Ti-basierte Legierungen, wie beispielsweise in der Orthopädie [GUILLEMOT 2005], der Unfallchirurgie [DISEGI 2000] und der Zahnmedizin [PALMQUIST et al. 2010].

Aufgrund ihrer physikochemischen Eigenschaften spielen Titan und seine Legierungen eine führende Rolle im Bereich der klinisch eingesetzten metallischen Biomaterialien [WILLIAMS 2001]. Gegenwärtig werden pro Jahr mehr als 1.000 Tonnen Titan für medizinische Implantate verwendet [IMPLANT TRIBUNE 2012]. So wird es beispielsweise für Hüft- und Kniegelenksprothesen, für Zahnimplantate, zur Schädelrekonstruktion sowie für Marknägel und andere Implantate zur Osteosynthese von Knochenbrüchen eingesetzt. Es gilt als leichtes und festes Übergangsmetall und ist durch eine Passivierung aufgrund einer chemisch stabilen und korrosionsbeständigen Titanoxid-Schicht ( $TiO_2$ ) auf der Oberfläche gekennzeichnet [PALMQUIST et al. 2010]. Als wesentlicher Parameter im Hinblick auf die Integration des Implantats in das umliegende Gewebe hat sich die Oberflächentopografie erwiesen [TRIPPLETT et al. 2003]. Diese wird je nach Dicke der  $TiO_2$ -Schicht, in Abhängigkeit von der Verarbeitung wenige Nanometer bis einige Mikrometer, entweder vorrangig durch die Struktur der Metalloberfläche oder durch die Rauigkeit des  $TiO_2$  bestimmt [PALMQUIST et al. 2010].

Trotz jahrzehntelanger Erfahrungen kommt es beim Einsatz von Ti-basierten Implantaten zu verschiedenen Komplikationen wie Infektionen [ARCIOLA et al. 2005; CAMPOCCIA et al. 2006], aseptischer Prothesenlockerung [SCHWEIZER et al. 2003; BAUMANN et al. 2007] oder Periimplantitis [ESPOSITO et al. 1998]. Eine Möglichkeit zur Minimierung solcher Probleme ist die Modulation der Oberflächeneigenschaften der Implantate, um die Anheftung und das Wachstum von Bakterien zu reduzieren [CAMPOCCIA et al. 2013] oder biologische Prozesse wie Proteinadsorption und Zell-Material-Interaktionen gezielt zu beeinflussen [RATNER & BRYANT 2004; GOODMAN et al. 2013]. Zur Modifizierung der Oberfläche von Ti-basierten Implantaten sind unter anderem verschiedene Beschichtungen [AVILA et al. 2009; DE JONGE et al. 2008; NARAYANAN et al. 2008] sowie chemische und physikalische Methoden [BAGNO & DI BELLO 2004; LE GUÉHENNEC et al. 2007] untersucht worden.

Physikalische Plasmen bieten hierfür aufgrund ihrer Eigenschaften sowie der Variabilität ihrer Zusammensetzung und Prozessparameter vielfältige Möglichkeiten. Bei einem solchen Plasma handelt es sich um ein teilweise oder vollständig ionisiertes Gas. Die Aufspaltung der Molekülbindungen und die Ionisierung der freien Atome erfolgt durch Energiezufuhr. Ein Plasma besteht damit aus positiv und negativ geladenen Ionen, negativ geladenen Elektronen und Radikalen sowie neutralen und angeregten Atomen und Molekülen [CONRADS & SCHMIDT 2000]. Plasmen mit einem geringen Ionisierungsgrad bei niedrigen Temperaturen werden als Niedertemperaturplasmen bezeichnet. Zu deren Erzeugung wird eine Substanz in den gasförmigen Aggregatzustand überführt und anschließend Energie in Form von Wärme, elektrischer Spannung, Strahlung oder Laserlicht zugeführt. Insbesondere bei empfindlichen Werkstoffen wie zum Beispiel Polymeren ermöglichen Niedertemperaturplasmen eine vergleichsweise schonende Anwendung ohne unerwünschte Materialveränderungen.

Durch den Einsatz von Niedertemperaturplasmen können Materialoberflächen zum Beispiel mit chemischen Gruppen ausgestattet sowie Parameter wie die elektrochemische Ladung oder der Oxidationszustand beeinflusst werden. Dadurch ist es möglich, funktionale Eigenschaften wie die Härte, die Resistenz gegenüber chemischer Korrosion oder mechanischem Abrieb, die Benetzbarkeit oder die Affinität zu bestimmten Molekülen gezielt zu verändern. Mögliche Anwendungen bei Ti-Implantaten ergeben sich daraus beispielsweise hinsichtlich der Modulation der Topografie [WANG et al. 2008a], der Reduzierung der Thrombogenität [YE et al. 2009], der Erzeugung antibakteriell wirksamer Oberflächen [POLAK et al. 2010] oder der Beeinflussung der Zelladhäsion [MORRA & CASSINELLI 1997; ZHAO et al. 2011].

## 1.4 Zielstellung

In-vitro-Untersuchungen, die in Zusammenarbeit zwischen der Universität Rostock und dem Greifswalder Leibniz-Institut für Plasmaforschung und Technologie durchgeführt wurden, zeigten für die Beschichtung von Ti-Oberflächen mit positiv geladenen Aminogruppen-reichen Schichten auf der Basis von plasma-polymerisiertem Allylamin (PPAAm) positive Effekte hinsichtlich der Adhäsion, Ausbreitung und Proliferation von Osteoblasten [NEBE et al. 2007]. Darüber hinaus verbesserte eine PPAAm-Beschichtung die Ausbildung von Zell-Material-Verbindungen, die als fokale Adhäsionen bezeichnet werden [FINKE et al. 2007]. Negativ geladene Carboxylgruppen-reiche Schichten auf der Basis von plasma-polymerisierter Acrylsäure (PPAAC) steigerten die Expression der osteogenen Differenzierungsmarker Alkalische Phosphatase und Typ-I-Kollagen sowie des Transkriptionsfaktors RUNX2 in humanen mesenchymalen Stammzellen [FINKE et al. 2009a].

Aufbauend auf diesen In-vitro-Ergebnissen war es Ziel der vorliegenden Arbeit, als zentralen Aspekt der In-vivo-Biokompatibilität die lokalen und systemischen Entzündungsreaktionen nach intramuskulärer Implantation von PPAAm- und PPAAC-modifizierten Ti-Plättchen im Tiermodell Ratte detailliert zu analysieren. Dazu sollte zunächst eine Methode zur quantitativen Untersuchung der lokalen Gewebsreaktionen mittels digitaler Bildanalyse etabliert werden. Diese Methode wurde anschließend für eine morphometrische Analyse der Gesamt-Monozyten und -Makrophagen, der gewebsständigen Makrophagen, der T-Lymphozyten und der MHC-Klasse-II-positiven antigen-präsentierenden Zellen im Peri-implantatgewebe eingesetzt. Im Hinblick auf die systemische Entzündungsantwort sollte zudem das Serumprofil der pro-inflammatorischen Zytokine IL-2, IFN $\gamma$  und IL-6 sowie der anti-inflammatorischen Zytokine IL-4, IL-10 und IL-13 nach Implantation von plasma-modifizierten Ti-Plättchen im zeitlichen Verlauf analysiert werden.

# Experimentelle Arbeiten

## 2.1 Quantitative immunhistochemische Untersuchung der lokalen Gewebsreaktionen nach Implantation von Biomaterialien

Veröffentlicht in: Walschus et al. (2011) *J Microsc* 242:94–99

Wie in der Einleitung dargestellt wurde, ist die Analyse der zellulären Reaktionen im Perimplantatgewebe ein wichtiger Teil der In-vivo-Untersuchung der Biokompatibilität von Implantatmaterialien. In den meisten bisher veröffentlichten Studien wurden allerdings nur qualitative oder semiquantitative Ansätze auf der Basis histochemischer beziehungsweise immunhistochemischer Methoden genutzt. Dadurch ist jedoch ein Vergleich zwischen verschiedenen Studien nicht oder nur eingeschränkt möglich. Zudem ist die Genauigkeit und Aussagekraft der Ergebnisse limitiert. Diese Probleme könnten durch die Kombination einer differenzierten immunhistochemischen Untersuchung unterschiedlicher Populationen von Entzündungszellen mit einem quantitativen Verfahren zur digitalen Bildanalyse basierend auf der Nutzung von Computersoftware reduziert werden. Viele der in diesem Bereich eingesetzten Programme sind allerdings kostenpflichtig und oft durch Hardware-Schlüssel oder entsprechende Lizenzbestimmungen an einen bestimmten Arbeitsplatz gebunden.

Das am National Institutes of Health (Bethesda, Maryland, USA) entwickelte Softwaresystem ImageJ [GALLAGHER 2010] ist demgegenüber frei im Internet verfügbar und ohne Einschränkungen auf verschiedenen Computern nutzbar. Es ist im Quellcode erhältlich und umfangreich dokumentiert, aufgrund der Programmiersprache Java plattformunabhängig und wird von einer aktiven Entwickler- und Nutzergemeinschaft betreut und weiterentwickelt. Wiederholte Abläufe können durch Makros automatisiert werden. Außerdem besteht die Möglichkeit, den Funktionsumfang des Programms durch Plugins zu erweitern und an die eigenen Bedürfnisse anzupassen. Aus diesen Gründen sollte die Eignung von ImageJ zur schnellen, einfachen und reproduzierbaren Quantifizierung der Gewebsantwort nach Implantation von Biomaterialien untersucht werden. Das Verfahren beruht auf einer Gitternetz-unterstützten manuellen Zählung von immunhistochemisch detektierten Zellen im Perimplantatgewebe auf der Basis der beiden Plugins Grid und CellCounter.

Die Testung der Methode erfolgte anhand von Gewebsproben, die nach intramuskulärer Implantation von PAAc-behandelten Ti-Implantaten in die Nackenmuskulatur von Lewis-Ratten nach 56 Tagen entnommen wurden. Unmittelbar nach der Explantation wurde das Gewebe zunächst durch Kältespray mit einer Temperatur von etwa -50 °C gefroren. Anschließend erfolgte mit einem Skalpell die Öffnung der Gewebsproben entlang einer

Implantatkante und mittels einer Pinzette die vorsichtige Entnahme der Ti-Plättchen aus dem Gewebe. Nach Füllung der dadurch entstandenen Implantattasche mit dem Einbettungsmedium Shandon Cryomatrix™ wurden die Proben in flüssigem Stickstoff schockgefroren. Danach wurden Gefrierschnitte mit einer Dicke von 5 µm angefertigt, die mit den monoklonalen Primärantikörpern ED1, spezifisch für Monozyten und Makrophagen, sowie OX6, spezifisch für MHC-Klasse-II-positive Zellen, entsprechend den Herstellerangaben inkubiert wurden. Der Nachweis positiv markierter Zellen erfolgte mit der Alkalische-Phosphatase-Anti-Alkalische-Phosphatase-Methode (APAAP). Von den gefärbten Schnitten wurden mit einem Lichtmikroskop bei 125facher Vergrößerung digitale Aufnahmen mit einer Auflösung von 768 × 576 Pixeln angefertigt.

Zur Quantifizierung der Zahl positiv gefärbter Zellen wurden die Bilder mit ImageJ geöffnet. Die Anwendung des Plugins Grid erzeugte dann über dem Bild ein Gitternetz mit quadratischen Zellen einstellbarer Größe. Für die genutzte Bildauflösung erwiesen sich 5.000 Pixel pro Gitterquadrat als optimal, durch Variation der Quadratgröße ist eine Anpassung an andere Bildgrößen möglich. Das Plugin CellCounter ermöglichte dann die Zählung positiv gefärbter Zellen durch manuelles Markieren im Bild. Dies erfolgte in einer zuvor festgelegten Anzahl an Quadrate, die unmittelbar an die Implantattasche angrenzten. In der vorliegenden Studie wurden fünf Quadrate analysiert, was etwa 5 % der gesamten Bildfläche entsprach. Modifikationen der Helligkeit beziehungsweise des Kontrastes vor Beginn der Analyse mit CellCounter ermöglichen in einigen Fällen eine bessere Differenzierung von Zellen in Bereichen mit hoher Zelldichte oder starker Hintergrundfärbung. Nach dem Ende der Auszählung wurden die Bilder im Plugin CellCounter in ein neues Bild exportiert. In diesem wurden Bereiche mit Artefakten beziehungsweise ohne Gewebe in den analysierten Quadrate mittels der Auswahlfunktion von ImageJ markiert. Mit der Messfunktion des Programms erfolgte die Ermittlung der Größe dieser Bereiche, die von der analysierten Gesamtfläche subtrahiert wurden. Die einem Pixel entsprechende Fläche wurde mit Hilfe eines Objektträgers mit aufgedruckter Maßskala ermittelt. Für die untersuchte Bildfläche von 25.000 Pixeln ergab sich daraus eine Schnittfläche von 7.500 µm<sup>2</sup>. Die Ergebnisse wurden als positiv gefärbte Zellen pro µm<sup>2</sup> angegeben.

Zur Evaluierung des Verfahrens wurden ED1- und OX6-gefärbte Präparate von drei individuellen Tieren einerseits durch drei verschiedene Untersucher und andererseits durch den gleichen Untersucher an drei unterschiedlichen Tagen analysiert. Dabei ergab sich für den Marker ED1 ein mittlerer Variationskoeffizient von 13,8 % für die Ergebnisse der drei verschiedenen Untersucher und von 10,0 % für die Ergebnisse des gleichen Untersuchers an drei unterschiedlichen Tagen. Beim Marker OX6 betrug der Variationskoeffizient durchschnittlich 19,6 % zwischen den drei verschiedenen Untersuchern und 13,8 % an den drei

unterschiedlichen Tagen des gleichen Untersuchers. Damit war zum einen für beide Marker der Variationskoeffizient zwischen den verschiedenen Untersuchern höher als für den gleichen Untersucher an unterschiedlichen Tagen. Zum anderen zeigte sich, dass der Variationskoeffizient für ED1 kleiner war als für den Marker OX6, der im Vergleich zu ED1 kleinere Zellzahlen aufwies.

Obwohl das untersuchte Verfahren aufgrund der manuellen Zählung subjektiven Faktoren unterliegt, zeigten die Ergebnisse ein hohes Maß an Reproduzierbarkeit sowohl zwischen verschiedenen Untersuchern als auch für den gleichen Untersucher an unterschiedlichen Tagen. Beim Marker OX6 hatten Abweichungen der absoluten Werte aufgrund der geringeren Zellzahlen im Vergleich zu ED1 einen stärkeren Einfluss auf die Variabilität. Sowohl die Auswirkungen von kleinen Zellzahlen als auch von subjektiven Faktoren könnten zusätzlich reduziert werden, indem zum einen die Analyse durch weitere Untersucher durchgeführt wird, und zum anderen die einbezogene Fläche im Gitternetz vergrößert wird. Darüber hinaus war eine Analyse von Testbildern durch verschiedene Untersucher hilfreich, um mögliche Gründe für Diskrepanzen zu ermitteln. Diese lagen nach den Erfahrungen in der vorliegenden Studie vor allem in Unterschieden bei der Auswahl der Quadrate sowie bei der Auszählung von Zellakkumulationen. Testbilder ermöglichten dabei die Festlegung gemeinsamer Standards. Das verwendete Verfahren erwies sich als reproduzierbare und flexible Methode zur Analyse der lokalen zellulären Reaktionen im Periimplantatgewebe von Biomaterialien und wurde im weiteren Verlauf der Arbeit entsprechend genutzt.

## **2.2 Chronische lokale Entzündungsreaktionen gegen Titan-Implantate mit unterschiedlich geladenen Plasmapolymer-Beschichtungen**

*Veröffentlicht in: Schröder et al. (2010) J Adh Sci Technol 24:1191–1205*

Vorhergehende In-vitro-Analysen zeigten, wie in der Einleitung beschrieben, dass positiv geladene Plasmapolymer-Beschichtungen auf der Basis von PPAAm und negativ geladene PPAAc-Filme das Wachstum beziehungsweise die Differenzierung von Zellen beeinflussen. Aus diesem Grund sollten die lokalen Gewebsreaktionen nach Implantation von PPAAm- und PPAAc-beschichteten Ti-Plättchen nach 56 Tagen Implantationsdauer untersucht werden. Ziel war es im Hinblick auf weiterführende Studien, für beide Schichten erste Hinweise hinsichtlich ihrer In-vivo-Biokompatibilität zu erhalten.

Acrylsäure wurde als Präkursor zur Erzeugung einer negativ geladenen Plasmapolymer-Schicht ausgewählt, da Untersuchungen verschiedener Arbeitsgruppen gezeigt hatten, dass dies im Vergleich zu anderen Substanzen zu linearen Kettenstrukturen und damit zu einer höheren Carboxylgruppendichte sowie zu stabileren Filmen aufgrund von Quervernetzung bei

höheren Plasmaenergien führte. Analog dazu resultierte aus der Verwendung von Allylamin als Präkursor eine hohe Dichte an Aminogruppen in den darauf basierenden positiv geladenen PPAAm-Filmen. Für solche positiv geladenen Schichten wurden Interaktionen mit Hyaluronsäure, einem Bestandteil der Extrazellulärmatrix, postuliert. Zudem erwiesen sich sowohl PPAAm- als auch PPAc-Filme als unempfindlich gegenüber der Ablösung durch Wasser im Ultraschallbad, was ihre physikochemische Stabilität belegt [FINKE et al. 2009b].

Für die Untersuchung der lokalen Entzündungsreaktionen wurden PPAAm- und PPAc-beschichtete Ti-Plättchen in die Nackenmuskulatur von je 8 Lewis-Ratten implantiert. Zusätzlich zur PPAAm- und PPAc-Gruppe erhielt eine Kontrollgruppe von 8 Tieren Ti-Plättchen ohne Plasmapolymer-Beschichtung. Nach 56 Tagen wurden die Tiere euthanasiert und die Implantate zusammen mit dem umliegenden Gewebe entnommen. Die weitere Behandlung der Gewebsproben zwecks Anfertigung von Gefrierschnitten, deren immunhistochemische Färbung und die morphometrische Analyse der histologischen Präparate erfolgten wie im Abschnitt 2.1 beschrieben.

Es zeigte sich, dass die Zahl der ED1-positiven Monozyten und Makrophagen sowie der OX6-positiven antigen-präsentierenden Zellen im Periimplantatgewebe bei den Tieren der PPAc-Gruppe höher war als bei den Tieren der PPAAm-Gruppe. Dieser Unterschied erwies sich jedoch nur für die antigen-präsentierenden Zellen als statistisch signifikant. Im Vergleich mit den Tieren der Kontrollgruppe war bei den Tieren der PPAc-Gruppe sowohl die Zahl der Monozyten und Makrophagen als auch die Anzahl der antigen-präsentierenden Zellen signifikant erhöht, was auf eine verstärkte chronische Entzündungsreaktion hindeutet. Demgegenüber unterschieden sich die Tiere der PPAAm-Gruppe hinsichtlich beider Zellpopulationen nicht signifikant von den Tieren der Kontrollgruppe. Aufgrund dieser Daten, der zuvor bereits beschriebenen In-vitro-Effekte sowie positiver Befunde zu den mechanischen Eigenschaften [FRITSCHE et al. 2009] wurden Schichten auf der Basis von PPAAm im Vergleich zu den PPAc-Filmen als geeigneter für die Erzeugung von bioaktiven Ti-Oberflächen mit dem Ziel einer besseren Knochenregeneration eingeschätzt.

## **2.3 Akute und chronische lokale Entzündungsreaktionen gegen Titan-Implantate mit plasma-polymerisiertem Allylamin**

*Veröffentlicht in: Hoene et al. (2010) Acta Biomater 6:676–683*

Nach den im Abschnitt 2.2 dargestellten In-vivo-Befunden zu den Entzündungsreaktionen nach Langzeitimplantation von PPAAm- und PPAc-beschichteten Ti-Plättchen sollten die akuten und chronischen Reaktionen gegen Ti-Implantate mit PPAAm-Filmen detaillierter charakterisiert werden. Dies umfasste die Analyse der Reaktionen nach 7 Tagen

Implantationsdauer als Zeitpunkt der akuten Phase, nach 14 Tagen als Zeitpunkt des Überganges zwischen akuter und chronischer Phase und nach 56 Tagen als Zeitpunkt der chronischen Phase der Entzündungsantwort. Des Weiteren sollte der Einfluss unterschiedlicher Plasmaparameter auf die Entzündungsreaktionen untersucht werden, um Rückschlüsse auf Zusammenhänge zwischen Variationen in den Prozessbedingungen, den daraus resultierenden physikochemischen Eigenschaften und deren Einfluss auf die In-vivo-Reaktionen zu erhalten.

Dementsprechend wurden drei verschiedene Serien PPAAm-beschichteter Ti-Plättchen mit den Bezeichnungen RM76AB, RM77AB und RM78AB präpariert. Der wesentliche Unterschied zwischen diesen drei Serien hinsichtlich der Plasmaparameter lag in den Pulsbedingungen, also dem Verhältnis zwischen der Zeit, in der das Plasma eingeschaltet war (Pulsdauer  $t_{on}$ ), und der Zeit, in der das Plasma abgeschaltet war (Pulspause  $t_{off}$ ). Diese Parameter betrugen für die RM76AB-Proben  $t_{on} = 0,30$  s und  $t_{off} = 1,70$  s, für die RM77AB-Proben  $t_{on} = 0,01$  s und  $t_{off} = 0,19$  s und für die RM78AB-Proben  $t_{on} = 0,10$  s und  $t_{off} = 0,70$  s. Aus einer einheitlichen Plasmabehandlungsdauer von 144 s für alle drei PPAAm-Serien resultierte eine Gesamtbehandlungszeit von 960 s für die RM76AB-Proben, 2880 s für die RM77AB-Proben und 1152 s für die RM78AB-Proben. Das als Duty cycle (DC) bezeichnete Verhältnis aus der Pulsdauer  $t_{on}$  und der Pulswiederholzeit  $t_{on} + t_{off}$  war somit für die RM77AB-Proben ( $DC = 0,05$ ) deutlich kleiner als für die RM76AB- ( $DC = 0,15$ ) und die RM78AB-Proben ( $DC = 0,125$ ). Zusätzlich zu den drei verschiedenen PPAAm-Proben kamen Kontrollimplantate zum Einsatz, die nur mit dem bei den PPAAm-Proben zur Aktivierung und Dekontamination verwendetem Sauerstoffplasma behandelt wurden, jedoch anschließend keine Allylamin-Beschichtung erhielten.

Im Gegensatz zu den vorherigen Untersuchungen, in denen pro Versuchstier ein Implantat eingesetzt wurde, erfolgte die Implantation der vier verschiedenen Implantate simultan in denselben Versuchstieren ( $n = 24$  Lewis-Ratten) in die Nackenmuskulatur mit einer quadratischen Anordnung der Implantate im Abstand von etwa 2 cm. Dieser bereits in anderen Studien [WALSCHUS et al. 2009; KOCHANOWSKI et al. 2011] verwendete Ansatz ermöglichte den intraindividuellen Vergleich der Gewebsreaktionen gegen die verschiedenen Implantate, wodurch sich der Einfluss der individuellen Variabilität zwischen einzelnen Versuchstieren am gleichen experimentellen Tag reduzierte. Darüber hinaus verringerte sich im Vergleich zu einem Studiendesign mit Einzelimplantation die Zahl der notwendigen Versuchstiere. Von den 24 Lewis-Ratten wurden je acht Tiere nach 7, 14 und 56 Tagen euthanasiert. Die Entnahme der Implantate zusammen mit Proben des Periimplantatgewebes sowie deren weitere Verarbeitung erfolgten wie im Abschnitt 2.1 beschrieben. Die von den Gewebsproben angefertigten Gefrierschnitte wurden mit den monoklonalen Primärantikörpern ED1, ED2,

R73 und OX6 inkubiert. Analog zu den vorherigen Untersuchungen erfolgte der Nachweis der Antikörper-markierten Zellen mittels der APAAP-Methode.

Im zeitlichen Verlauf der Gewebsantwort zeigte sich für die ED1-positiven Monozyten und Makrophagen für keine der vier Implantatserien eine signifikante Veränderung. Alle drei PAAm-Implantatserien wiesen am Tag 14 im Vergleich zu den Kontrollimplantaten signifikant weniger Monozyten und Makrophagen im Periimplantatgewebe auf. Auch am Tag 56 lag deren Zahl für die RM76AB- und RM78AB-Implantate signifikant unter den Kontrollen, während die RM77AB-Implantate sich nicht von den Kontrollen unterschieden.

Auch für die Anzahl der ED2-positiven Gewebsmakrophagen war für keine der vier Implantatserien eine signifikante Veränderung zwischen Tag 7 und Tag 56 nachweisbar. Für die RM76AB-Implantate zeigte sich eine zwar nicht signifikante aber konsistente Abnahme im zeitlichen Verlauf. Am Tag 56 war die Anzahl der Gewebsmakrophagen für alle drei PAAm-Implantatserien, dabei insbesondere für die RM76AB- und die RM78AB-Proben, signifikant geringer als bei den Kontrollen.

Die Anzahl der R73-positiven T-Lymphozyten lag für alle vier Implantatserien und an allen experimentellen Tagen deutlich unter der Anzahl der Makrophagen. Änderungen im zeitlichen Verlauf oder signifikante Unterschiede zwischen den Implantaten waren für die T-Lymphozyten nicht feststellbar. Im Vergleich zu den Kontrollen zeigte sich am Tag 14 für die RM76AB- und die RM77AB-Implantate tendenziell eine erhöhte sowie am Tag 56 für alle drei PAAm-Implantate eine geringere Anzahl an T-Lymphozyten. Analog zu den Befunden für die ED1- und ED2-positiven Makrophagen wurde dies am Tag 56 vor allem für die RM76AB- und RM78AB-Implantate beobachtet.

Hinsichtlich der Anzahl der OX6-positiven antigen-präsentierenden Zellen zeigte sich für die RM78AB-Implantate eine signifikante Abnahme zwischen Tag 7 und Tag 56. Obwohl zu keinem Zeitpunkt signifikante Unterschiede zwischen den vier Implantatserien feststellbar waren, lag die Anzahl der antigen-präsentierenden Zellen an den Tagen 7 und 14 für die drei PAAm-Implantatserien tendenziell über der für die Kontrollimplantate. Demgegenüber waren am Tag 56 alle vier Implantatserien vergleichbar.

Zusammenfassend lässt sich feststellen, dass das Ausmaß der lokalen Entzündungsreaktionen für die PAAm-beschichteten Ti-Implantate im Langzeitverlauf geringer war als für die Kontrollimplantate. Dies galt hinsichtlich der ED2-positiven Monozyten und Makrophagen für alle drei PAAm-Serien und bei Gesamtbetrachtung aller untersuchten Zellpopulationen primär für die Serien RM76AB und RM78AB, bei denen zur Plasmabeschichtung ein höherer DC-Wert verwendet wurde. Untersuchungen der physikochemischen Eigenschaften unmittelbar nach der Beschichtung ergaben für diese Proben ein geringeres Stickstoff/Kohlenstoff-Verhältnis, eine höhere Sauerstoffaufnahme und eine geringere

Stickstoffabgabe nach Ultraschallbehandlung, eine geringere PPAAm-Schichtdicke sowie eine geringere Proteinadsorption. Die Analyse der explantierten Proben zeigte zudem, dass das Sauerstoff/Kohlenstoff-Verhältnis von Tag 7 bis Tag 56 für die RM76AB- und die RM78AB-Proben zunahm, während es sich für die RM77AB-Proben nicht änderte. Das Stickstoff/Kohlenstoff-Verhältnis blieb für die RM76AB- und die RM78AB-Proben im zeitlichen Verlauf unverändert und nahm für die RM77AB-Proben tendenziell ab. Von möglicher Relevanz hinsichtlich eines Einflusses auf die zellulären Reaktionen könnte dabei insbesondere die geringere initiale Proteinadsorption der RM76AB- und RM78AB-Proben im Vergleich zu den RM77AB-Proben sein. Insgesamt zeigen die Ergebnisse zum einen, dass die PPAAm-Beschichtung die Stärke der untersuchten lokalen Entzündungsreaktionen reduzierte. Zum anderen wurde deutlich, dass Unterschiede in den Prozessbedingungen und den daraus resultierenden physikochemischen Eigenschaften die Gewebsantwort beeinflussten.

## **2.4 Serumprofil pro- und anti-inflammatorischer Zytokine nach Implantation von Plasmapolymer-beschichteten Titan-Implantaten**

*Veröffentlicht in: Walschus et al. (2012) J Mater Sci Mater Med 23:1299–1307*

Da insbesondere Zytokine für die Aktivierung der an den Entzündungsreaktionen beteiligten Zellpopulationen und für deren Kommunikation untereinander eine zentrale Rolle spielen, könnte deren quantitative Bestimmung in Körperflüssigkeiten Rückschlüsse auf die Entzündungsreaktionen nach Implantation von Biomaterialien ermöglichen. Entsprechende Untersuchungen wurden in den letzten Jahren beispielsweise für die Gewebsflüssigkeit in implantierten Polyurethanröhren [WANG et al. 2008b] sowie für Exsudate in einem Cage-Implant-Modell [MARCHANT et al. 1983] nach subkutaner Implantation von Stahlkäfigen mit Proben verschiedener Polymermaterialien in Ratten beschrieben [RODRIGUEZ et al. 2009]. In einer weiteren Studie untersuchten die Autoren nach 7, 14 und 28 Tagen verschiedene Zytokine im Serum nach subkutaner Implantation von Hydroxylapatit, Polycaprolacton und Typ-1-Kollagen in Mäusen [SCAGLIONE et al. 2011].

In Ergänzung zu den histologischen Untersuchungen der lokalen zellulären Reaktionen, die in den vorherigen Abschnitten beschrieben wurden, sollte mittels Analyse des Serumprofils ausgewählter Zytokine die systemische Entzündungsantwort nach Implantation von Plasmapolymer-beschichteten Ti-Implantaten untersucht werden. Aus diesem Grund wurden drei pro-inflammatorisch wirkende Zytokine, und zwar das für die Funktion und Proliferation von T-Lymphozyten sowie für das Wachstum und die Differenzierung von NK-Zellen wichtige Interleukin-2 (IL-2), das für die Stimulation beziehungsweise Aktivierung von Makrophagen und NK-Zellen essentielle IFN $\gamma$  sowie das die Proliferation von

B-Lymphozyten und die Expression des IL-2-Rezeptors auf T-Lymphozyten regulierende IL-6, quantitativ bestimmt. Darüber hinaus wurden mit IL-4, das im Wesentlichen den Effekten von IFN $\gamma$  entgegenwirkt, IL-10, das die Aktivität von Makrophagen hemmt und humorale Immunreaktionen aktiviert, sowie IL-13, das synergistisch mit IL-4 wirkt, drei anti-inflammatorisch wirkende Zytokine in die Analyse einbezogen.

Wie im Abschnitt 2.2 beschrieben, erhielten je 8 Lewis-Ratten ein PPAAm- beziehungsweise PPAc-beschichtetes Ti-Plättchen oder als Kontrolle ein Ti-Plättchen ohne Plasmapolymer-Beschichtung in die Nackenmuskulatur implantiert. Präoperativ und wöchentlich postoperativ wurde den Tieren über die gesamte Studiendauer von 56 Tagen Blut entnommen. In den Serumproben erfolgte mittels Enzyme-linked Immunosorbent Assays (ELISA-Assays) auf der Basis kommerziell verfügbarer Antikörperpaare die Messung der Zytokine IL-2, IFN $\gamma$ , IL-6, IL-4, IL-10 und IL-13. Zur Auswertung wurden die an den postoperativen Tagen gemessenen Zytokinkonzentrationen jeweils mit den präoperativen Werten verglichen. Darüber hinaus wurden mögliche Interaktionen zwischen den einzelnen Zytokinen mittels Korrelationsanalyse untersucht.

In der Gruppe mit den PPAAm-beschichteten Implantaten zeigte sich für IL-2 ein vorübergehender Anstieg an den Tagen 7 und 14 und, nach einem zwischenzeitlichen Absinken, erneut am Tag 35. Der Anstieg in der Frühphase fiel auf den gleichen Zeitpunkt wie die tendenziell erhöhte Zahl an T-Lymphozyten am Tag 14 in den im Abschnitt 2.3 beschriebenen Untersuchungen zu den lokalen Gewebsreaktionen. Da IL-2 das Wachstum und die Proliferation von T-Lymphozyten induziert, ist ein diesbezüglicher Zusammenhang plausibel. Neben der IL-2- war auch die IFN $\gamma$ -Konzentration am Tag 35 erhöht. Darüber hinaus war die IL-10-Konzentration von diesem Tag bis zum Studienende verringert, während sich für IL-4 im gesamten Studienverlauf keine Veränderungen der Serumkonzentration zeigten. Der Zeitraum um den Tag 35 könnte somit einen Übergang zwischen zwei verschiedenen Phasen der Entzündungsreaktionen darstellen, der möglicherweise durch Veränderungen der Materialeigenschaften bedingt ist. Wie bereits im Abschnitt 2.3 beschrieben, wurden in der Studie zu den lokalen Gewebsreaktionen Änderungen verschiedener physikochemischer Schichtparameter zwischen den Tagen 7 und 56 nachgewiesen, die auf einen schrittweisen Abbau der PPAAm-Schicht hindeuten. Da aus diesen Untersuchungen jedoch keine Daten zum Tag 35 vorliegen, kann aus den Ergebnissen beider Studien kein direkter Zusammenhang zwischen den Änderungen der Materialeigenschaften und den an diesem experimentellen Tag beobachteten Veränderungen im Zytokinprofil postuliert werden. Hinsichtlich der Analyse der Interaktionen zwischen den Zytokinen ergaben sich in der PPAAm-Gruppe negative Korrelationen zwischen den Konzentrationen

von IL-2 und IL-4 sowie IL-2 und IL-10, während positive Korrelationen zwischen IFN $\gamma$  und IL-10 sowie IL-4 und IL-10 gefunden wurden.

Bei den Tieren mit den PPAc-beschichteten Implantaten kam es zu keinem Zeitpunkt zu signifikanten Änderungen in der Konzentration der pro-inflammatorischen Zytokine IL-2 und IFN $\gamma$ . Für die Konzentrationen der anti-inflammatoryisch wirkenden Zytokine IL-4 und IL-10 zeigte sich in dieser Gruppe ein divergenter Verlauf. Während die IL-4-Konzentration ab dem Tag 28 erhöht war und bis zum Studienende anstieg, war die IL-10-Konzentration vom Tag 42 bis zum Studienende verringert. Die PPAc-Gruppe war damit die einzige, in der es zu Änderungen der IL-4-Serumkonzentration kam. Dementsprechend ergab die Korrelationsanalyse in dieser Gruppe negative Korrelationen zwischen IL-4 und IL-2, zwischen IL-10 und IFN $\gamma$  sowie zwischen IL-4 und IL-10, während zwischen IL-10 und IL-2 sowie IL-4 und IFN $\gamma$  positive Korrelationen bestanden. Hinsichtlich der positiven Korrelation zwischen IL-4 und IFN $\gamma$  und zwischen IL-10 und IL-2 sowie der negativen Korrelation zwischen IL-10 und IFN $\gamma$  wichen diese Befunde von den Ergebnissen in den beiden anderen Gruppen ab. Dies deutet möglicherweise auf spezifische Änderungen in den Interaktionen zwischen verschiedenen Entzündungszellpopulationen als Ursache des entgegengesetzten Verlaufs der Serumkonzentrationen von IL-4 und IL-10 hin.

In der Kontrollgruppe waren die IL-2-Konzentration am Tag 42 sowie die IFN $\gamma$ -Konzentration an den Tagen 42 und 56 erhöht, während sich die Konzentrationen von IL-4 und IL-10 im gesamten Studienverlauf nicht änderten. In dieser Gruppe zeigte sich eine negative Korrelation zwischen IL-2 und IL-10, während zwischen IL-4 und IL-10 sowie zwischen IL-2 und IFN $\gamma$  positive Korrelationen gefunden wurden. Die Befunde zum Zytokinprofil und die Ergebnisse der Korrelationsanalyse waren mit der PPAAm-Gruppe vergleichbar. Für IL-6 und IL-13 lagen die Konzentrationen im gesamten Studienverlauf in allen Gruppen unter der Nachweisgrenze des jeweiligen ELISA-Kits.

Zusammenfassend zeigten die Ergebnisse, dass die Veränderungen im Serumprofil der untersuchten Zytokine nach der Implantation von Ti-Plättchen mit unterschiedlichen Plasmapolymer-Beschichtungen materialspezifisch waren. Dieser Befund ist im Einklang mit den bereits erwähnten Untersuchungen anderer Autoren [SCAGLIONE et al. 2011]. Darüber hinaus ist bei einer vergleichenden Betrachtung der hier vorliegenden Daten mit der Studie von Scaglione et al. erkennbar, dass die systemischen Entzündungsreaktionen nicht nur vom Material, sondern wahrscheinlich auch von der Empfängerspezies (Maus vs. Ratte) und dem Implantationsort (subkutan vs. intramuskulär) abhängen. Die Tatsache, dass in den vorliegenden Untersuchungen die meisten Änderungen im Zytokinprofil nach Tag 28 gefunden wurden, unterstreicht zudem die Bedeutung von Langzeituntersuchungen der chronischen Entzündungsreaktionen.

Eine kombinierte Analyse der Interaktionen zwischen den lokalen Entzündungsreaktionen am Tag 56 und dem Verlauf der Serumkonzentrationen der pro- und anti-inflammatorischen Zytokine kann darüber hinaus mögliche Zusammenhänge zwischen frühen Änderungen im Zytokinprofil und der chronischen Gewebsreaktion aufzeigen. Die Anwendung eines multivariaten Korrelationsverfahrens auf der Basis eines generalisierten linearen Modells mit Messwiederholung erbrachte diesbezüglich, dass zwischen der IFN $\gamma$ -Konzentration im Serum und der Zahl der ED1-positiven Monozyten und Makrophagen im Periimplantatgewebe ein positiver Zusammenhang besteht. Dieser Befund war bei einer Untersuchung der einzelnen Zeitpunkte an den Tagen 14 und 21 besonders stark ausgeprägt. Dies deutet darauf hin, dass eine Bestimmung der IFN $\gamma$ -Serumkonzentration möglicherweise eine prädiktive Bedeutung für das Ausmaß der chronischen Entzündungsreaktionen am Implantationsort haben könnte und somit, wie bereits von anderen Autoren gezeigt [CARUSO et al. 2010], die Untersuchung von Entzündungsmarkern wie Zytokinen möglicherweise zur frühzeitigen Erkennung von Komplikationen nach einer Implantation geeignet ist.

## Zusammenfassung

In-vitro-Studien zur Oberflächenmodifizierung von Ti-Plättchen mit verschiedenen Niedertemperatur-Plasmapolymer-Schichten zeigten für einen positiv geladenen, Amino-gruppen-reichen Film aus plasma-polymerisiertem Allylamin (PPAAm) positive Effekte auf das Wachstum von Osteoblasten. Eine negativ geladene, Carboxylgruppen-reiche Schicht auf der Basis von plasma-polymerisierter Acrylsäure (PPAAC) steigerte die Expression verschiedener osteogener Differenzierungsmarker humaner mesenchymaler Stammzellen. Aufgrund dieser Ergebnisse wurden in der vorliegenden Arbeit die lokalen und systemischen Entzündungsreaktionen nach Implantation von PPAAm- und PPAAC-modifizierten Ti-Implantaten im Tiermodell Ratte untersucht.

Um im Rahmen dieser In-vivo-Studien eine morphometrische Analyse der zellulären Reaktionen im Periimplantatgewebe von Ti-Implantaten zu ermöglichen, wurde zunächst ein Verfahren zur digitalen Bildanalyse etabliert und evaluiert (siehe Abschnitt 2.1). Dieses erwies sich als reproduzierbare Methode zur quantitativen Analyse der lokalen Gewebsreaktionen nach Implantation von metallischen Biomaterialien und war Grundlage der nachfolgenden tierexperimentellen Studien.

Die histologische Untersuchung der lokalen Entzündungsantwort nach Implantation von PPAAC-beschichteten Ti-Plättchen zeigte im Vergleich zu Kontrollimplantaten eine verstärkte chronische Entzündungsreaktion im Periimplantatgewebe (siehe Abschnitt 2.2). Eine serologische Analyse des Serumzytokinprofils als Marker der systemischen Entzündungsantwort ergab für diese Implantate zudem einen gegensätzlichen Verlauf der anti-inflammatoryischen Zytokine IL-4 und IL-10 (siehe Abschnitt 2.4).

Demgegenüber waren die lokalen Gewebsreaktionen nach Implantation von PPAAm-beschichteten Ti-Plättchen im Langzeitverlauf schwächer als bei den Kontrollimplantaten (siehe Abschnitt 2.3). Im Serumzytokinprofil zeigte sich zum einen ein vorübergehender Anstieg der pro-inflammatoryischen Zytokine IL-2 und IFN $\gamma$  und zum anderen eine moderate Verringerung der IL-10-Konzentration (siehe Abschnitt 2.4). Diese Beobachtungen stehen möglicherweise in Zusammenhang mit Änderungen verschiedener physikochemischer Parameter der Implantatoberflächen im zeitlichen Verlauf, die als Hinweis auf einen Abbau der PPAAm-Schicht gedeutet werden könnten. Die durch die PPAAm-beschichteten Implantate induzierten systemischen Reaktionen und die Interaktionen zwischen den Zytokinen waren insgesamt mit den Befunden in der Kontrollgruppe vergleichbar.

Den durchgeführten In-vivo-Studien lagen zwei verschiedene experimentelle Ansätze im Tiermodell Ratte zugrunde. Die Untersuchung der lokalen Gewebsreaktionen im zeitlichen Verlauf erfolgte durch simultane Implantation mehrerer unterschiedlich modifizierter Ti-Plättchen in dieselben Versuchstiere. Dadurch verringerte sich gegenüber einem Ansatz mit Einzelimplantation und einer vergleichbaren Anzahl an experimentellen Tagen die Zahl der Tiere. Darüber hinaus reduzierte der intraindividuelle Vergleich der Reaktionen den Einfluss der individuellen Variabilität der Versuchstiere einer Gruppe. Für die Analyse des Serumzytokinprofils war hingegen die Implantation eines einzelnen Ti-Plättchens pro Tier notwendig, da bei einer Simultanimplantation mehrerer Implantate die Zytokin-konzentrationen eine Mischantwort repräsentieren würden und damit keine material-spezifische Differenzierung möglich wäre. Beide Ansätze orientieren sich damit an den jeweiligen Fragestellungen und ermöglichen eine umfassende Bewertung der Implantatbedingten akuten und chronischen Entzündungsreaktionen.

Die Gesamtbetrachtung der In-vitro- und In-vivo-Ergebnisse zeigt, dass positiv geladene PAAm-beschichtete Ti-Oberflächen in vitro positive Effekte auf das Wachstum von Osteoblasten haben, ohne dabei in vivo die lokalen oder systemischen Entzündungsreaktionen negativ zu beeinflussen. Eine PAAm-Beschichtung ist damit ein vielversprechender Ansatz zur Erzeugung von zelladhäsiven Implantatoberflächen mit dem Ziel einer Verbesserung des Einwachsens von Ti-Implantaten. Die beobachteten Zusammenhänge zwischen den Plasmaprozessbedingungen, den physikochemischen Schichtparametern und den daraus resultierenden In-vivo-Reaktionen zeigen darüber hinaus, dass prinzipiell eine anwendungs-spezifische Anpassung der Schichteigenschaften möglich ist. Eine statistische Analyse der lokalen Gewebsreaktionen und der systemischen Zytokinprofile unter Verwendung eines multivariaten Korrelationsverfahrens ergab darüber hinaus, dass die Messung der IFN $\gamma$ -Serumkonzentration in der Frühphase ein prädiktiver Parameter zur Vorhersage der Stärke der lokalen Entzündungsreaktion in der chronischen Phase sein könnte.

## Referenzen

- ALMEIDA CR**, Vasconcelos DP, Gonçalves RM, Barbosa MA (2012). Enhanced mesenchymal stromal cell recruitment via natural killer cells by incorporation of inflammatory signals in biomaterials. *Journal of the Royal Society Interface* 9:261–271
- ANDERSON JM** (2001). Biological responses to materials. *Annual Review of Materials Research* 31:81–110
- ANDERSON JM**, Rodriguez A, Chang DT (2008). Foreign body reaction to biomaterials. *Seminars in Immunology* 20:86–100
- ANDERSON JM & McNALLY AK** (2011). Biocompatibility of implants: lymphocyte/ macrophage interactions. *Seminars in Immunopathology* 33:221–233
- ARCIOLA CR**, Alvi FI, An YH, Campoccia D, Montanaro L (2005). Implant infection and infection resistant materials: a mini review. *International Journal of Artificial Organs* 28:1119–1125
- AVILA G**, Misch K, Galindo-Moreno P, Wang HL (2009). Implant surface treatment using biomimetic agents. *Implant Dentistry* 18:17–26
- BAGNO A & DI BELLO C** (2004). Surface treatments and roughness properties of Ti-based biomaterials. *Journal of Materials Science: Materials in Medicine* 15:935–949
- BAUMANN B**, Hendrich C, Barthel T, Bockholt M, Walther M, Eulert J, Rader CP (2007). 9- to 11-year results of cemented titanium mueller straight stem in total hip arthroplasty. *Orthopedics* 30:551–557
- BIOMARKET GROUP** (2009). Global Biomaterial Market (2009–2014). Zusammenfassung online veröffentlicht (abgerufen am 1. Oktober 2013):  
<http://www.biemarketgroup.com/market-research-report/factsheet-pdf/global-biomaterial-market-2009-2014.pdf>
- CAMPOCCIA D**, Montanaro L, Arciola CR (2006). The significance of infection related to orthopedic devices and issues of antibiotic resistance. *Biomaterials* 27:2331–2339
- CAMPOCCIA D**, Montanaro L, Arciola CR (2013). A review of the biomaterials technologies for infection-resistant surfaces. *Biomaterials* 34:8533–8554
- CARUSO R**, Trunfio S, Milazzo F, Campolo J, De Maria R, Colombo T, Parolini M, Cannata A, Russo C, Paino R, Frigerio M, Martinelli L, Parodi O (2010). Early expression of pro- and anti-inflammatory cytokines in left ventricular assist device recipients with multiple organ failure syndrome. *ASAIO Journal* 56:313–318
- CONRADS H & SCHMIDT M** (2000). Plasma generation and plasma sources. *Plasma Sources Science and Technology* 9:441–454

- DAVIS C**, Fischer J, Ley K, Sarembock IJ (2003). The role of inflammation in vascular injury and repair. *Journal of Thrombosis and Haemostasis* 1:1699–1709
- DE JONGE LT**, Leeuwenburgh SC, Wolke JG, Jansen JA (2008). Organic-inorganic surface modifications for titanium implant surfaces. *Pharmaceutical Research* 25:2357–2369
- DISEGI JA** (2000). Titanium alloys for fracture fixation implants. *Injury* 4:S14–S17
- ESPOSITO M**, Hirsch JM, Lekholm U, Thomsen P (1998). Biological factors contributing to failures of osseointegrated oral implants. (I). Success criteria and epidemiology. *European Journal of Oral Sciences* 106:527–551
- FINKE B**, Lüthen F, Schröder K, Mueller PD, Bergemann C, Frant M, Ohl A, Nebe BJ (2007). The effect of positively charged plasma polymerization on initial osteoblastic focal adhesion on titanium surfaces. *Biomaterials* 28:4521–4534
- FINKE B**, Bergemann C, Lüthen F, Rothe H, Schröder K, Rychly J, Ohl A (2009a). Plasma polymer deposition for improved cell differentiation control. *Proceedings of the 19th International Symposium on Plasma Chemistry* P3.13.12; Online veröffentlicht (abgerufen am 1. Oktober 2013):  
<http://www.ispc-conference.org/ispcproc/papers/232.pdf>
- FINKE B**, Schröder K, Ohl A (2009b). Structure retention and water stability of microwave plasma polymerized films from allylamine and acrylic acid. *Plasma Processes and Polymers* 6:S70–S74
- FRITSCHE A**, Haenle M, Zietz C, Mittelmeier W, Neumann HG, Heidenau F, Finke B, Bader R (2009). Mechanical characterization of anti-infectious, anti-allergic, and bioactive coatings on orthopedic implant surfaces. *Journal of Materials Science: Materials in Medicine* 20:5544–5551
- GALLAGHER SR** (2010). Digital image processing and analysis with ImageJ. *Current Protocols Essential Laboratory Techniques* 3:A.3C.1–A.3C.24
- GOODMAN SB** (2007). Wear particles, periprosthetic osteolysis and the immune system. *Biomaterials* 28:5044–5048
- GOODMAN SB**, Yao Z, Keeney M, Yang F (2013). The future of biologic coatings for orthopaedic implants. *Biomaterials* 34:3174–3183
- GRAMMATOPOULOS G**, Pandit H, Kamali A, Maggiani F, Glyn-Jones S, Gill HS, Murray DW, Athanasou N (2013). The correlation of wear with histological features after failed hip resurfacing arthroplasty. *Journal of Bone and Joint Surgery (American Volume)* 95:e81(1–10)
- GUILLEMOT F** (2005). Recent advances in the design of titanium alloys for orthopedic applications. *Expert Review of Medical Devices* 2:741–748
- HEYMANN D**, Pradal G, Benahmed M (1999). Cellular mechanisms of calcium phosphate ceramic degradation. *Histology and Histopathology* 14:871–877

- HUSS RS**, Huddleston JI, Goodman SB, Butcher EC, Zabel BA (2010). Synovial tissue-infiltrating natural killer cells in osteoarthritis and periprosthetic inflammation. *Arthritis & Rheumatism* 62:3799–3805
- IMPLANT TRIBUNE** (2012). Herausgegeben von Dental Tribune America, LLC. U.S. Edition, Band 7/ Ausgabe 8 (August 2012), S. C1
- INGHAM E & FISHER J** (2005). The role of macrophages in osteolysis of total joint replacement. *Biomaterials* 26:1271–1286
- KOCHANOWSKI A**, Hoene A, Patrzyk M, Walschus U, Finke B, Luthringer B, Feyerabend F, Willumeit R, Lucke S, Schlosser M (2011). Examination of the inflammatory response following implantation of titanium plates coated with phospholipids in rats. *Journal of Materials Science: Materials in Medicine* 22:1015–1026
- KOU PM & BABENSEE JE** (2011). Macrophage and dendritic cell phenotypic diversity in the context of biomaterials. *Journal of Biomedical Materials Research Part A* 96:239–260
- LE GUÉHENNEC L**, Soueidan A, Layrolle P, Amouriq Y (2007). Surface treatments of titanium dental implants for rapid osseointegration. *Dental Materials* 23:844–854
- MARCHANT R**, Hiltner A, Hamlin C, Rabinovitch A, Slobodkin R, Anderson JM (1983). In vivo biocompatibility studies. I. The cage implant system and a biodegradable hydrogel. *Journal of Biomedical Materials Research* 17:301–325
- MARTINEZ FO**, Helming L, Gordon S (2009). Alternative activation of macrophages: an immunologic functional perspective. *Annual Review of Immunology* 27:451–483
- MEDSUM** (2013). MEDSUM – The MEDLINE summary tool. Institute for Biostatistics and Medical Informatics, Medical Faculty, University of Ljubljana, Slovenia. Online verfügbar (Abfrage am 1. Oktober 2013 für die Stichworte „biomaterials“, 104.522 Einträge, beziehungsweise „biocompatibility“, 14.063 Einträge):  
<http://www.medsum.info>
- MORRA M & CASSINELLI C** (1997). Organic surface chemistry on titanium surfaces via thin film deposition. *Journal of Biomedical Materials Research* 37:198–206
- NARAYANAN R**, Seshadri SK, Kwon TY, Kim KH (2008). Calcium phosphate-based coatings on titanium and its alloys. *Journal of Biomedical Materials Research Part B: Applied Biomaterials* 85:279–299
- NEBE B**, Finke B, Lüthen F, Bergemann C, Schröder K, Rychly J, Liefelth K, Ohl A (2007). Improved initial osteoblast functions on amino-functionalized titanium surfaces. *Biomolecular Engineering* 24:447–454
- PALMQUIST A**, Omar OM, Esposito M, Lausmaa J, Thomsen P (2010). Titanium oral implants: surface characteristics, interface biology and clinical outcome. *Journal of the Royal Society Interface* 7:S515–S527

- POLAK M**, Ohl A, Quaas M, Lukowski G, Lüthen F, Weltmann KD, Schröder K (2010). Oxygen and water plasma-immersion ion implantation of copper into titanium for antibacterial surfaces of medical implants. *Advanced Engineering Materials* 12:B511–B518
- RATNER BD** (2011). The biocompatibility manifesto: biocompatibility for the twenty-first century. *Journal of Cardiovascular Translational Research* 4:523–527
- RATNER BD & BRYANT SJ** (2004). Biomaterials: where we have been and where we are going. *Annual Review of Biomedical Engineering* 6:41–75
- REVELL PA** (2008). The combined role of wear particles, macrophages and lymphocytes in the loosening of total joint prostheses. *Journal of the Royal Society Interface* 5:1263–1278
- RODRIGUEZ A**, Voskerician G, Meyerson H, Macewan SR, Anderson JM (2008). T cell subset distributions following primary and secondary implantation at subcutaneous biomaterial implant sites. *Journal of Biomedical Materials Research Part A* 85:556–565
- RODRIGUEZ A**, Meyerson H, Anderson JM (2009). Quantitative in vivo cytokine analysis at synthetic biomaterial implant sites. *Journal of Biomedical Materials Research Part A* 89:152–159
- SCAGLIONE S**, Cilli M, Fiorini M, Quarto R, Pennesi G (2011). Differences in chemical composition and internal structure influence systemic host response to implants of biomaterials. *International Journal of Artificial Organs* 34:422–331
- SCHLOSSER M**, Wilhelm L, Urban G, Ziegler B, Ziegler M, Zippel R (2002). Immunogenicity of polymeric implants: long-term antibody response against polyester (Dacron) following the implantation of vascular prostheses into LEW.1A rats. *Journal of Biomedical Materials Research* 61:450–457
- SCHLOSSER M**, Zippel R, Hoene A, Urban G, Ueberrueck T, Marusch F, Koch A, Meyer L, Wilhelm L (2005). Antibody response to collagen after functional implantation of different polyester vascular prostheses in pigs. *Journal of Biomedical Materials Research Part A* 72:317–325
- SCHWEIZER A**, Riede U, Maurer TB, Ochsner PE (2003). Ten-year follow-up of primary straight-stem prosthesis (MEM) made of titanium or cobalt chromium alloy. *Archives of Orthopaedic and Trauma Surgery* 123:353–356
- TANG L**, Jennings TA, Eaton JW (1998). Mast cells mediate acute inflammatory responses to implanted biomaterials. *Proceedings of the National Academy of Sciences* 95:8841–8846
- TRIPLETT RG**, Frohberg U, Sykaras N, Woody RD (2003). Implant materials, design, and surface topographies: their influence on osseointegration of dental implants. *Journal of Long Term Effects of Medical Implants* 13:485–501
- WALSCHUS U**, Hoene A, Neumann HG, Wilhelm L, Lucke S, Lüthen F, Rychly J, Schlosser M (2009). Morphometric immunohistochemical examination of the inflammatory tissue

reaction after implantation of calcium phosphate-coated titanium plates in rats. *Acta Biomaterialia* 5:776–784

**WANG GX**, Shen Y, Zhang H, Quan XJ, Yu QS (2008a). Influence of surface microroughness by plasma deposition and chemical erosion followed by TiO<sub>2</sub> coating upon anticoagulation, hydrophilicity, and corrosion resistance of NiTi alloy stent. *Journal of Biomedical Materials Research Part A* 85:1096–1102

**WANG X**, Lennartz MR, Loegering DJ, Stenken JA (2008b). Multiplexed cytokine detection of interstitial fluid collected from polymeric hollow tube implants - a feasibility study. *Cytokine* 43:15–19

**WILLIAMS DF** (1987). Definitions in Biomaterials. Proceedings of a Consensus Conference of the European Society for Biomaterials. Elsevier, Amsterdam und New York; S. 1–72

**WILLIAMS DF** (1999). The Williams Dictionary of Biomaterials. Liverpool University Press, Liverpool; S. 40–42

**WILLIAMS DF** (2001). The golden anniversary of titanium biomaterials. *Medical Device Technology* 12:8–11

**WILLIAMS DF** (2008). On the mechanisms of biocompatibility. *Biomaterials* 29:2941–2953

**WILLIAMS DF** (2009). On the nature of biomaterials. *Biomaterials* 30:5897– 5909

**XIA Z & TRIFFITT T** (2006). A review on macrophage responses to biomaterials. *Biomedical Materials* 1:R1–9

**YE SH**, Johnson CA Jr, Woolley JR, Oh HI, Gamble LJ, Ishihara K, Wagner WR (2009). Surface modification of a titanium alloy with a phospholipid polymer prepared by a plasma-induced grafting technique to improve surface thromboresistance. *Colloids and Surfaces B: Biointerfaces* 74:96–102

**ZHAO JH**, Michalski WP, Williams C, Li L, Xu HS, Lamb PR, Jones S, Zhou YM, Dai XJ (2011). Controlling cell growth on titanium by surface functionalization of heptylamine using a novel combined plasma polymerization mode. *Journal of Biomedical Materials Research Part A* 87:127–134

**ZIPPEL R**, Wilhelm L, Hoene A, Walschus U, Ueberrueck T, Schlosser M (2008). Local tissue reaction and differentiation of the prosthesis-specific antibody response following functional implantation of vascular grafts in pigs. *Journal of Biomedical Materials Research Part B: Applied Biomaterials* 85:334–342

# 5

## Anhang

### 5.1 Eidesstattliche Erklärung

Hiermit erkläre ich, dass ich die vorliegende Dissertation selbständig verfasst und keine anderen als die angegebenen Hilfsmittel benutzt habe.

Die Dissertation ist bisher keiner anderen Fakultät und keiner anderen wissenschaftlichen Einrichtung vorgelegt worden.

Ich erkläre, dass ich bisher kein Promotionsverfahren erfolglos beendet habe und dass eine Aberkennung eines bereits erworbenen Doktorgrades nicht vorliegt.

---

Ort, Datum

---

Unterschrift

## **5.2 Lebenslauf**

Entsprechend §16(2) der Promotionsordnung der Universitätsmedizin der Ernst-Moritz-Arndt-Universität Greifswald vom 3. Februar 2011 ist der Lebenslauf in der zur Veröffentlichung der Dissertation vorgesehenen Fassung für die Pflichtexemplare und die elektronische Version nicht enthalten.

## 5.3 Publikationsliste

### 5.3.1 Originalarbeiten

1. **Walschus U**, Witt S, Wittmann C (2002). Development of monoclonal antibodies against Cry1Ab protein from *Bacillus thuringiensis* and their application in an ELISA for detection of transgenic Bt-maize. *Food and Agricultural Immunology* 14:231–240
2. Zippel R, Hoene A, **Walschus U**, Jarchow T, Ueberrueck T, Patrzyk M, Schlosser M, Wilhelm L (2006). Digital image analysis for morphometric evaluation of tissue response after implanting alloplastic vascular prostheses. *Microscopy and Microanalysis* 12:366–375
3. Schlosser M, **Walschus U**, Klöting I, Walther R (2008). Determination of glutamic acid decarboxylase (GAD65) in pancreatic islets and its in vitro and in vivo degradation kinetics in serum using a highly sensitive enzyme immunoassay. *Disease Markers* 24:191–198
4. **Walschus U**, Goldmann H, Ueberrueck T, Hoene A, Wilhelm L, Schlosser M (2008). Evaluation of the biocompatibility of a new vascular prosthesis coating by detection of prosthesis-specific antibodies. *Journal of Materials Science: Materials in Medicine* 19:1595–1600
5. Zippel R, Wilhelm L, Hoene A, **Walschus U**, Ueberrueck T, Schlosser M (2008). Local tissue reaction and differentiation of the prosthesis-specific antibody response following functional implantation of vascular grafts in pigs. *Journal of Biomedical Materials Research Part B: Applied Biomaterials* 85:334–342
6. **Walschus U**, Hoene A, Neumann HG, Wilhelm L, Lucke S, Lüthen F, Rychly J, Schlosser M (2009). Morphometric immunohistochemical examination of the inflammatory tissue reaction after implantation of calcium phosphate-coated titanium plates in rats. *Acta Biomaterialia* 5:776–784
7. Hoene A, **Walschus U**, Patrzyk M, Finke B, Lucke S, Nebe B, Schröder K, Ohl A, Schlosser M (2010). In vivo investigation of the inflammatory response against allylamine plasma polymer coated titanium implants in a rat model. *Acta Biomaterialia* 6:676–683
8. Schröder K, Finke B, Ohl A, Lüthen F, Bergemann C, Nebe B, Rychly J, **Walschus U**, Schlosser M, Liefeth K, Neumann HG, Weltmann KD (2010). Capability of differently charged plasma polymer coatings for control of tissue interactions with titanium surfaces. *Journal of Adhesion Science and Technology* 24:1191–1205
9. Patrzyk M, Hoene A, Jarchow R, Wilhelm L, **Walschus U**, Zippel R, Schlosser M (2010). Time course of fibronectin in the peri-implant tissue and neointima formation after functional implantation of polyester-based vascular prostheses with different porosity in pigs. *Biomedical Materials* 5:055003

10. Walschus U, Hoene A, Kochanowski A, Neukirch B, Patrzyk M, Wilhelm L, Schröder K, Schlosser M (2011). Quantitative immunohistochemical examination of the local cellular reactions following implantation of biomaterials. *Journal of Microscopy* 242:94–99
11. Kochanowski A, Hoene A, Patrzyk M, **Walschus U**, Finke B, Luthringer B, Feyerabend F, Willumeit R, Lucke S, Schlosser M (2011). Examination of the inflammatory response following implantation of titanium plates coated with phospholipids in rats. *Journal of Materials Science: Materials in Medicine* 22:1015–1026
12. **Walschus U**, Hoene A, Patrzyk M, Finke B, Polak M, Lucke S, Nebe B, Schröder K, Podbielski A, Wilhelm L, Schlosser M (2012). Serum profile of pro- and anti-inflammatory cytokines in rats following implantation of low temperature plasma-modified titanium plates. *Journal of Materials Science: Materials in Medicine* 23:1299–1307
13. Hoene A, Patrzyk M, **Walschus U**, Straňák V, Hippler R, Testrich H, Meichsner J, Finke B, Rebl H, Nebe B, Zietz C, Bader R, Podbielski A, Schlosser M (2013). In vivo examination of the local inflammatory response after implantation of Ti6Al4V samples with a combined low-temperature plasma treatment using pulsed magnetron sputtering of copper and plasma-polymerized ethylenediamine. *Journal of Materials Science: Materials in Medicine* 24:761–771
14. Hoene A, Prinz C, **Walschus U**, Lucke S, Patrzyk M, Wilhelm L, Neumann HG, Schlosser M (2013). In vivo evaluation of copper release and acute local tissue reactions after implantation of copper-coated titanium implants in rats. *Biomedical Materials* 8:035009

### 5.3.2 Buchbeiträge

1. Luderer F, **Walschus U** (2005). Immobilization of oligonucleotides for biochemical sensing by self-assembled monolayers: Thiol-organic bonding on gold and silanization on silica surfaces. In: Wittmann C (Hrsg.): Immobilization of DNA on Chips I. Reihe: *Topics in Current Chemistry*. Band 260. Springer, Berlin und New York; S. 37–56
2. **Walschus U**, Schröder K, Finke B, Nebe B, Meichsner J, Hippler R, Bader R, Podbielski A, Schlosser M (2011). Application of low-temperature plasma processes for biomaterials. In: Pignatello R (Hrsg.): Biomaterials Applications for Nanomedicine. InTech, Rijeka und Wien; S. 127–142

## **5.4 Danksagung**

Für die Überlassung des Themas, die herausragende Betreuung und für das fortwährend in mich gesetzte Vertrauen danke ich Herrn PD Dr. Michael Schlosser von ganzem Herzen. Auch Dr. Silke Lucke, deren langjährige Erfahrungen im Bereich der Histologie große Teile dieser Arbeit wesentlich erleichtert haben, gilt mein herzlicher Dank. Kirsten Tornow möchte ich dafür danken, dass sie mir, nicht nur im Labor, bei allen großen und kleinen Problemen stets mit Herz, Rat und Tat zur Seite stand.

Den Chirurgen OA Dr. Andreas Hoene und OA Dr. Maciej Patrzyk (Chirurgische Universitätsklinik Greifswald) sowie CA Dr. Lutz Wilhelm (Kreiskrankenhaus Demmin) danke ich für ihre Mitarbeit bei den tierexperimentellen Arbeiten sowie ihre Beiträge zur Erstellung der Publikationen.

Dem Direktor des Instituts für Medizinische Biochemie und Molekularbiologie Herrn Prof. Reinhard Walther gilt mein Dank für die jederzeit gewährte Unterstützung. Herrn Prof. Dr. Heinrich Brinkmeier, Direktor des Instituts für Pathophysiologie, danke ich für die Möglichkeit zur Nutzung der Labore und Räumlichkeiten des Instituts in Karlsruhe.

Die Ergebnisse dieser Arbeit entstanden im Rahmen von zwei Drittmittelprojekten (VH-MV1 „Regenerative Medizin“ und 13N9779 „Campus PlasmaMed“). Den Mitarbeitern der beteiligten Arbeitsgruppen, insbesondere allen Mitautoren der dieser Arbeit zugrunde liegenden Veröffentlichungen, danke ich herzlich für die vertrauensvolle Zusammenarbeit. Dies betrifft insbesondere Dr. Karsten Schröder und Dr. Birgit Finke vom Greifswalder Leibniz-Institut für Plasmaforschung und Technologie und ihre Aktivitäten zur Etablierung der untersuchten Niedertemperaturplasma-Prozesse. Dem Andenken an Karsten, der im August 2011 unerwartet im Alter von nur 47 Jahren verstarb, ist diese Arbeit gewidmet.

Meiner Mutter danke ich für ihren Rückhalt, ihre Geduld und ihren Optimismus im Hinblick auf das Gelingen dieser Arbeit.

## 5.5 Beigefügte Veröffentlichungen

Die Ergebnisse dieser Arbeit sind in den folgenden vier Veröffentlichungen in begutachteten wissenschaftlichen Zeitschriften erschienen.

**Walschus U, Hoene A, Kochanowski A, Neukirch B, Patrzyk M, Wilhelm L, Schröder K, Schlosser M** (2011). Quantitative immunohistochemical examination of the local cellular reactions following implantation of biomaterials. *Journal of Microscopy* 242:94–99

Schröder K, Finke B, Ohl A, Lüthen F, Bergemann C, Nebe B, Rychly J, **Walschus U**, Schlosser M, Liefelth K, Neumann HG, Weltmann KD (2010). Capability of differently charged plasma polymer coatings for control of tissue interactions with titanium surfaces. *Journal of Adhesion Science and Technology* 24:1191–1205

Hoene A, **Walschus U**, Patrzyk M, Finke B, Lucke S, Nebe B, Schröder K, Ohl A, Schlosser M (2010). In vivo investigation of the inflammatory response against allylamine plasma polymer coated titanium implants in a rat model. *Acta Biomaterialia* 6:676–683

**Walschus U, Hoene A, Patrzyk M, Finke B, Polak M, Lucke S, Nebe B, Schröder K, Podbielski A, Wilhelm L, Schlosser M** (2012): Serum profile of pro- and anti-inflammatory cytokines in rats following implantation of low-temperature plasma-modified titanium plates. *Journal of Materials Science: Materials in Medicine* 23:1299–1307

Eine zusammenfassende Darstellung der Anwendung von Niedertemperaturplasmen für Biomaterialien, die auch auf Ergebnisse der vorliegenden Arbeit eingeht, wurde darüber hinaus in Form des folgenden Buchbeitrags veröffentlicht.

**Walschus U, Schröder K, Finke B, Nebe B, Meichsner J, Hippler R, Bader R, Podbielski A, Schlosser M** (2011). Application of low-temperature plasma processes for biomaterials. In: Pignatello R (Hrsg.): Biomaterials Applications for Nanomedicine. InTech, Rijeka und Wien; S. 127–142

Die vier genannten Veröffentlichungen sowie der Buchbeitrag sind der Arbeit im Folgenden als Anhang beigefügt.

# Quantitative immunohistochemical examination of the local cellular reactions following implantation of biomaterials

U. WALSCHUS<sup>\*#</sup>, A. HOENE<sup>†#</sup>, A. KOCHANOWSKI<sup>\*</sup>,  
B. NEUKIRCH<sup>\*</sup>, M. PATRZYK<sup>†</sup>, L. WILHELM<sup>‡</sup>,  
K. SCHRÖDER<sup>§</sup> & M. SCHLOSSER<sup>\*</sup>

<sup>\*</sup>Research Group of Predictive Diagnostics of the Department of Medical Biochemistry and Molecular Biology, Ernst Moritz Arndt University Greifswald, Karlsburg, Germany

<sup>†</sup>Department of Surgery, Ernst Moritz Arndt University Greifswald, Greifswald, Germany

<sup>‡</sup>Department of Surgery, Hospital Demmin, Demmin, Germany

<sup>§</sup>Leibniz Institute for Plasma Science and Technology (INP), Greifswald, Germany

**Key words.** Biomaterials, digital image analysis, immunohistochemistry, implantation.

## Summary

Examining the biocompatibility of implant materials includes the *in vivo* investigation of the local tissue response following implantation in experimental animals. By contrast to qualitative and semi-quantitative approaches often used in this field, a quantitative technique would facilitate a more accurate determination and better comparability of different studies. Therefore, this study aimed at evaluating the applicability of the free image analysis software IMAGEJ for fast, easy and reproducible quantification of the tissue response following implantation of titanium samples in rats with subsequent immunohistochemical examination of peri-implant tissue samples for monocytes and macrophages (ED1) and MHC class II positive antigen presenting cells (OX6). The quantification of positively stained cells in the vicinity of the implant pockets was based on a grid-supported manual count carried out using two IMAGEJ plugins (CellCounter, Grid) and resulted in a mean coefficient of variation of 13.8% (ED1) and 19.6% (OX6) between different investigators and 10.0% (ED1) and 13.8% (OX6) for repeated counting by the same investigator. In conclusion, IMAGEJ was found to be suitable for morphometric evaluation of the tissue response following implantation, particularly the analysis of discrete cellular events at the tissue–biomaterial interface. The procedure which was used is described in detail, and its advantages and disadvantages are discussed.

#These authors have contributed equally to this work.

Correspondence to: Dr. M. Schlosser. Department of Medical Biochemistry and Molecular Biology, Ernst Moritz Arndt University of Greifswald, Greifswalder Str. 11c; D-17495 Karlsburg, Germany. Tel: +49 3834 8619178; fax: +49 3834 8680118; e-mail: schlosse@uni-greifswald.de

## Introduction

Medical implants made from different materials such as metals, polymers and ceramics are widely used in surgery, orthopaedics, dentistry and other fields. The introduction of new or modified materials into clinical practice requires comprehensive examination in a number of *in vitro* as well as *in vivo* tests to assess their biocompatibility, defined as ‘the ability of a material to perform with an appropriate host response in a specific application’ (Williams, 1989). Therefore, a factor of prime importance regarding the biocompatibility is the response of the body following implantation. As all biomaterials are foreign from an immunological point of view, they cause a sequence of local and systemic inflammatory reactions altogether known as the foreign body response. It consists of an acute phase immediately following the implantation and a chronic phase which is maintained as long as the implant is present in the body (Anderson, 1993; Tang & Eaton, 1995).

The intensity and duration of the acute inflammatory reactions as well as the level of the chronic inflammation are measures of the bio(in)compatibility when comparing different materials for the same application or when testing an established material for a new application. Material properties which affect the initial protein absorption as well as cell adhesion and migration, thereby influencing the outcome of implantation, include the chemistry, topography and roughness of the surface (Chilkoti *et al.*, 1995; Marchisio *et al.*, 2005; Pessková *et al.*, 2007). The cellular response after implantation is characterized by tissue damage from the surgical procedure which causes an influx of neutrophils and monocytes into the implant site. Within this context, monocyte-derived macrophages being involved in phagocytosis of cellular debris and foreign materials are

the dominant cell population. Additionally, they release a number of cytokines and other factors (Refai *et al.*, 2004; Suska *et al.*, 2005) which attract other immune cells, smooth vascular muscle cells, fibroblasts and endothelial cells as well as promote fibroblast proliferation, collagen synthesis and the formation of the extracellular matrix (Anderson, 1993; Tang & Eaton, 1995; Pribila *et al.*, 2004). Furthermore, in recent years the differentiation of macrophages into distinctly different phenotypes called pro-inflammatory M1 macrophages and immunomodulatory M2 macrophages, the latter being mainly responsible for tissue remodelling, has been a topic of increasing interest in biomaterials research and other fields (Badylak *et al.*, 2008; Martinez *et al.*, 2008). For quantitative examination of differentially activated and polarized macrophages, digital image analysis methods could especially be useful.

The histological examination, differentiation and quantification of these cell populations are therefore an important part of the *in vivo* examination of the biocompatibility of implant materials. However, most studies published use only qualitative and semi-quantitative approaches to examine the tissue response, limiting the comparability of different studies as well as the accuracy of the results. A quantitative approach using digital image analysis software could help to overcome these problems. Most of these programs such as the ks400 system (Carl Zeiss MicroImaging GmbH, Jena, Germany) used in our previous study (Zippel *et al.*, 2006), its successor AxioVISION and similar systems are costly proprietary solutions which are often hardware locked or bound by license restrictions to a specific microscopy workstation within a lab. As an alternative, the software IMAGEJ is freely available for download from the Internet. It can be installed and used on multiple computers without any limitations and is actively maintained by a large developer and user community. Due to the platform-independent programming language Java, it runs on all popular operating systems including Microsoft Windows, Apple MacOS and Linux. Its open nature and extensive documentation make it easy to extend its capabilities by macros and plugins. Therefore, the aim of this study was to demonstrate the applicability of IMAGEJ for fast, easy and reproducible quantification of the tissue response following implantation of biomaterials. The analysis procedure is based on a grid-supported manual count of positively stained cells in the vicinity of the implant pockets and carried out using two IMAGEJ plugins (CellCounter, Grid). The approach is outlined in a detailed step-by-step manner to help other researchers with using it in their own work.

## Materials and methods

### *In vivo* experiments

Three male Lewis rats received via i.m. implantation into the neck musculature one implant (square plate, 5 × 5 × 1 mm)

made from polished titanium with a surface modified with a plasma-polymerized acrylic acid film. The anaesthesia and surgical procedure as well as the plasma treatment are described in detail elsewhere (Walschus *et al.*, 2008; Schröder *et al.*, 2010). The animals were kept for a post-implantation period of 56 days after which they were killed to remove the implant together with a sample of the surrounding tissue for histological examination of the tissue response. All aspects of the animal experiments were conducted in accordance with the animal protection law of the Federal Republic of Germany in its new version of 1 January 1987, with the principles of care for animals in laboratories (drawn up by the National Society for Medical Research) and with the Guidelines for Keeping and Using Laboratory Animals (NIH Publication No. 80–23, revised 1985).

### Histological examination

Immediately after explantation, the tissue samples were frozen with laboratory freezer spray New Envi-Ro-Tech™ (Thermo Electron Corporation, Pittsburgh, PA, U.S.A.) and then cut using a scalpel with the section plane at right angles with the implants. The implants were carefully removed from the frozen tissue using tweezers. The respective tissue pockets were filled with the embedding medium Shandon Cryomatrix™ (Thermo Electron Corporation). Subsequently, the samples were shock frozen in liquid nitrogen and stored at –80°C until preparation of frozen sections (thickness: 5 µm) using a Cryotome 2800 Frigocut N (Reichert-Jung, Nussloch, Germany). The cryosections were incubated with the monoclonal antibodies ED1 (Dijkstra *et al.*, 1985) for monocytes and macrophages and OX6 (McMaster and Williams, 1979) for MHC class II positive cells (MorphoSys AbD Serotec GmbH, Duesseldorf, Germany) according to the manufacturer's protocols. For detection of positive cells, the alkaline phosphatase anti-alkaline phosphatase method (DakoCytomation GmbH, Hamburg, Germany) was used. To exclude unspecific staining and tissue alkaline phosphatase activity, respective control staining samples were performed in which either the primary antibody, the secondary antibody, both antibodies or the colorimetric substrate were omitted. All samples were examined at a microscope magnification of 125× using a digital image analysis system which consists of a light microscope Jenamed 2 (Carl Zeiss Jena, Jena, Germany), and a colour camera (RGB Camera, CCD-chip 768\*576 Pixel, JVC, Yokohama, Japan) was used to obtain digital images of the microscopic samples.

### Image analysis procedure

The underlying principle of the quantitative image analysis procedure which is outlined in the following is a manual count of positively stained cells in defined areas using the image analysis program IMAGEJ v1.43 (U.S. National Institutes of Health, Bethesda, MD, U.S.A.) and the IMAGEJ plugins Grid and CellCounter. Both plugins are included in the

installation package of recent versions of IMAGEJ but can also be downloaded from external websites for installation on earlier IMAGEJ versions. After starting IMAGEJ, the first step is to load the image via the 'File -> Open' command. Next, a grid is superimposed onto the image using the Grid plugin. In the default IMAGEJ installation, this is performed via the 'Plugins -> Analyse -> Grid' command. In the next window, the square size of the grid (in pixels) has to be chosen for a specific application depending on the resolution of the images and the desired level of coverage. For example, we found a value of 5000 pixels per square for images with a resolution of  $768 \times 576$  and of 20 000 pixels per square for images with a resolution of  $1600 \times 1200$  to be suitable for our purposes. However, the exact choice is up to each user. In the next step, the Plugin CellCounter is called via the 'Plugins -> Analyse -> CellCounter' command. Now the image has to be initialized using the 'Initialize' button of the plugin window, and a counter type must be selected by clicking on one of the counter types in the CellCounter window. For counting positively stained cells, only one counter type is needed and it is sufficient to choose any of the available counter types. Now the positively stained cells are counted by repeated pointing and clicking in the image window. For examining the tissue response after implantation of biomaterials, the approach consists of counting the cells in a defined number of representative grid squares in the vicinity of the implants. Although we have found five squares, corresponding to coverage of about 5% of the total image area with the square size mentioned before, to be suitable for our application, a higher number would increase the coverage of the counted area. For better discrimination of cells in areas with a high background staining it was found to be helpful to modify the brightness and/or contrast of the images via the 'Image -> Adjust -> Brightness/Contrast' command before initialization via the CellCounter plugin.

After finishing the count, the counter window is exported to a new image window via the 'Export Image' button of the CellCounter plugin. In the resulting Markers Counter window, artefacts and other regions within a counted square which did not contain tissue are now marked using the Freehand selections tool of IMAGEJ. This tool can be selected via the fourth button from the left in the main program window. To select multiple areas, the 'Shift' key has to be pressed while drawing the selections. The total selected area is measured by the 'Analyse -> Measure' command. Using a microscopic slide with a printed length scale, the area which corresponds to one pixel can be calculated in micrometre square for a specific microscopic magnification. The final results are calculated as positively stained cells per micrometre square after deducting the excluded area from the total area of the counted grid squares.

#### Statistical data analysis

To examine the reproducibility of the image analysis procedure between different investigators and between different days for the same investigator, the counting was performed by three independent persons. Furthermore, one of the investigators counted the samples three times on different days. To assess the variability between different investigators and between different counts from the same investigator, the respective mean, standard deviation and coefficient of variation (CV) were calculated. Statistical analysis was performed using the software system GraphPad Prism version 4.02 (GraphPad Software, Inc., San Diego, CA, U.S.A.).

#### Results

The results are given in Table 1. For the comparison between the three different investigators, the CV ranged from 6.2%

**Table 1.** Morphometric immunohistochemical analysis of ED1-positive cells (macrophages and monocytes) and OX6-positive cells (MHC class II antigen presenting cells) performed by three different investigators (i1, i2, i3) and by the same investigator (i3) on three different days (c1, c2, c3). Data are number of cells  $10^{-3}$  per  $\mu\text{m}^2$ . For statistical evaluation between different investigators and between different counts from the same investigator, the respective mean and standard deviation (SD) as well as the CV are given.

| Marker: ED1 |       |       |       |       |       | Mean $\pm$ SD (CV)     |
|-------------|-------|-------|-------|-------|-------|------------------------|
| Sample      | i1-c1 | i2-c1 | i3-c1 | i3-c2 | i3-c3 | c1: i1 i2 i3           |
| Rat 1       | 3.05  | 2.20  | 2.54  | 2.88  | 2.20  | $2.60 \pm 0.4$ (16.5%) |
| Rat 2       | 3.32  | 4.66  | 3.52  | 2.96  | 3.29  | $3.83 \pm 0.7$ (18.7%) |
| Rat 3       | 2.40  | 2.62  | 2.33  | 2.65  | 2.71  | $2.45 \pm 0.2$ (6.2%)  |
| Mean        | 2.92  | 3.16  | 2.80  | 2.83  | 2.73  | (13.8%)                |
| Marker: OX6 |       |       |       |       |       | i3: c1 c2 c3           |
| Rat 1       | 1.44  | 1.27  | 1.02  | 0.93  | 1.19  | $1.24 \pm 0.2$ (17.0%) |
| Rat 2       | 1.24  | 0.76  | 1.04  | 1.37  | 1.14  | $1.01 \pm 0.2$ (23.7%) |
| Rat 3       | 1.19  | 0.85  | 0.93  | 0.76  | 1.02  | $0.99 \pm 0.2$ (18.1%) |
| Mean        | 1.29  | 0.96  | 1.00  | 1.02  | 1.12  | (19.6%)                |
|             |       |       |       |       |       | (13.8%)                |

to 18.7% (mean 13.8%) for ED1 samples and from 17.0% to 23.7% (mean 19.6%) for the OX6 samples. The CV for the three different counts from the same investigator was in a range between 8.0% and 13.4% (mean 10.0%) for the ED1 samples and 12.6% and 14.5% (mean 13.8%) for the OX6 samples. Overall, the mean CV for the comparison between different investigators was higher than for the comparison between different counts from the same investigator for both markers. Furthermore, in comparison between the ED1 and the OX6 samples, the mean CV was higher for the lower cell count data (OX6) for the comparison between different investigators as well as for the comparison between different counts from the same investigator. Exemplary immunohistological images for both markers are given in Figure 1.

## Discussion

*In vivo* studies regarding the local tissue response following implantation of biomaterials play an increasingly important role in the development of new or modified implant materials. To compare the results between different materials, studies and laboratories, quantitative approaches are required. Despite this need, such methods were rarely used so far in the field of biomaterial science (Hunt *et al.*, 1996; Burugapalli *et al.*, 2004). One possible reason might be the fact that the necessary digital camera equipment as well as the image analysis software systems available in the market have been quite expensive until some years ago. However, this has changed in recent time with the availability of affordable cameras and, more importantly, the free image analysis software IMAGEJ.

In this paper, the application of IMAGEJ for digital image analysis of immunohistochemically stained images obtained from tissue samples after implantation of biomaterials is presented. The chosen method is based on a manual count in a defined grid-based area, similar to counting cells or bacteria in a microscope counting chamber (haemocytometer). It is therefore a 2D morphometric approach for evaluation of digital images obtained from stained tissue sections. In principle, extrapolation by stereology to obtain 3D data (cell number per volume) could provide more detailed information about the examined tissue reactions, for example about the spatial distribution and density of the inflammatory cells in the peri-implant tissue. However, the data obtained by the method which is described (cell number per tissue section area) nonetheless allow a comparative quantitative examination of different samples, which was the primary aim for the intended applications. The approach presented here was used in studies in which the inflammatory reactions for different materials were examined and compared in course of time (Walschus *et al.*, 2008; Schröder *et al.*, 2010). The results of these studies enabled us to detect statistically significant differences in the cellular responses which are consistent with the intensity of inflammation as assessed by hematoxylin/eosin staining.

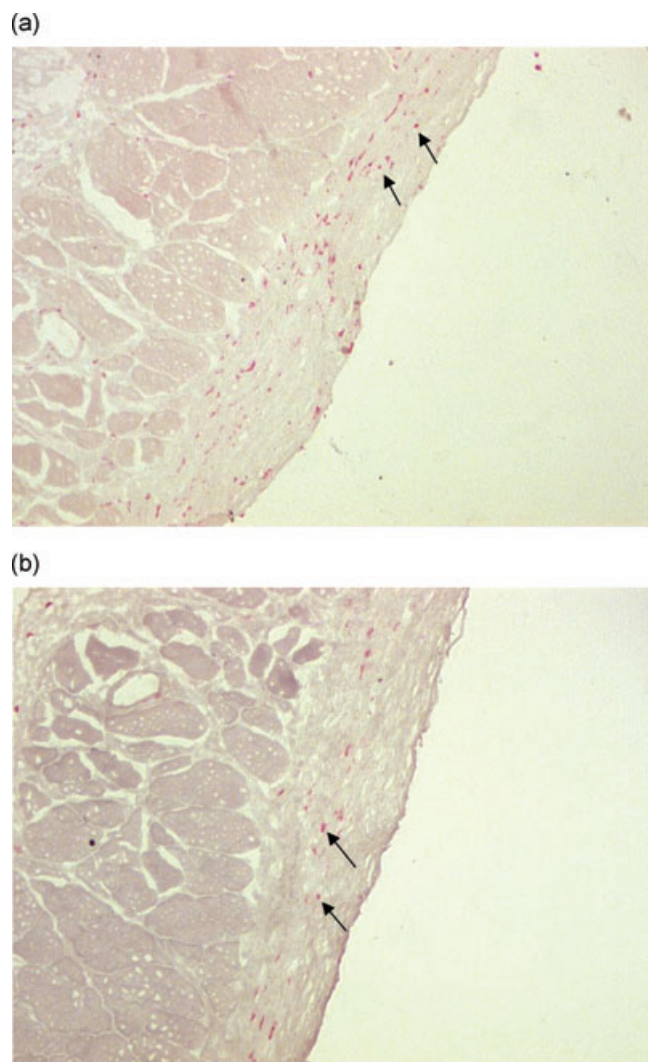


**Fig. 1.** Exemplary immunohistochemical images for the ED1 staining (a) and OX6 staining (b) of cryosections (thickness 5  $\mu\text{m}$ ) using alkaline phosphatase anti-alkaline phosphatase method as detection system (magnification: 125 $\times$ ). The samples were prepared from the peri-implant tissue after implantation of titanium plates in rats for 56 days. Black arrows indicate positively stained cells.

Although the chosen approach might seem to be prone to subjective factors, we found a good level of reproducibility for the same investigator as well as between different investigators. The mean CV was 13.8% (ED1, total monocytes and macrophages) and 19.6% (OX6, MHC class II positive antigen presenting cells) between different investigators and 10.0% (ED1) and 13.8% (OX6) for repeated counting by the same investigator. The OX6 samples had a higher level of variation because the number of positive cells in these samples was lower, resulting in a higher relative influence of variations in the absolute numbers. Although we routinely examine our experimental samples with two investigators, it might be advisable to use three investigators for other

applications. Furthermore, the level of subjectivity could be further reduced by increasing the coverage of the examined area using a higher grid square size or a higher number of grid squares. Both of these measures could be especially helpful for images with relatively low numbers of positively stained cells such as the OX6 samples as discussed above. The deviation between the results from different investigators could also be minimized by analysing a series of test images followed by an examination of the reasons for possible discrepancies. From our experience, the main reasons for a high discordance and therefore subjectiveness are differences regarding the selection of squares as well as differences regarding the counting of cell accumulations in which the staining of cells overlaps. Working out common standards regarding these aspects and other reasons for discrepancies by analysing a test series helps to reduce the deviation between different investigators.

In a previous study, we used the ks400 software system for a nearly fully-automatic processing of images (Zippel *et al.*, 2006). This was based on segmentation of the colour image to a binary image using a threshold which defined the difference for positive staining. This thresholding process was performed manually as automatic thresholding requires images with sufficient colour differences between positively stained areas and the surrounding tissue as well as a comparable staining intensity between different images. The process of adjusting the threshold level manually has to be performed for each individual image and thus is also affected by subjective judgement of the investigator. It therefore depends on the characteristics of the samples and staining whether a thresholding-based approach or a manual counting is better suited for the specific application. As long as no adjustment of brightness and contrast is necessary, experienced investigators are able to perform the manual counting procedure in a straightforward manner with a sufficient level of throughput for low or moderate cell numbers. However, a threshold-based near-fully automated approach is advantageous for samples with a high cell number, diffusely expressed markers or when the number of positively stained cells should be expressed relative to the total number of cells (Zippel *et al.*, 2006). Images with an insufficient difference between positively stained cells and the surrounding tissue, for example due to high background staining, are problematic with both methods. Moreover, it is difficult or impossible to process them by manual or automatic segmentation. On the other hand, manually adjusting brightness and contrast to differentiate positively stained cells from the background staining is time consuming and not always successful.

In conclusion, the manual procedure for counting stained cells in immunohistochemical images as presented in this paper was found to be a reproducible, flexible and versatile method for the quantitative examination of the local inflammatory response following implantation of biomaterials. Whether the method is suitable for a specific application depends on the exact characteristics of the

respective samples. As discussed before, analysing samples with very low cell numbers could require additional efforts to get statistically sound results. On the other hand, the method has its limits for samples with very high cell numbers for which a near-automatic approach based on colour thresholding might be more suitable to save time. However, due to the open and free nature of IMAGEJ it should easily be possible to test the suitability of this method and to adapt it for analysis of histological samples from other fields of application with little or no modification.

### Acknowledgements

We are grateful to Kirsten Tornow for excellent technical support. This study was supported by the Federal state of Mecklenburg-Vorpommern and the Helmholtz Association of German Research Centres (grant no. VH-MV1) and by the Federal Ministry of Education and Research (grant no. 13N9779, Campus PlasmaMed).

### References

- Anderson, J.M. (1993) Mechanisms of inflammation and infection with implanted devices. *Cardiovasc. Pathol.* **2**, 33–41.
- Badylak, S.F., Valentin, J.E., Ravindra, A.K., McCabe, G.P. & Steward-Akers, A.M. (2008) Macrophage phenotype as a determinant of biologic scaffold remodeling. *Tissue Eng. A* **14**, 1835–1842.
- Burugapalli, K., Koul, V. & Dinda, A.K. (2004) Effect of composition of interpenetrating polymer network hydrogels based on poly(acrylic acid) and gelatin on tissue response: a quantitative in vivo study. *J. Biomed. Mater. Res. A* **68**, 210–218.
- Chilkoti, A., Schmierer, A.E., Perez-Luna, V.H. & Ratner, B.D. (1995) Investigating the relationship between surface chemistry and endothelial cell growth: partial least squares regression of the static secondary ion mass spectra of oxygen containing plasma deposited films. *Anal. Chem.* **67**, 2883–2891.
- Dijkstra, C.D., Dopp, E.A., Joling, P. & Kraal, G. (1985) The heterogeneity of mononuclear phagocytes in lymphoid organs: distinct macrophage subpopulations in the rat recognized by monoclonal antibodies ED1, ED2 and ED3. *Immunology* **54**, 589–599.
- Hunt, J.A., Flanagan, B.F., McLaughlin, P.J., Strickland, I. & Williams, D.F. (1996) Effect of biomaterial surface charge on the inflammatory response: evaluation of cellular infiltration and TNF alpha production. *J. Biomed. Mater. Res.* **31**, 139–144.
- Marchisio, M., Di Carmine, M., Pagone, R., Piattelli, A. & Mischia, S. (2005) Implant surface roughness influences osteoclast proliferation and differentiation. *J. Biomed. Mater. Res. B Appl. Biomater.* **75**, 251–256.
- Martinez, F.O., Sica, A., Mantovani, A. & Locati, M. (2008) Macrophage activation and polarization. *Front. Biosci.* **13**, 453–461.
- McMaster, W.R. & Williams, A.F. (1979) Identification of Ia glycoproteins in rat thymus and purification from rat spleen. *Eur. J. Immunol.* **9**, 426–433.
- Pessková, V., Kubies, D., Hulejová, H. & Himmlová, L. (2007) The influence of implant surface properties on cell adhesion and proliferation. *J. Mater. Sci. Mater. Med.* **18**, 465–473.
- Pribila, J.T., Quale, A.C., Mueller, K.L. & Shimizu, Y. (2004) Integrins and T cell-mediated immunity. *Ann. Rev. Immunol.* **22**, 157–180.

- Refaï, A.K., Textor, M., Brunette, D.M. & Waterfield, J.D. (2004) Effect of titanium surface topography on macrophage activation and secretion of proinflammatory cytokines and chemokines. *J. Biomed. Mater. Res. A* **70**, 194–205.
- Schröder, K., Finke, B., Ohl, A. *et al.* (2010) Capability of differently charged plasma polymer coatings for control of tissue interactions with titanium surfaces. *J. Adhes. Sci. Technol.* **24**, 1191–1205.
- Suska, F., Gretzer, C., Esposito, M., Emanuelsson, L., Wennerberg, A., Tengvall, P. & Thomsen, P. (2005) In vivo cytokine secretion and NF- $\kappa$ B activation around titanium and copper implants. *Biomaterials* **26**, 519–527.
- Tang, L. & Eaton, J.W. (1995) Inflammatory responses to biomaterials. *Am. J. Clin. Pathol.* **103**, 466–471.
- Walschus, U., Hoene, A., Neumann, H.-G. *et al.* (2008) Morphometric immunohistochemical examination of the inflammatory tissue reaction after implantation of calcium phosphate-coated titanium plates in rats. *Acta Biomater.* **5**, 776–784.
- Williams, D.F. (1989) A model for biocompatibility and its evaluation. *J. Biomed. Eng.* **11**, 185–191.
- Zippel, R., Hoene, A., Walschus, U. *et al.* (2006) Digital image analysis for morphometric evaluation of tissue response after implanting alloplastic vascular prostheses. *Microsc. Microanal.* **12**, 366–375.

# Capability of Differently Charged Plasma Polymer Coatings for Control of Tissue Interactions with Titanium Surfaces

**K. Schröder<sup>a,\*</sup>, B. Finke<sup>a</sup>, A. Ohl<sup>a</sup>, F. Lüthen<sup>b</sup>, C. Bergemann<sup>b</sup>, B. Nebe<sup>b</sup>, J. Rychly<sup>b</sup>, U. Walschus<sup>c</sup>, M. Schlosser<sup>c</sup>, K. Liefelth<sup>d</sup>, H.-G. Neumann<sup>e</sup> and K.-D. Weltmann<sup>a</sup>**

<sup>a</sup> Leibniz Institute for Plasma Science and Technology (INP), F.-Hausdorff Straße 2,  
17489 Greifswald, Germany

<sup>b</sup> University of Rostock, Medical Faculty, Laboratory of Cell Biology, Schillingallee 69,  
18057 Rostock, Germany

<sup>c</sup> University of Greifswald, Department of Medical Biochemistry and Molecular Biology,  
Greifswalder Str. 11c, 17495 Karlsburg, Germany

<sup>d</sup> Institute for Bioprocessing and Analytical Measurement Techniques, Rosenhof,  
37308 Heilbad Heiligenstadt, Germany

<sup>e</sup> DOT GmbH, Charles-Darwin-Ring 1a, 18059 Rostock, Germany

Received in final form 10 December 2009

## Abstract

Titanium surfaces were equipped with positively and negatively charged chemical functional groups by plasma polymerization. Their capability to influence the adhesion of human mesenchymal stem cells (hMSCs) and inflammation processes was investigated on titanium substrates, which are representative of real implant surfaces.

For these purposes, titanium samples were coated with plasma polymers from allylamine (PPAAm) and acrylic acid (PPAAC). The process development was accompanied by physicochemical surface analysis using XPS, FT-IR and contact angle measurements. Very thin plasma polymer coatings were created, which are resistant to hydrolysis and delamination. Positively charged amino groups improve considerably the initial adhesion and spreading steps of hMSCs. PPAAm and PPAAC surfaces have an effect on the differentiation of hMSCs, e.g., the expression of osteogenic markers in dependence on culturing conditions. Acrylic acid groups appear to stimulate early mRNA differentiation markers (ALP, COL, Runx2) under basal conditions, whereas positively and negatively charged groups both stimulate late differentiation markers, like BSP and OCN, after 3 days of osteogenic stimulation.

Long-term intramuscular implantation in rats revealed that PPAAC surfaces caused significantly stronger reactions by macrophages and antigen-presenting cells compared to untreated control (polished titanium) samples, while PPAAm films did not show a negative influence on the inflammatory reaction after implantation.

© Koninklijke Brill NV, Leiden, 2010

\* To whom correspondence should be addressed. Tel.: +49 3834 554 428; Fax: +49 3834 554 301; e-mail: schroeder@inp-greifswald.de

**Keywords**

Plasma polymer, microwave plasma, amino functionalization, carboxylic acid functionalization, human stem cells (hMSCs), *in vivo* investigations

## 1. Introduction

Today, metallic implants, especially made from titanium (Ti) and its alloys, are the state of the art in bone replacement surgery [1]. Correspondingly, continued improvement of tissue integration of implants is of great interest and many different surface modifications have been developed following this intention [2]. Within this development, there exists a special, growing interest in chemical surface modifications of pure titanium surfaces. Although natural oxide-covered titanium surfaces exhibit remarkable inherent interface biocompatibility, it is expected that a controlled shift of the interface chemistry from the naturally inorganic towards an organic character could be useful. Simply speaking, except for variations of the titanium oxides crystallographic constitution and of the density of the surface terminal hydroxyl groups, possibilities for major chemical modifications of the oxide surface itself are limited. Introduction of organic chemical groups can appreciably change this situation. There is a vast spectrum of available organic chemical groups encompassing inert groups such as hydrocarbons, fluoro(hydro)carbons CC<sub>x</sub>, CH<sub>x</sub> and –CF<sub>x</sub> groups, bioactive groups like C–OH, C=O, C–NH<sub>2</sub> and –COOH as well as bioactive coatings which may stimulate cell behavior. In any case, surfaces covered with organic groups can be expected to be more suited to living tissue. Indeed, it was demonstrated that such groups can influence implant integration. For example, Kamath *et al.* [3] reported on the influence of hydroxyl, carbonyl, amino and carboxylic acid groups fixed onto polypropylene particles on host tissue fibrotic reactions. A detailed description of the different modification approaches would be beyond the scope of this contribution. The interested reader is referred to the literature (see, e.g., [2, 4]).

Here we focus on the topic of gas discharge plasma-assisted chemical surface modification. Deposition of nanometer-thin, so-called plasma polymers, is a convenient method to attach organic groups onto surfaces, regardless of the chemical composition of the substrate. This is of great interest for titanium since its surface chemistry is strongly dominated by its high oxygen affinity. As a consequence, it is difficult to control surface charging in aqueous biological environments. As will be shown here, despite the existing, favourable, slightly negative natural surface charge of titanium such an opportunity could be helpful for further tuning of surface biocompatibility. Surface charges exert an overall control on protein attachment from liquids to surfaces, as it will be the case in the initial phase of implant integration.

The most interesting organic groups suitable for cell- and tissue-adhesion are carboxyls and amines. Due to their dominant share in the structure of proteins they are favoured for biointerface improvement *in vitro*. While carboxyls lead to negative surface charges, amines are strongly basic at biological pH of 7.5, leading to positive surface charges.

Carboxylated surfaces are reported to be a convenient platform for the immobilization of cell adhesion molecules (CAMs), cell-stimulating molecules like insulin or cytokines or fatty acids, sugars, or proteins to trigger cell behavior on artificial surfaces. A useful plasma-assisted approach to carboxylation is plasma polymerization of acrylic acid in RF-plasmas [5–7]. This precursor is reported to result in plasma polymers with more linear chain structure and, therefore, higher carboxylic group densities than other plasma polymers. The reason is a noticeable tendency for thermally induced polymerization [5, 8, 9]. High fragmentation at high discharge power of RF plasmas results in greater cross-linking which is reported to be the basic prerequisite for stable films [10–12]. Indeed, films insoluble in aqueous environments could be obtained under such conditions, but with a decreased COOH group density. The fraction of O=C=O groups in the C<sub>1s</sub> XPS-peak lies between 4% at high discharge power (20 W) and 22% at low power (2 W) [13].

Titanium surfaces equipped with amino groups are considered to be beneficial for the interaction with hyaluronan [14]. Hyaluronic acid is a substance of the extracellular matrix, which plays a key role in the initial adhesion of osteoblasts to artificial surfaces. Several research groups [15–17] have reported on plasma polymerized allylamine by pulsed low-pressure RF-plasmas. High densities of amino groups were obtained along with structure retention of the monomer due to less fragmentation under very mild plasma conditions. Probably, this effect is due to the double bonds in allylamine which encourages deposition by a combination of plasma polymerization and conventional free-radical polymerization [8]. Comparable to plasma polymerized acrylic acid coatings, the problem of solubility occurs for plasma polymers of allylamine prepared under inappropriate conditions [8]. Water-stable aminofunctionalized surfaces are reported to be advantageous for the improvement of the adhesion of different cells to polymer materials, for instance human skin fibroblasts to poly(ethylene terephthalate) (PET) membranes and silicones [18, 19] and Chinese hamster ovary (CHO) cells [20, 21].

In the context of improvement of titanium implant surfaces, success has to be demonstrated stepwise: first the technical usefulness of the modification, i.e., stability and appropriate composition, then by *in vitro* and *in vivo* tests. *In vitro* tests, as a matter of course, must be performed using the appropriate cell types. Actually, osteoblasts and human mesenchymal stem cells (hMSCs) are most important in this context. Our results showed that osteoblasts adhere to and proliferate on microwave plasma polymers of allylamine on titanium more as compared to pure or cleaned titanium [14, 22, 23]. This promises improvement of bone ingrowth. Stimulation of human mesenchymal stem cells (hMSCs) promises a new way for bone regeneration. A very important point concerning the use of hMSCs is control of their differentiation behavior. In this regard, surface functional groups and surface charges may play a decisive role. This was demonstrated using a model system of silane-modified glass surfaces with self-assembled monolayers presenting –CH<sub>3</sub>, –NH<sub>2</sub>, –SH, –OH and –COOH functional groups [24, 25]. The –CH<sub>3</sub> surfaces maintained the hMSC phenotype. The NH<sub>2</sub>- and SH-modified surfaces promoted

and maintained osteogenesis both in the presence and absence of biological stimuli. Unfortunately, there are still open questions concerning the results. In another investigation, an osteogenic differentiation on aminofunctionalized polypropylene foil was found [26].

In the present contribution, we report on investigations which were carried out to tentatively evaluate the possibility of using differently charged plasma polymer coatings for improvement of implant integration. Special emphasis was given to observe a wide range of relevant aspects, including materials chemical properties, specific stimulation of human mesenchymal stem cells (hMSCs) to evolve into osteoblasts, and inflammatory reactions *in vivo*.

## 2. Materials and Methods

### 2.1. Surface Functionalization of Titanium

Polished titanium discs (TiP) (99+% purity) were employed throughout these investigations with an arithmetic mean roughness ( $R_a$ ) of 0.19  $\mu\text{m}$ .

For thin film preparation, substrates were treated in a microwave plasma reactor V55G (2.45 GHz; Plasma Finish, Schwedt, Germany) in a downstream position (9 cm from the microwave coupling window) with respect to a disc-like planar plasma of about 2 cm thickness. At first, TiP was cleaned and activated by continuous wave (cw) low pressure oxygen plasma (500 W, 50 Pa, 100 sccm  $\text{O}_2$ /25 sccm Ar, 60 s). Then, coating was performed using either allylamine ( $\text{H}_2\text{C}=\text{CH}-\text{CH}_2-\text{NH}_2$ ) or acrylic acid ( $\text{H}_2\text{C}=\text{CH}-\text{COOH}$ ) as the monomers in argon carrier gas. Thin layers (<100 nm) of plasma polymerized allylamine (TiP-PPAAm) or acrylic acid (TiP-PPAAC) were deposited using pulsed discharges with different ‘plasma on’ times and duty cycles (DC). DC is the ratio of plasma  $t_{\text{on}}$  divided by the overall pulse duration  $t_{\text{on}} + t_{\text{off}}$ . (TiP-PPAAm: DC = 0.15; total pulse length of 2 s and TiP-PPAAC: DC = 0.5; total pulse length of 100 ms.) A liquid handling system allowed exact dosing of the precursors, allylamine or acrylic acid, by a calibrated needle valve ( $84 \pm 11 \text{ mg/min}$ ).

### 2.2. Physicochemical Surface Characterization

#### 2.2.1. XPS

X-ray photoelectron spectra were recorded with an Axis Ultra spectrometer (Kratos, Manchester, UK). Irradiation by monochromatic Al  $K_\alpha$  line at 1486 eV (150 W) was used for the determination of the elemental surface composition and chemical binding properties. Spectra were recorded with a pass energy of 80 eV for the estimation of the elemental composition and of 10 eV for highly resolved  $\text{C}_{1s}$  and  $\text{N}_{1s}$  peaks (i.e., for binding properties). Each reported surface composition value represents an average over three XPS measurements. The C–C/C–H component (abbreviated in Fig. 2 as C–C) of the  $\text{C}_{1s}$  peak was adjusted to 285.0 eV [27]. The other components of the  $\text{C}_{1s}$  peak were assigned to known values [27] as follows: Amines ( $\text{C}-\text{NH}$ ) at  $285.7 \pm 0.1 \text{ eV}$ ; hydroxyls, ethers and imines ( $\text{C}-\text{O}$ ), at

$286.6 \pm 0.2$  eV; aldehydes, ketones and amides ( $\text{C}=\text{O}$ ) at  $288.0 \pm 0.3$  eV; and esters and acids ( $\text{O}-\text{C}=\text{O}$ ) at  $289.2 \pm 0.2$  eV. Amino groups were labeled by reaction with 4-trifluoromethyl-benzaldehyde (TFBA) at  $40^\circ\text{C}$  in a saturated gas phase for 2 h [14].

#### 2.2.2. FT-IR

TiP-PPAAm and TiP-PPAAC films were further investigated by Fourier-Transform-Infrared Spectroscopy using the diamond ATR-unit of the FT-IR spectrometer Spectrum One (Perkin-Elmer, Rodgau-Jügesheim, Germany). The sensitivity of the FT-IR equipment was improved by using Au sputter-coated small polystyrene discs as substrates for plasma polymer deposition.

#### 2.2.3. Water Contact Angle

Water contact angles were measured by the sessile drop method using a contact angle meter DIGIDROP (GBX Instrumentation Scientifique, France). At least five measurements were averaged. Values are given as arithmetic means with standard deviations (SD).

#### 2.2.4. Zeta Potential

Zeta potential measurements were carried out by means of an Electrokinetic Analyzer (A. Paar KG, Ostfildern, Germany). The measurements were performed in 0.001 M potassium chloride (KCl) solution at pH 6. Poly(diallyldimethyl ammonium chloride) was used as reference surface with a positive zeta potential.

#### 2.2.5. Film Stability

The stability of films against water was studied by sonication of the samples in an ultrasonic bath (Transsonic T570H, HF-frequency 35 kHz, Elma, Singen, Germany) using ultra-pure water for 10 min. XPS analyses were performed to investigate the changes in the surface composition.

#### 2.2.6. Investigations with a Quartz Crystal Microbalance

The overall attraction of proteins from physiological liquids was measured with a quartz crystal microbalance with dissipation monitoring (D 300, Q-Sense, Göteborg, Sweden). DMEM cell culture medium (GIBCO, Invitrogen, Karlsruhe, Germany) supplemented with 10% fetal calf serum (FCS) ('GOLD', PAA Laboratories, Coelbe, Germany) was taken as an example of a biological liquid.

### 2.3. Culture of Human Mesenchymal Stem Cells (hMSCs)

Human mesenchymal stem cells (6000 cells/cm<sup>2</sup>, Lonza) were cultivated on modified surfaces in MSCBM medium under basal and osteogenic conditions. Spreading (cell area in  $\mu\text{m}^2$ ) of PKH26 stained cells (PKH26 General Cell Linker Kit, Sigma, Germany) [28] was measured using confocal microscopy (LSM 410, Carl Zeiss, Oberkochen, Germany). Quantitative real time reverse transcriptase–polymerase chain reaction (RT–PCR) assays were performed for the osteogenic markers alkaline phosphatase (ALP), collagen 1 (COL), bone sialo protein (BSP), osteocalcin (OCN), and runt related transcription factor 2 (Runx2,

also known as Cbfa1, AML-3 and PEBP2 $\alpha$ A, supports commitment and differentiation of progenitor cells to hypertrophic chondrocytes and osteoblasts), and monitored in triplicate using an ABI PRISM 7500 Sequence Detection System (Applied Biosystems, Darmstadt, Germany) and the following primer/probe sets: Hs99999905\_m1GAPDH, Hs00758162\_m1ALP, Hs00164004\_m1COL1A1, Hs00173720\_m1IBSP, Hs01587813\_g1BGLAP and Hs00231692\_m1RUNX2 (Applied Biosystems, Darmstadt, Germany). Gene expression was calculated with ABI PRISM 7500 Sequence Detection Software included in the system by the comparative CT-method and normalized to TiP (control).

#### 2.4. In Vivo Investigation

For examination of the long-term inflammatory response, intramuscular (i.m.) implantation into small pockets in the neck musculature of male LEWIS rats (age 100 days) was performed ( $n = 8$  animals/group). In addition to the PPAAm group and the PPAAc group with the plasma-modified implants, a control group received unmodified titanium implants. After 56 days, the rats were euthanized to remove the implants together with the peri-implant tissue. The tissue samples were immediately frozen with freezer spray New Envi-Ro-Tech™ (Thermo Electron Corporation, Waltham, MA, USA) and cut open using a scalpel to carefully remove the implants from the tissue using tweezers. Shandon Cryomatrix™ medium (Thermo Electron Corporation, Waltham, MA, USA) was used to fill the remaining tissue pockets, and the samples were shock-frozen in liquid nitrogen. For immunohistochemical examination, cryosections (thickness: 5  $\mu\text{m}$ ) were prepared with a Cryotome 2800 Frigocut N (Reichert-Jung, Nussloch, Germany). The antibodies ED1 for total macrophages and OX6 for MHC-class-II-positive cells (MorphoSys AbD Serotec, Duesseldorf, Germany) were used for staining according to the manufacturer's protocols and detected by Alkaline-phosphatase–anti-Alkaline-phosphatase method (AAPAAP; DakoCytomation, Hamburg, Germany). A counterstaining with hematoxylin was performed according to standard protocols. Representative digital images were prepared using a microscope (magnification 100 $\times$ ) with a digital camera. The stained cells were counted using the image analysis software ImageJ 1.40 (U.S. National Institutes of Health, Bethesda, MD, USA) with the software modules Grid and CellCounter. The results are given as cells (per  $10^3 \mu\text{m}^2$ ) and represent the average from two independent investigators.

### 3. Results and Discussion

#### 3.1. Physicochemical Surface Characterization of Plasma Polymerized Coatings on Ti

The most important points for the investigation of surface modifications in cell culture as well as in implantation studies are stable and well-characterized sample surfaces. The present study additionally necessitates sufficient densities of the desired chemical functionalities.

Plasma treatment durations for plasma polymer deposition were chosen such that coatings with thicknesses of  $50 \pm 10$  nm were obtained. Coatings of this thickness usually completely cover the surface of substrates, if their morphology is smooth enough. Further, they are thin enough not to develop large interfacial stress to facilitate a very good adhesion to Ti [30]. The composition and uniformity of such coatings and the absence of holes can be checked with XPS, based on the analysis depth of about 10 nm which is much smaller than coating thickness.

PPAAm or PPAc equipped the Ti surface with positively charged  $-\text{NH}_2$ -groups or negatively charged  $-\text{COOH}$ -groups, respectively (Fig. 1). The required absence of pinholes could be verified for both coatings even after sonication in water for 10 min by the absence of any  $\text{Ti}_{2p}$  signal (data not shown). The results of  $\text{C}_{1s}$  high resolution spectrum of PPAc (Fig. 2) does not show any changes after sonication, and that for PPAAm illustrate only small changes, which indicate surface oxidation [31]. While the error of such peak-fitting procedures is at least 10%, the reduction of carbon–carbon and carbon–hydrogen bonds (285.0 eV) is clearly visible. This means that carbon-based radicals react with water to form oxygen-containing groups, preferentially hydroxyls and carboxyls as indicated by the increasing contents of these groups.

The density of amino groups on PPAAm was calculated to be  $-\text{NH}_2/\text{C} = 2.5 \pm 0.5\%$  after derivatization [14]. Carboxyl group density was determined from  $\text{C}_{1s}$  peak fitting to be  $6.0 \pm 0.5\%$ . Note that carboxylic acid density is not necessarily equal to carboxyl density, because carboxylic esters cannot be distinguished from acids by XPS.

FT-IR studies (see Fig. 3) of TiP–PPAAm confirmed a high retention of the structural properties of the allylamine monomer in the plasma polymer coating. The basic features of the monomer are still dominant in PPAAm: the stretching vibrations of the aliphatic C–H groups,  $\nu\text{-CH}_{2,3}$  at  $2980\text{--}2880\text{ cm}^{-1}$ , the deformation vibrations of amines,  $\delta\text{-NH}$  at  $1650\text{--}1510\text{ cm}^{-1}$  and the  $\nu\text{-NH}$  stretching vibrations between  $3380\text{--}3200\text{ cm}^{-1}$ . The broader band at  $1700\text{ cm}^{-1}$  is associated with partial conversion of amines into amides. A new band for imines and nitriles arises between  $2300\text{--}2200\text{ cm}^{-1}$ , the stretching vibration of nitrile groups,  $\nu\text{-CN}$ .

Differences between acrylic acid monomer and TiP–PPAc film are more pronounced. But, all in all the acidic character of the surfaces is obvious. Associated carboxylic acids groups can be verified by strong  $\nu\text{-OH}$  stretching vibrations at

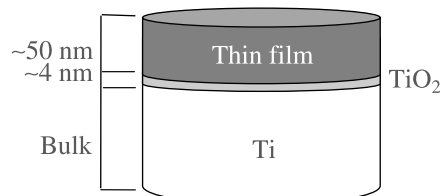


**Figure 1.** Schematic of surface structure of coated titanium samples. The plasma-cleaned titanium oxide layer is covered with layers of plasma-polymerized thin films of PPAAm or PPAc.

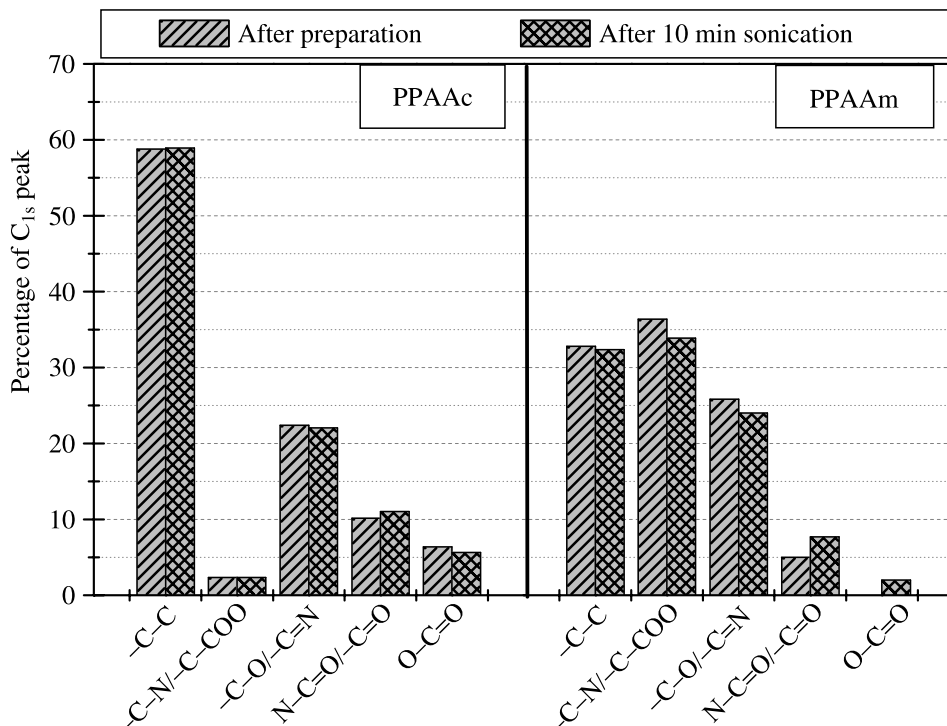


**Figure 2.** Percentages of bonding components in  $\text{C}_{1s}$  peak after film preparation and after subsequent sonication in a water bath for 10 min for TiP-PPAAm (right) and TiP-PPAAC (left).

3650–3200  $\text{cm}^{-1}$ . This band interferes with  $\nu\text{-CH}_{2,3}$  stretching vibrations at 2980–2880  $\text{cm}^{-1}$ . The small ‘combination band’ at 2650–2630  $\text{cm}^{-1}$  is also characteristic of associated carboxylic acids groups. Furthermore, the  $\nu\text{-C=O}$  stretching vibration can be seen quite clearly at 1740–1650  $\text{cm}^{-1}$ .  $\delta\text{-CH}_{2,3}$  and  $\nu\text{-CO}$  and  $\delta\text{-C-OH}$  vibrations are superimposed in the fingerprint region.

TiP-PPAAm and TiP-PPAAC surfaces exhibit similar, medium water contact angles of  $50^\circ \pm 10^\circ$ . This means an increased wettability compared to TiP (contact angle of  $78^\circ \pm 2^\circ$ ). This increase of surface energy was shown to be advantageous for fibroblast adhesion to polymer surfaces of different wettabilities [31]. Such investigations are the basis of the so-called ‘biocompatibility window’ of polymers, which lies in between  $40^\circ$  and  $60^\circ$  water contact angle [32]. Not surprisingly, zeta potential measurements show surfaces with completely different charging. TiP-PPAAm films have sufficient amounts of  $-\text{C}-\text{NH}_2$  functional groups at the surface which can counterbalance the existing negatively charging functional moieties. Their zeta potential is +7.7 mV, i.e., weakly positive. In contrast, TiP exhibits weak negative charging (zeta potential –3.4 mV, found also in [33]). Negative surface charges can be expected for PPAAC; indeed, a zeta potential of –62.8 mV was determined. The high value corresponds to the dominance of negatively charged surface groups as determined by XPS and FT-IR-spectroscopy.

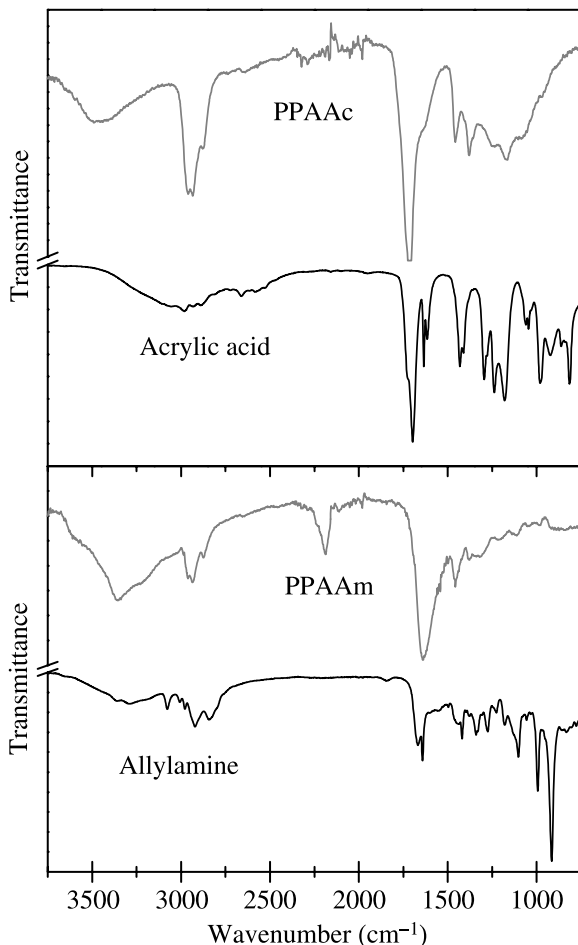


**Figure 3.** Comparison of FT-IR spectra of acrylic acid and allylamine with the corresponding plasma polymers PPAAm and PPAAc.

Interestingly, the capability of protein adhesion from DMEM + 10% FCS-solution was not influenced by these differences. A viscoelastic adhesion layer of 8 nm was estimated for both TiP-PPAAm and TiP-PPAAC by using the quartz crystal microbalance with dissipation monitoring. Possibly, this effect can be explained by a multi-layered structure of the layer which is indicated by the thickness. In that case, a protein–protein interaction could be more determining for the layer build-up than the protein–surface interaction.

### 3.2. Manipulation/Stimulation of hMSC behavior by Plasma Polymer Coatings on Ti

As mentioned above, different surface functional groups are reported to induce different differentiation of stem cells. On the molecular level, such effects may be

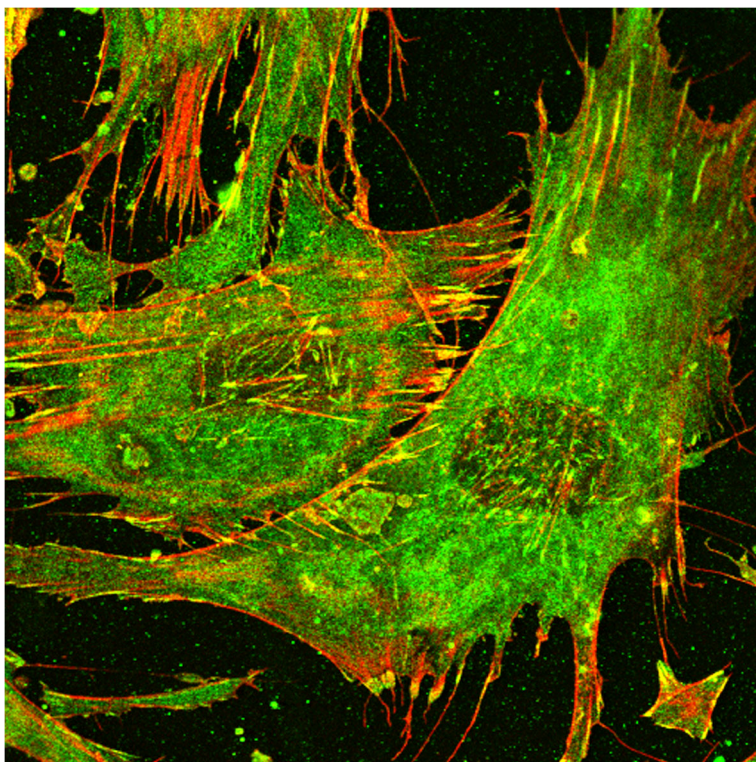


**Figure 4.** Confocal image of MSCs cultured on PPAAm. The actin cytoskeleton (red) and vinculin (green) are fluorescently labelled.

related to different bindings of cell-specific adhesion molecules like integrins but also to different charge induced attachments of adhesion-related molecules. For the case of the present investigation, differences in surface charging are considerable. Therefore, information on the relevance of charge-related effects can be expected.

Indeed, experimental results demonstrate differences in hMSC spreading between PPAAm and PPAAc. A confocal image of a well-spread cell on PPAAm is shown in Fig. 4. Staining of the cytoskeletal associated protein vinculin and the actin cytoskeleton reveals that cell extensions contain focal adhesion with colocalized actin and vinculin. While the positively charged PPAAm film improves considerably the spreading of hMSC as an initial cellular effect compared with TiP, the PPAAc coating reduces the cell area compared with TiP (Fig. 5).

Also, differences in differentiation could be observed. According to a human osteoblast differentiation model [34], COL and ALP mRNA expressions are early differentiation markers in the osteoblast lineage and decline again later during osteoblast maturation. On the other hand, BSP and OCN mRNA are expressed at very low levels in the early osteoblast differentiation stage, but transcription is enhanced during later differentiation stages [35].

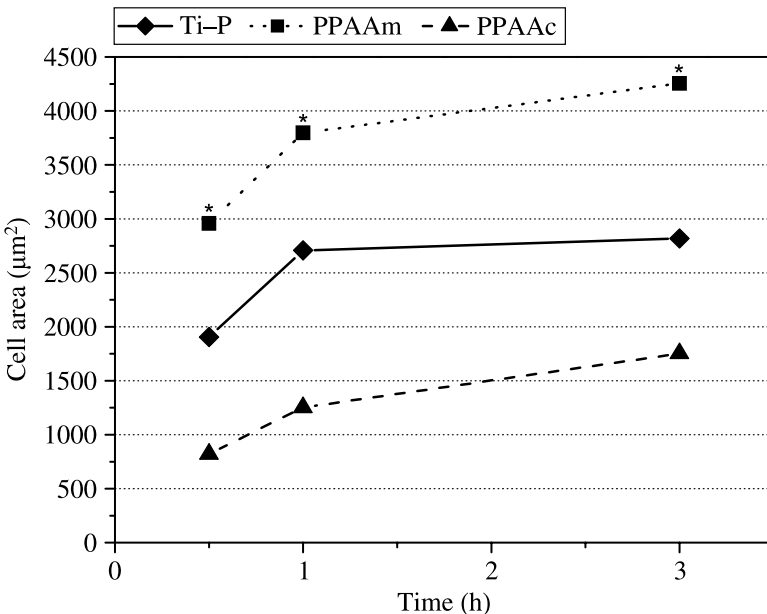


**Figure 5.** Initial spreading phase of hMSCs in basal medium (0.5–3 h). Cells spread significantly faster on PPAAm compared to TiP and PPAAc. Values with significant differences are marked by \*. Significance was calculated by the U-test with  $n = 40$  and  $p < 0.01$ .

Here, it was observed that in osteogenic medium the mRNA expression of BSP rises significantly in cells on both PPAAm and PPAAc surfaces, whereas OCN increases only on PPAAm (Fig. 6(a)). Under basal conditions, the mRNA expression of ALP and COL in hMSCs is significantly increased 2-fold and 1.5-fold for Runx2 after 3 days on PPAAc compared to TiP (Fig. 6(b)).

These results show that both PPAAm and PPAAc facilitate osteogenic differentiation. BSP late-stage differentiation-related mRNA expression was enhanced in cells cultivated on PPAAm and PPAAc in osteogenic medium, compared with the results for TiP.

Following these results, it can be assumed that surface charging has no crucial influence on enhancement of osteogenic differentiation. Even the mechanisms regarding how functional groups influence differentiation seem not straightforward. However, it must be kept in mind that attachment and spreading of cells is a prerequisite for tissue integration. Therefore, further investigation of the effects occurring on PPAAm seems promising.

### 3.3. In Vivo Investigation of Inflammation in Rats

Next to cell culture investigations, the influence of plasma-coated surfaces was explored by intramuscular implantation in rats (see Fig. 7). This model is advantageous to mimic the clinical situation of this kind of implants to examine inflammatory reactions in a muscular tissue well-perfused with blood.

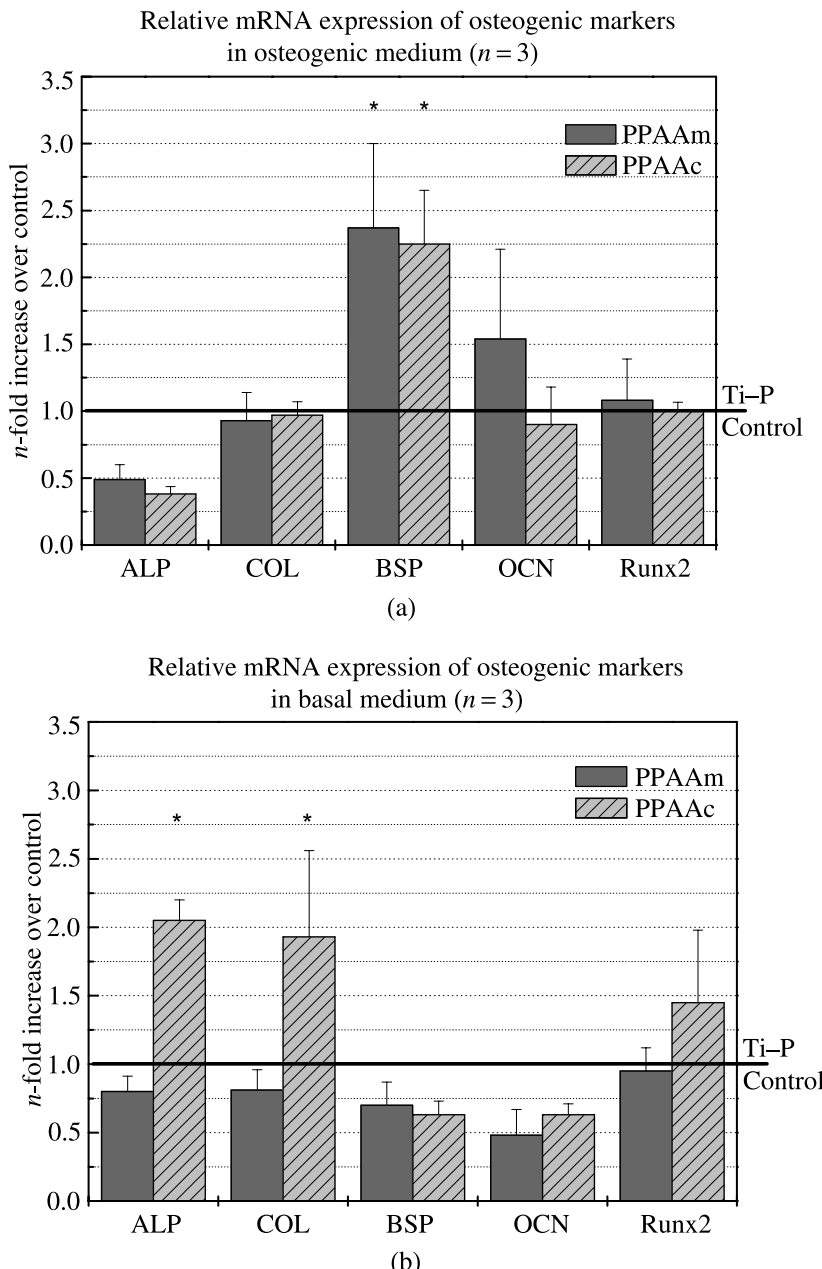


**Figure 6.** mRNA expression for osteogenic differentiation markers in hMSCs after culture on PPAAm and PPAc in osteogenic (a) and basal (b) media for 3 days, compared to cells on TiP (control). Values with significant differences are marked by an \*. Significance was calculated by the U-test with  $p < 0.05$ . Abbreviations: ALP — alkaline phosphatase, COL — collagen 1, BSP — bone sialo protein, OCN — osteocalcin, Runx2 — runt-related transcription factor 2.

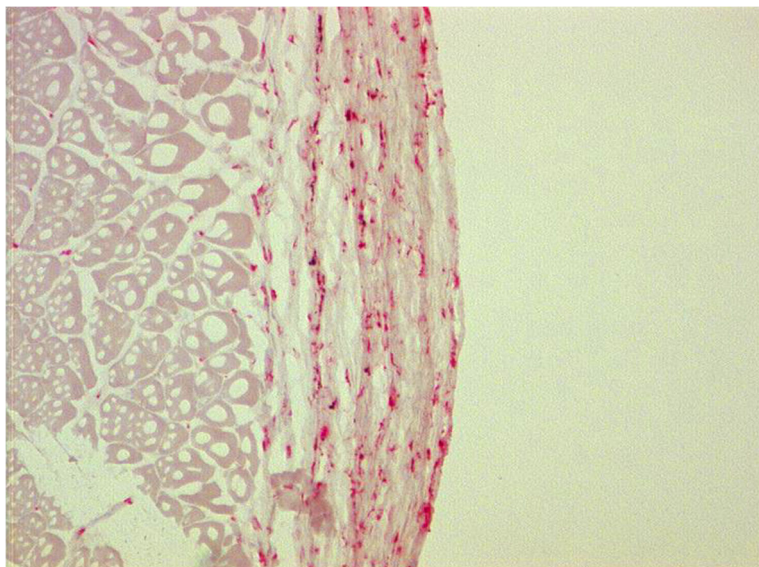


**Figure 7.** Exemplary image illustrating the morphometric evalution of the peri-implant tissue. The tissue samples (5 µm cryosections after careful removal of the titanium implants) were stained with Hemalaun/Eosin according to standard protocols. For immunohistochemical examination, the monoclonal antibody ED1 was used in this example to stain monocytes and macrophages. Based on the APAAP detection system, the positively stained cells appear red within the pink fibrous tissue (image center) which contacts the empty area where the implant was located before removal (right side of the image). The purple muscular tissue (left side of the image) adjacent to the fibrous tissue is nearly free of macrophages.

**Table 1.**  
Results of *in vivo* examination of inflammatory cells

|   | Control group            | PPAAm group              | PPAAC group              |
|---|--------------------------|--------------------------|--------------------------|
| Macrophages<br>(per $10^3 \mu\text{m}^2$ )              | 1.55<br>(IQR: 0.79–2.60) | 2.57<br>(IQR: 1.04–3.95) | 3.96<br>(IQR: 2.58–4.62) |
| Antigen-presenting cells<br>(per $10^3 \mu\text{m}^2$ ) | 0.09<br>(IQR: 0.00–0.64) | 0.04<br>(IQR: 0.00–0.51) | 1.19<br>(IQR: 1.10–1.84) |

Examination of the number of ED1-positive macrophages and OX6-positive antigen-presenting cells in the peri-implant tissue of rats ( $n = 8$  per group) after long-term implantation (56 days) of uncoated titanium implants (control group) as well as titanium implants modified with a layer of plasma-polymerized allylamine (PPAAm group) and plasma-polymerized acrylic acid (PPAAC group). Data given are the median and interquartile range (IQR).

The morphometric evaluation of the peri-implant tissue after 56 days revealed a lower number of ED1-positive macrophages and OX6-positive antigen-presenting cells in the PPAAm group compared to the PPAAC group (see Table 1). However, this difference was only significant for the antigen-presenting cells ( $p = 0.003$ ,

Mann Whitney test). Compared to the control group, the PPAc group had significantly higher numbers of macrophages ( $p = 0.007$ ) and antigen-presenting cells ( $p = 0.0148$ ) while the PPAAm group did not differ significantly from the control group for either cell population.

### 3.4. Summary

Titanium samples were coated with thin and stable plasma polymers carrying amino or carboxyl groups. These plasma modifications yielded positively and negatively charged surfaces which were investigated with respect to the behavior of hMSCs in cell culture and inflammation reactions *in vivo*. Positively charged amino groups improve considerably the initial spreading step. Both PPAAm and PPAc facilitate osteogenic differentiation, which became evident by increased expression of osteogenic differentiation-related mRNA on these surfaces.

Long-term intramuscular implantation in rats revealed that the PPAAm surfaces were comparable to untreated control (polished titanium) samples regarding the reaction of macrophages and antigen-presenting cells. This indicates that these PPAAm films do not have a negative influence on the inflammatory reaction after implantation. In contrast, the PPAc surfaces caused significantly stronger reactions by macrophages and antigen-presenting cells compared to untreated controls.

Although we do not know the molecular mechanism for the stimulation of cell spreading and osteogenic differentiation, we suggest that adhesion receptor-mediated signaling events are modified by additional reactive chemical groups which were immobilized on the material surface. In addition, the surface charge may have an influence on the cellular behavior. Because of the inflammatory reactions of PPAc *in vivo*, the PPAAm surfaces are regarded as more suitable for applications to regenerate bone tissue.

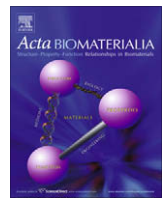
### Acknowledgements

The authors thank Urte Kellner, Uwe Lindemann and Gerd Friedrichs (INP), Kirsten Tornow (University of Greifswald) as well as Annelie Peters (University of Rostock) for excellent assistance. This study was supported by the Federal State of Mecklenburg-Vorpommern and the Helmholtz Association of German Research Centres (UR 0402210) and by the Federal Ministry of Education and Research (grant No. 13N9779, Campus PlasmaMed).

### References

1. M. Long and H. J. Rack, *Biomaterials* **19**, 1621 (1998).
2. X. Liu, P. K. Chu and C. Ding, *Mater. Sci. Eng.* **R47**, 49 (2004).
3. S. Kamath, D. Bhattacharyya, C. Padukudru, R. B. Timmons and L. P. Tang, *J. Biomed. Mater. Res. A* **86**, 617 (2008).
4. D. M. Brunette, P. Tengvall, M. Textor and P. Thomsen (Eds), *Titanium in Medicine*. Springer Verlag, Berlin (2001).

5. L. O'Toole, A. J. Beck and R. D. Short, *Macromolecules* **29**, 5172 (1996).
6. L. O'Toole, A. J. Beck, A. P. Ameen, F. R. Jones and R. D. Short, *J. Chem. Soc. Faraday Trans.* **91**, 3907 (1995).
7. J. M. Kelly, R. D. Short and M. R. Alexander, *Polymer* **44**, 3173 (2003).
8. K. S. Siow, L. Britcher, S. Kumar and H. J. Griesser, *Plasma Process. Polym.* **3**, 392 (2006).
9. J. Behnisch, F. Mehdorn, A. Holländer and H. Zimmermann, *Surf. Coat. Technol.* **98**, 875 (1998).
10. L. Detomato, R. Gristina, G. Senesi, R. d'Agostino and P. Favia, *Biomaterials* **26**, 3831 (2005).
11. V. Sciaratta, D. Hegemann, M. Müller, U. Vohrer and C. Oehr, in: *Plasma Processes and Polymers*, R. d'Agostino, P. Favia, C. Oehr and M. R. Wertheimer (Eds), p. 39ff. Wiley-VCH Weinheim, (2005).
12. T. M. Ko and S. L. Cooper, *J. Appl. Polym. Sci.* **47**, 1601 (1993).
13. M. R. Alexander and T. M. Duc, *J. Mater. Chem.* **8**, 937 (1998).
14. B. Finke, F. Lüthen, K. Schröder, P. D. Müller, C. Bergemann, M. Frant, A. Ohl and B. J. Nebe, *Biomaterials* **28**, 4521 (2007).
15. J. Friedrich, G. Kühn, R. Mix, A. Fritz and A. Schönhals *J. Adhesion Sci. Technol.* **17**, 1591 (2003).
16. A. Choukourov, H. Biederman, D. Slavinska, L. Hanley, A. Grinevich, H. Boldyryeva and A. Mackova, *J. Phys. Chem. B* **109**, 23086 (2005).
17. H. Biederman and Y. Osada, *Adv. Polym. Sci.* **95**, 57 (1990).
18. P. Hamerli, T. Weigel, T. Groth and D. Paul, *Biomaterials* **24**, 3989 (2003).
19. T. B. Ren, T. Weigel, T. Groth and A. Lendlein, *J. Biomed. Mater. Res. A* **86**, 209 (2008).
20. J. H. Lee, H. W. Jung, I.-K. Kang and H. B. Lee, *Biomaterials* **15**, 705 (1994).
21. J. H. Lee, J. W. Lee, G. Khang and H. B. Lee, in: *Science and Technology of Polymers and Advanced Materials*, P. N. Prasad (Ed.), p. 535ff. Plenum Press, New York, NY (1998).
22. B. Nebe, B. Finke, F. Lüthen, C. Bergemann, K. Schröder, J. Rychly, K. Liefelth and A. Ohl, *Biomol. Eng.* **24**, 447 (2007).
23. K. Schröder, B. Finke, H. Jesswein, F. Lüthen, A. Diener, R. Ihrke, A. Ohl, K.-D. Weltmann, J. Rychly and J. B. Nebe, *J. Adhesion. Sci. Technol.*, in print.
24. J. M. Curran, R. Chen and J. A. Hunt, *Biomaterials* **26**, 7057 (2005).
25. J. M. Curran, R. Chen and J. A. Hunt, *Biomaterials* **27**, 4783 (2006).
26. F. Mwale, H. T. Wanga, V. Nelea, L. Luo, J. Antoniou and M. R. Wertheimer, *Biomaterials* **27**, 2258 (2006).
27. G. Beamson and D. Briggs, *The Scienta ESCA 300 Database*. Wiley, Chichester (1992).
28. F. Lüthen, R. Lange, P. Becker, J. Rychly, U. Beck and B. Nebe, *Biomaterials* **26**, 2423 (2005).
29. A. Fritzsche, M. Haenle, C. Zietz, W. Mittelmeier, H.-G. Neumann, F. Heidenau, B. Finke and R. Bader, *J. Mater. Sci. Mater. Med.* **44**, 5544 (2009).
30. B. Finke, K. Schröder and A. Ohl, *Plasma Process. Polym.* **6**, S70 (2009).
31. P. B. van Wachem, T. Beugeling, J. Feijen, A. Bantjes, J. P. Detmers and W. G. van Aken, *Biomaterials* **6**, 403 (1985).
32. H. Höcker and D. Klee, *Macromol. Symp.* **102**, 421 (1996).
33. S. Roessler, R. Zimmermann, D. Scharnweber, C. Werner and H. Worch, *Colloids Surfaces B* **26**, 387 (2002).
34. J. Billiard, R. A. Moran, M. Z. Whitley, M. Chatterjee-Kishore, K. Gillis, E. L. Brown, B. S. Komm and P. V. Bodine, *J. Cell Biochem.* **89**, 389 (2003).
35. N. Chosa, M. Taira, S. Saitoh, N. Sato and Y. Araki, *J. Dental Res.* **83**, 465 (2004).



## In vivo investigation of the inflammatory response against allylamine plasma polymer coated titanium implants in a rat model

A. Hoene<sup>a,1</sup>, U. Walschus<sup>b,1</sup>, M. Patrzyk<sup>a</sup>, B. Finke<sup>c</sup>, S. Lucke<sup>b</sup>, B. Nebe<sup>d</sup>, K. Schroeder<sup>c</sup>, A. Ohl<sup>c</sup>, M. Schlosser<sup>b,\*</sup>

<sup>a</sup> Department of Surgery, University of Greifswald, Greifswald, Germany

<sup>b</sup> Department of Medical Biochemistry and Molecular Biology, University of Greifswald, Karlsburg, Germany

<sup>c</sup> Leibniz Institute for Plasma Science and Technology (INP), Greifswald, Germany

<sup>d</sup> Department of Internal Medicine, University of Rostock, Rostock, Germany

### ARTICLE INFO

#### Article history:

Received 28 May 2009

Received in revised form 10 August 2009

Accepted 4 September 2009

Available online 12 September 2009

#### Keywords:

Biocompatibility

*In vivo* investigation

Titanium

Plasma polymerization

Morphometry

### ABSTRACT

Titanium (Ti) is an established biomaterial for bone replacement. However, facilitation of osteoblast attachment by surface modification with chemical groups could improve the implant performance. Therefore, this study aimed to evaluate the effect of a plasma polymerized allylamine (PPAAm) layer on the local inflammation in a rat model. Three series (RM76AB, RM78AB, RM77AB) of PPAAm-treated Ti plates were prepared using different plasma conditions. Twelve male LEW.1A rats received one plate of each series and one uncoated control plate implanted into the back musculature. After 7, 14 and 56 days, four rats were euthanized to remove the implants with surrounding tissue. Total monocytes/macrophages, tissue macrophages, T-cells and MHC-class-II-positive cells were morphometrically counted. On day 14, the macrophage/monocyte number was significantly higher for the controls than for the PPAAm samples. On day 56, the RM76AB and RM78AB samples had significantly lower numbers than RM77AB and the controls. The same was found for the tissue macrophages. No change over time and no differences between the implants were found for the T-cells. For the number of MHC-class-II-positive cells, a significant decrease was found only for the RM78AB implants between day 14 and day 56. Physico-chemical analysis of the PPAAm implants revealed that the RM77AB implants had the lowest water absorption, the highest nitrogen loss and the lowest oxygen uptake after sonication. These results demonstrate that the PPAAm samples and the controls were comparable regarding local inflammation, and that different plasma conditions lead to variations in the material properties which influence the tissue reaction.

© 2009 Acta Materialia Inc. Published by Elsevier Ltd. All rights reserved.

### 1. Introduction

Implanted biomaterials have to fulfil multifactorial requirements regarding physical and chemical stability as well as biocompatibility. Accordingly, improvement of implant performance is a complex task. When a single aspect of performance is to be improved, it is essential to maintain the current level of performance of the other aspects. This circumstance requires consideration by a step-by-step integration of increasingly demanding biocompatibility tests *in vitro* and *in vivo* throughout the whole development procedure.

Among the materials which are used for bone replacement, titanium is a metal with very good natural surface biocompatibility and excellent mechanical strength. Thus, titanium implants usually

perform well for up to 10 years after implantation and beyond [1]. Current research activities focus on improvement of implant ingrowth with the help of additional surface modifications. It has been shown that the success of the implantation procedure can be improved in this way by, for example, effectively enhancing bone apposition [2] and soft tissue integration [3]. A crucial factor of rapid metal implant in-growth is the cellular acceptance of the surrounding tissue after implantation. In this regard, it was found that the matrix substance hyaluronan which is produced by the cells themselves plays an important role in the initial interactions between the surface of an implant and its surrounding tissue, because it acts as mediator and modulator of the first steps of cellular adhesion [4,5]. As hyaluronan is negatively charged, an implant surface with a positive charge would improve attachment of hyaluronan, thereby facilitating better cell–material contact. However, titanium does not fit this requirement. The natural oxidized titanium surface is believed to be highly hydroxylated and to carry a slight negative charge in aqueous environments at or close to the

\* Corresponding author. Tel.: +49 3834 8619178; fax: +49 3834 8680118.

E-mail address: schlosse@uni-greifswald.de (M. Schlosser).

<sup>1</sup> These authors contributed equally to this work.

physiological pH [6]. In principle, this situation could be improved by the introduction of amino groups on the Ti implant surface, as amino groups are positively charged in aqueous environments in physiological conditions and could thus enhance the attachment of hyaluronan and subsequent cell adhesion. However, it is difficult to couple amino groups to titanium directly, owing to the special chemistry of titanium oxide. However, coating of the titanium surface with a thin plasma polymer film from allylamine (plasma polymerized allylamine, henceforth designated PPAAm) was found to be possible and efficient [7]. Recently, a comparable approach using a plasma polymerization technique with ethylenediamine has been described using subcutaneous implantation into mice to examine the host tissue response [8]. In previous *in vitro* experiments, PPAAm-coated titanium surfaces exhibited beneficial effects regarding the rapid formation of osteoblastic focal adhesions of MG63 cells through the important focal contact proteins paxillin, vinculin and the phosphorylated focal adhesion kinase. Furthermore, it could be demonstrated that the coating is advantageous for cell morphology and spreading. These effects could be traced back to an enhanced hyaluronan-mediated attachment [9]. No adverse effects of the coating on the cell behaviour *in vitro* could be observed.

An important part of the *in vivo* biocompatibility of an implant in the host environment is the inflammatory response of the body, as it influences the long-term stability and functionality of the implant. In the context of this response, macrophages and other phagocytic cells play a central role [10]. Furthermore, T-cells have been implicated in the host reaction after implantation of biomaterials [11], although their exact role remains unknown [12,13]. In the context of the present implant improvement approach, study of inflammatory response is of special importance, since the coated titanium surface will be the cell contacting material. It is known that hyaluronan is only temporarily present during the early phase of cell contact. However, PPAAm must be assumed to be stable for a longer time, since its properties were specifically adjusted for low water solubility and good adhesion to titanium. Whether it can be removed by biodegradation, e.g., through phagocytosis, is not yet known. However, the inflammatory response caused by the additional PPAAm layer should be as low as that caused by the untreated titanium surface.

To evaluate the PPAAm-coated titanium implants *in vivo*, the aim of this study was an examination of four different cell populations which are involved in the inflammatory reaction following implantation in a rat model. For this purpose, an intramuscular implantation in Lewis rats was performed, which was previously established for calcium-phosphate-coated titanium implants [14]. Each animal simultaneously received a titanium control implant as well as three implants with different PPAAm coatings. The coating conditions were chosen based on previous *in vitro* results and on physico-chemical aspects such as film stability, as described previously [7]. Small variations in film properties were chosen for the different implant series, to gain insights into possible causes of inflammatory response for further improvements in film quality. To measure the inflammatory response, the number of total and tissue macrophages as well as total T-lymphocytes and MHC-class-II-positive cells was quantitatively determined in the peri-implant tissue.

## 2. Materials and methods

### 2.1. Thin film preparation on Ti implants

Small square Ti platelets ( $5 \times 5 \times 1$  mm; DOT GmbH, Rostock, Germany) were cut from a sheet of chemically pure titanium (TiP) with roughness  $R_a = 0.28 \mu\text{m}$  on both sides. Polished discs

( $R_a = 0.19 \mu\text{m}$ ) from the same sheet material and thin gold films sputtered on small polystyrene or polyetheretherketone wafers were used for plasma polymer film analysis. All samples were decontaminated and activated by a continuous wave oxygen-plasma (microwave plasma reactor V55G, PlasmaFinish, Schwedt, Germany, 500 W, 50 Pa, 100 sccm O<sub>2</sub>/25 sccm Ar) and immediately thereafter, without breaking the vacuum, coated with a thin film of PPAAm  $\sim 50$ – $100$  nm. During plasma treatment, the samples were located on an aluminium table. Therefore, the complete treatment procedure was repeated once again with the samples upside down, to ensure complete coverage of the implant surfaces. Film properties were controlled by means of duty cycle variation and pulse length variation of pulsed plasma excitation [15]. The duty cycle is the ratio of plasma  $t_{\text{on}}$  divided by the overall pulse duration  $t_{\text{on}} + t_{\text{off}}$ . Three series of samples, RM76AB, RM78AB and RM77AB, were produced using pulse conditions of 0.30 s on + 1.70 s off, 0.10 s on + 0.70 s off, and 0.01 s on + 0.19 s off, respectively. In all cases the total plasma-on time was 144 s. This means that the overall processing duration was 960 s, 1152 s and 2880 s, respectively. Owing to plasma deposition, all samples were sterile by procedure.

### 2.2. Thin film analysis of PPAAm-modified samples

#### 2.2.1. X-ray photoelectron spectroscopy

The elemental chemical surface composition and chemical binding properties of films on polished discs were determined by X-ray photoelectron spectroscopy (XPS) (AXIS ULTRA spectrometer, Kratos, Manchester, UK). The measurement conditions were described in detail previously [7]. Briefly, the monochromatic Al K<sub>α</sub> line at 1486 eV (150 W), implemented charge neutralization and pass energy of 80 eV were used for estimating the chemical elemental composition, and 10 eV for highly resolved C1s and N1s peaks, respectively. Each surface composition value represents an average over three XPS measuring steps on the surface.

Primary amino groups were reacted with 4-trifluoromethylbenzaldehyde (TFBA) at 40 °C for 2 h in a saturated gas phase to label them for detection.

For examination of the film stability, the samples were sonicated in an ultrasonic bath (T570H, Elma, Singen, Germany) in ultra pure water for 10 min at room temperature to analyse the change of the surface composition.

To examine the *in vivo* changes in the chemical composition, XPS analysis was also performed on the explanted samples of the three PPAAm series from one randomly selected animal on each experiment day. Explanted samples were rinsed for 5 min at 37 °C in a cell lysis agent (0.05% trypsin, 0.02% EDTA solved in distilled water at pH 7.2, PAA Laboratories GmbH, Cölbe, Germany) to remove adhering cells.

#### 2.2.2. Fourier transform infrared spectroscopy

The chemical compositions of the PPAAm films were further analysed by means of infrared absorption spectra taken with the help of the diamond ATR unit of a Fourier transform infrared spectroscopy (FT-IR) instrument (Spectrum One, Perkin-Elmer, Rodgau-Jügesheim, Germany). In this case, Au-sputtered polystyrene samples were used to improve sensitivity.

#### 2.2.3. Film thickness

The thickness of the deposited plasma polymer film was determined by three independent methods in parallel. Assuming a film density comparable with typical polymer densities ( $1 \text{ g} \times \text{cm}^{-3}$ ), it was calculated from the mass difference due to coating, which was determined using a laboratory microbalance (SE2 Ultra-Micro balance, Sartorius, Göttingen, Germany). Also the depth of scratches in the film was measured with the help of a surface profiler

Dektak3ST (Veeco, Santa Barbara, CA). Additional results were received by analysis with the quartz crystal microbalance. These three methods showed consistent results (<20% deviation).

#### 2.2.4. Surface charges

Existing surface charges were estimated on the basis of the zeta-potential by determining the streaming potential in dependence of the pressure with an Electrokinetic Analyzer (A. Paar, Ostfildern, Germany). Subsequently the zeta-potential was calculated according to the method of Fairbrother and Mastin. The measurements were performed in 0.001 M KCl solution at pH 6.

#### 2.2.5. Protein adsorption on TiP and PPAAm surfaces

A quartz crystal microbalance with dissipation monitoring (QCM-D-Q-Sense D 300, Fa. Q-Sense, Göteborg, Sweden) was used to study the capability of a material surface to attract proteins from liquids with protein concentrations typical for physiological conditions. This was done for the model case of DMEM cell culture medium (GIBCO, Invitrogen, Karlsruhe, Germany) supplemented with 10% fetal calf serum (FCS "GOLD", PAA Laboratories GmbH, Cölbe, Germany).

### 2.3. In vivo experiments

#### 2.3.1. Laboratory animals

Twelve male Lewis rats (age 100 days, median weight  $311 \pm 19$  g) were bred and maintained in in-house facilities under conventional housing and feeding conditions. All animal experiments were carried out in accordance with the animal protection law of the Federal Republic of Germany in its new version of 1 January 1987, with the principles of care for animals in laboratories (drawn up by the National Society for Medical Research) and with the Guidelines for Keeping and Using Laboratory Animals (NIH Publication No. 80-23, revised 1985).

#### 2.3.2. Implantation procedure and tissue sampling

Anaesthesia of the animals was performed by i.p. application of a mixture of Rompun (Bayer, Leverkusen, Germany) and Ketamin (Sanofi-Ceva, Düsseldorf, Germany). Each animal received four implants into small intramuscular pockets arranged in a rectangular formation: one implant of each PPAAm-modified series (RM76AB, RM77AB, RM78AB) as well as one untreated Ti control implant. The implants were separated by at least 2 cm from each other and fixed with a non-resorbable synthetic polypropylene suture (PROLENE, Ethicon Endo-Surgery, Inc., Hamburg, Germany). On experiment days 7, 14 and 56, four randomly selected animals were euthanized. The implantation site was cut open and the implants with a sample of the surrounding tissue were carefully explanted. The samples were immediately frozen with laboratory freezer spray New Envi-Ro-Tech (Thermo Electron Corporation, Pittsburgh, PA) and then cut using a scalpel, with the section plane at right angles to the implants. The implants were carefully removed from the frozen tissue using tweezers. The remaining tissue pockets were filled with the embedding medium Shandon Cryomatrix (Thermo Electron Corporation, Pittsburgh, PA). Subsequently, the samples were shock frozen in liquid nitrogen and stored at  $-80^{\circ}\text{C}$  until further histological examination.

### 2.4. Morphological examination

#### 2.4.1. Immunohistochemistry and histochemistry

For immunohistochemical examination, the samples were processed as frozen sections (thickness 5  $\mu\text{m}$ ) obtained from a Cryotome 2800 Frigocut N (Reichert-Jung, Nussloch, Germany). The staining was performed using the following antibodies according to the manufacturer's protocols: ED1 for monocytes and macro-

phages, ED2 for tissue macrophages, R73 for T-lymphocytes, and OX6 for MHC-class-II-positive cells (all obtained from MorphoSys AbD Serotec GmbH, Duesseldorf, Germany). For optical detection of bound antibodies, the alkaline phosphatase anti-alkaline phosphatase method (APAAP, DakoCytomation GmbH, Hamburg, Germany) was used. Counterstaining with hematoxylin was performed according to standard protocols. In addition to the immunohistochemical examination, hemalaun-eosin (HE) staining was also prepared according to standard protocols as an overview staining.

#### 2.4.2. Microscopic equipment

The samples were examined at a microscope magnification of  $125\times$  using a digital image analysis system consisting of a light microscope Jenamed 2 (Carl Zeiss Jena, Jena, Germany) and a colour camera (RGB Camera, CCD-chip 768 \* 576 Pixel, JVC, Japan).

#### 2.4.3. Image analysis procedure

The images obtained were examined quantitatively by counting positively stained cells in defined areas using the image analysis program ImageJ v1.38 (US National Institutes of Health, Bethesda, MD) with the software plug-ins Grid and CellCounter. Five representative squares in the direct vicinity of the implants pockets were selected, with an area of 2000 pixels per square, resulting in a total analysed area of 10,000 pixels per image. Artefacts and other regions within a square which did not contain tissue were deducted from the analysed area by selecting and measuring these regions with the Freehand selection tool and the Analyze/Measure feature of ImageJ. In the chosen microscopic magnification, 1 pixel corresponded to an area of  $0.3025 \mu\text{m}^2$ . This ratio was determined using a microscopic slide with a printed length scale. The final results for all images were given as positively stained cells per square micrometer, and represent the average of the counts from two independent investigators. For the HE-stained samples, the intensity of the cellular reaction was examined and assessed by both investigators with scoring on a scale of 0 (no reaction), 1 (low reaction), 2 (moderate reaction) to 3 (severe reaction). The results for the HE staining represent the mean of the ratings from both investigators.

### 2.5. Statistical data analysis

Differences between the numbers for each cell type for the four different implants on the same experiment day were examined with the non-parametric paired Friedman test. The non-parametric Kruskal-Wallis test was used for comparison of the results for each of the implants between the different experiment days as well as for analysis of the physico-chemical measurements. The level of significance was  $p < 0.05$  for all tests.

Statistical analysis was performed using the software system GraphPad Prism version 4.02 (GraphPad Software, Inc., San Diego, CA, USA).

## 3. Results

### 3.1. Thin film analysis

#### 3.1.1. Film properties of the samples after plasma treatment

A detailed physico-chemical comparison of the three implant series is given in Fig. 1a and b. There was only a small variation in amino group density as determined by chemical derivation and XPS. It was in the order of the estimated methodical uncertainty of  $\pm 0.005$ . Similarly, the results of the FT-IR spectroscopy and for the zeta-potential measurements (which were positive in any case) were not significantly different for the three

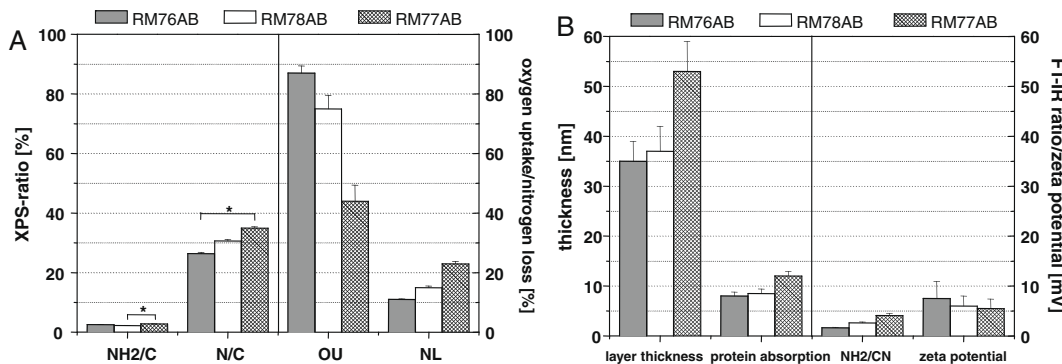


**Fig. 1.** Summarizing comparison of different film properties for RM76AB, RM78AB and RM77AB. Data are means  $\pm$  standard deviation of three measurements on one sample, *p*-values indicate significant differences by non-parametric Kruskal-Wallis test: (A) NH<sub>2</sub>/C, primary amino groups vs carbon content of the film surface determined by derivatized XPS measurements; N/C, elemental ratio from XPS; OU, oxygen uptake due to sonication; NL, nitrogen loss due to sonication (RM77AB: RM76AB, RM78AB; NH<sub>2</sub>/C: *p* = 0.027; N/C: *p* = 0.027; OU and NL are not significant; the single values are highly dispersive. (B) Layer thickness (nm), protein attachment *in vitro* (nm) and NH<sub>2</sub>/CN: ratio of 3380–3200 cm<sup>-1</sup> v-N—H stretching vibration band of primary amines —NH<sub>2</sub> and the 2300–2200 cm<sup>-1</sup> stretching vibration band of nitriles —C≡N of the FT-IR absorption spectra of the films, zeta-potential (mV).

PPAAm-coated implants. FT-IR spectra confirmed the low amino group retention during plasma polymerization. The ranking of the PPAAm samples for the ratio of the stretching vibrations of primary amino groups and nitriles vNH<sub>2</sub>vCN was RM76AB < R-M78AB < RM77AB. The film thickness was higher for the samples with a low duty cycle and short pulse duration (RM77AB). Also, these samples had the highest nitrogen loss (NL) of ~9% and the lowest oxygen uptake (OU) of ~2.3% after sonication (the values represent the difference between the N/C and O/C ratios after preparation and 10 min sonication in percent). While these differences were pronounced, they were not significant owing to a high variance of the individual values. Another effect was the increased capability of protein adhesion. For the model protein solution, a thickness of the elastic adhesion layer of ~12 nm was observed for RM77AB, compared with ~8 nm for the two other sample series RM76AB and RM78AB and the control samples. A survey of all the results in Fig. 1a and b shows that the low duty cycle condition actually leads to different films compared with the two other conditions. For RM77AB, the NH<sub>2</sub>/C and N/C ratios were significantly higher (*p* = 0.027) compared with the other two sample series.

Fig. 2 illustrates the characterization of the film properties of the three different PPAAm coatings examined before and after sonication in distilled water by XPS analysis of nitrogen-to-carbon and oxygen-to-carbon ratios as a measure of film stability. As-deposited films exhibited an N/C ratio close to that of the monomer allylamine H<sub>2</sub>C=CH—CH<sub>2</sub>—NH<sub>2</sub> (N/C = 33%). After the plasma process, only a small part of the total nitrogen still existed in the form of primary amino groups (NH<sub>2</sub>/C  $\approx$  2.5%). Therefore, more than 90% of the monomer amino groups were reacted during plasma polymer deposition. Sonication led to further surface oxidation of ~3%. In contrast, nitrogen loss was observed due to sonication ranging from 3% to 8% for the three different implant types. In particular, the N/C ratio of RM77AB was significantly higher (*p* = 0.027) than for the RM76AB and RM78AB implants.

### 3.1.2. Surface analysis of explanted samples after different implantation times

The three PPAAm implants from one randomly selected animal for each explantation day were examined by XPS analysis after trypsinization (Fig. 3). While the nitrogen ratio N/C decreased only by ~3%, the oxygen ratio O/C increased by ~10% with implantation time for implant series RM76AB and RM78AB, but not for RM77AB. The oxidation of the RM77AB surface over time was smaller, but the nitrogen loss higher. Also, traces of phosphorus were found (P/C 0.5–1.5%). A smaller P/C ratio was detected for RM77AB than

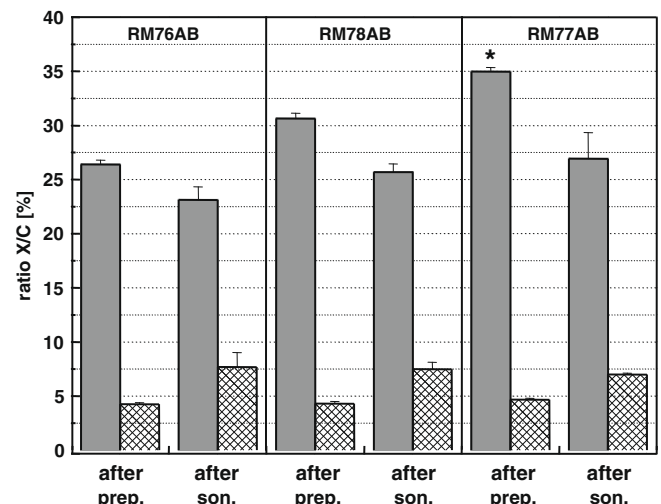


**Fig. 2.** Nitrogen and oxygen content relative to carbon for the different sample series, determined by XPS after preparation (left-hand columns) and after sonication in distilled water (right-hand columns). The grey columns represent the nitrogen-to-carbon ratio N/C and the cross-hatched columns the oxygen-to-carbon ratio O/C, respectively. The N/C ratio for RM77AB is significantly higher than for RM76AB and RM78AB (*p* = 0.027) while no significant difference was found for the O/C ratio. Data are means  $\pm$  standard deviation of three measurements on one sample. *p*-values indicate significant differences by non-parametric Kruskal-Wallis test.

for the other two surfaces. The increase in the Ti/C ratio was higher for the RM76AB and RM78AB than for RM77AB until day 56 (Ti/C < 4% at day 56).

The O/C, P/C and Ti/C ratios were significantly different for RM76AB after 7, 14 and 56 days explantation (*p* = 0.035–0.039) but not for RM78AB, where only the P/C demonstrated a significant change (*p* = 0.05). For RM77AB, only the Ti/C ratio changed significantly in the course of the study period (*p* = 0.05).

### 3.2. Morphological examination

#### 3.2.1. Total monocytes/macrophages (ED1)

For the number of total monocytes and macrophages, none of the implants demonstrated a significant change over the course of the study (Figs. 4 and 8A). However, a reduction in the ED1 cell count was observed for the RM76AB and RM78AB samples between day 7 and day 56, but not for the RM77AB and the control

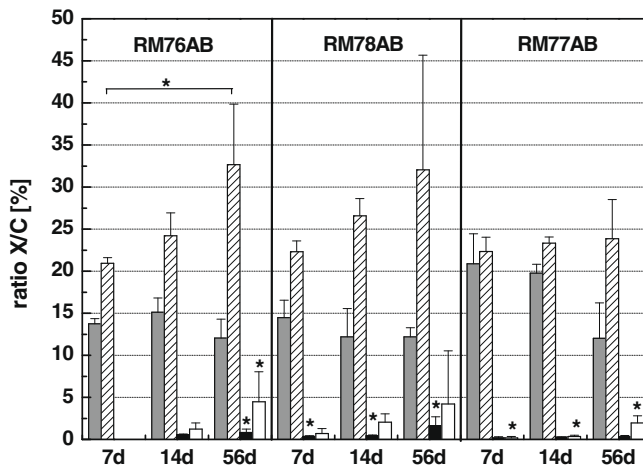


**Fig. 3.** Elemental surface composition of explanted samples as determined by XPS. The grey columns represent the N/C ratio, the hatched columns the O/C ratio, the black columns the P/C ratio, and the white columns the Ti/C ratio. Before analysis, tissue was removed from the surfaces by trypsinization and subsequent rinsing in distilled water. Significant differences in the time course were found for RM76AB regarding the O/C, P/C, Ti/C ratios ( $p = 0.039\text{--}0.046$ ), for RM78AB regarding the P/C ratio ( $p = 0.05$ ), and for RM77AB regarding the Ti/C ratio ( $p = 0.05$ ). Data represent means  $\pm$  standard deviation of three measurements on one sample,  $p$ -values indicate significant differences by non-parametric Kruskal-Wallis test.

samples, which demonstrated a slight increase during the same period. On day 14, the control samples had a higher count than the three PAAm-coated samples ( $p = 0.0539$ ). On day 56, there was a significant difference between the four implants ( $p = 0.0062$ ), with lower ED1-positive cell counts for the RM76AB and the RM78AB samples than for the RM77AB and the control samples.

### 3.2.2. Tissue macrophages (ED2)

Similarly to the ED1-positive cells, there was no significant change in the time course of tissue macrophage numbers for any of the four implant types, although a consistent decline was observed for the RM76AB samples from day 7 to day 56 (Fig. 5). A sig-

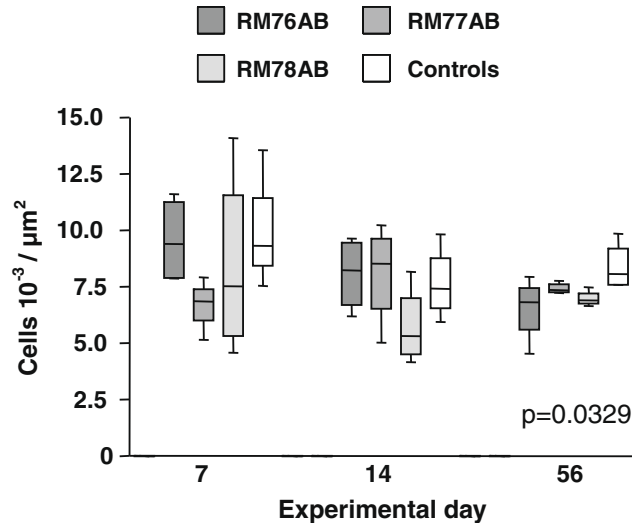


**Fig. 5.** Morphometric evaluation of ED2-positive cells (tissue macrophages) in the peri-implant tissue of Lewis rats following i.m. implantation of titanium plates coated with different PAAm layers (RM76AB, RM77AB and RM78AB; grey boxes) and uncoated titanium plates (white boxes) over a period of 56 days. Boxes indicate median and interquartile range and whiskers minimum and maximum values.  $p$ -values indicate differences by non-parametric Friedman test.

nificant difference between the implants was found on day 56 ( $p = 0.0329$ ), with lower cell counts for the RM76AB and RM78AB implants than for the RM77AB and the control samples.

### 3.2.3. T-lymphocytes (R73)

The number of T-lymphocytes was markedly lower than the number of ED1 and ED2 macrophages (Fig. 6). Furthermore, the number of T-lymphocytes demonstrated broad variability throughout all the experiment days, while the variability was markedly reduced on day 56 for the ED1 and ED2 macrophages (Figs. 4 and 5). None of the four implants showed a significant difference between the experiment days. Also, no significant difference between the implant types was found on any experiment day.

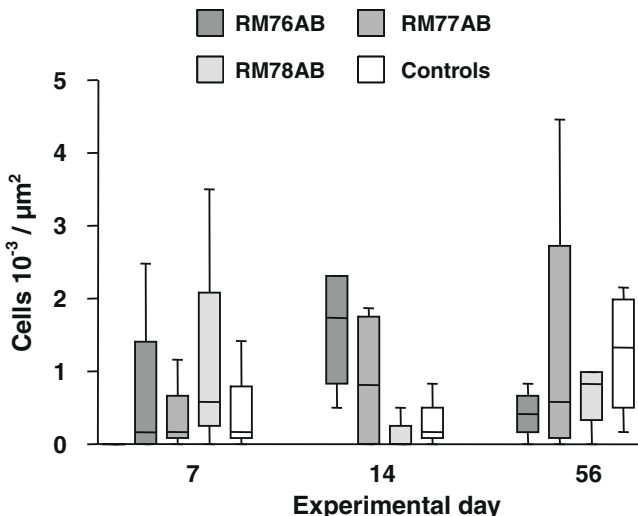


**Fig. 6.** Morphometric evaluation of R73 positive cells (T-cells) in the peri-implant tissue of Lewis rats following i.m. implantation of titanium plates coated with different PAAm layers (RM76AB, RM77AB and RM78AB; grey boxes) and uncoated titanium plates (white boxes) over a period of 56 days. Boxes indicate median and interquartile range and whiskers minimum and maximum values.

**Fig. 4.** Morphometric evaluation of ED1-positive cells (monocytes/macrophages) in the peri-implant tissue of Lewis rats following i.m. implantation of titanium plates coated with different PAAm layers (RM76AB, RM77AB and RM78AB; grey boxes) and uncoated titanium plates (white boxes) over a period of 56 days. Boxes indicate median and interquartile range and whiskers minimum and maximum values.  $p$ -values indicate differences by non-parametric Friedman test.

### 3.2.4. MHC-class-II-positive cells (OX6)

The number of MHC-class-II-positive cells decreased significantly for the RM78AB implants between day 14 and day 56 ( $p = 0.0178$ ; Figs. 7 and 8B). For the other three implant types, no significant change in the time course occurred. There were also no significant differences between the four implants on any experiment day. However, while the three PPAAm implants had a markedly higher number of MHC-class-II-positive cells on days 7 and 14, this difference was not observed on day 56, when the number was slightly higher for the control samples than for the PPAAm samples.

### 3.2.5. HE staining

For the HE staining, the RM76AB and RM78AB samples had a higher score on day 7 (2.5 and 2.0, respectively) than the RM77AB and the control samples (1.7 and 0.7, respectively; Fig. 9). However, both the RM76AB and the RM78AB implants had the lowest scores on day 56: 1.0 and 0.8, respectively, as compared with 1.5 for both the RM77AB and the control samples. Consequently, a pronounced decrease in the intensity of the HE-stained cellular reaction between day 7 and day 56 was observed for the RM76AB (from 2.5 to 1.0) and the RM78AB (from 2.0 to 0.8) implants, while the reaction remained nearly unchanged for the RM77AB samples

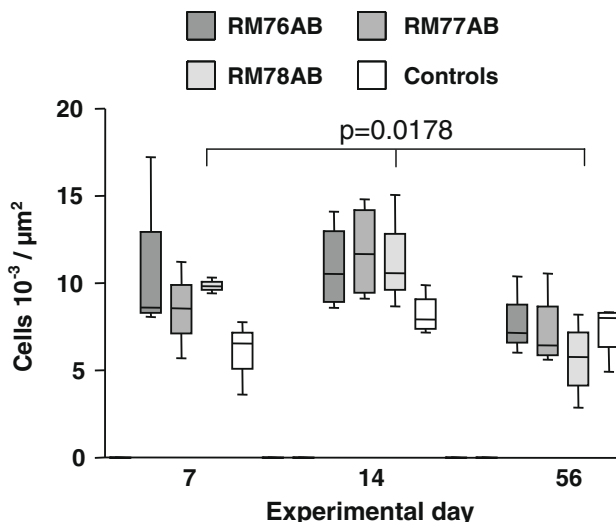


**Fig. 7.** Morphometric evaluation of OX6 positive cells (MHC-class-II-positive cells) in the peri-implant tissue of Lewis rats following i.m. implantation of titanium plates coated with different PPAAm layers (RM76AB, RM77AB and RM78AB; grey boxes) and uncoated titanium plates (white boxes) over a period of 56 days. Boxes indicate median and interquartile range, and whiskers minimum and maximum values.

(from 1.7 to 1.5) or was increased for the control samples (from 0.7 to 1.5).

## 4. Discussion

Following earlier *in vitro* experiments on titanium implants functionalized with a PPAAm layer, which demonstrated beneficial effects of such surfaces regarding the formation of osteoblastic focal adhesions [7], the aim of the study was to examine the local cellular reaction around these implants as an important part of their *in vivo* biocompatibility. As it is well known that macrophages [10] and lymphocytes [11] are both involved in the inflammatory response of the host, the cell populations which were examined by immunohistochemistry and digital image analysis were the total and tissue macrophages as well as total T-lymphocytes and MHC-class-II-positive cells.

As the experimental model, intramuscular (i.m.) implantation in the neck musculature of rats was chosen. The reason for selecting this site was the fact that the procedures for implantation and explantation of the samples were straightforward. The OP could be performed in an easy and uniform manner for all animals within a short period, as well as with minimal risk for surgical complications and with reduced post-operative stress. In addition, this experimental design resembles the clinical situation, as these kinds of implants are typically implanted into muscular tissue. Musculature is also well perfused with blood and therefore especially suitable for examining inflammatory reactions. The simultaneous implantation of the four implants into the same individual animals as performed in this study was similar to previous experiments on calcium-phosphate-coated titanium [14]. The advantage of this approach is that it eliminates the broad individual variability of host reactions which were observed, for example, in studies on the immunological reactions against vascular prostheses using inbred rats as well as pigs [16,17].

For the total monocytes and macrophages (ED1), the PPAAm samples had lower counts than the control samples on day 14 and day 56, though on day 56 this beneficial effect was only seen for the RM76AB and the RM78AB implants. Similarly, these two implant types had a lower number of tissue macrophages (ED2) than the controls on day 56. Furthermore, the RM78AB samples were the only implants which demonstrated a decrease in the number of MHC-class-II-positive cells (OX6 count) between day 14 and day 56. Overall, these results demonstrate that the inflammatory reactions which were caused by the PPAAm-treated titanium implants were not significantly higher than for the untreated control samples on any experiment day, and that the RM76AB and the RM78AB samples caused lower macrophage-related reactions than the control samples in the mid- and late-phase

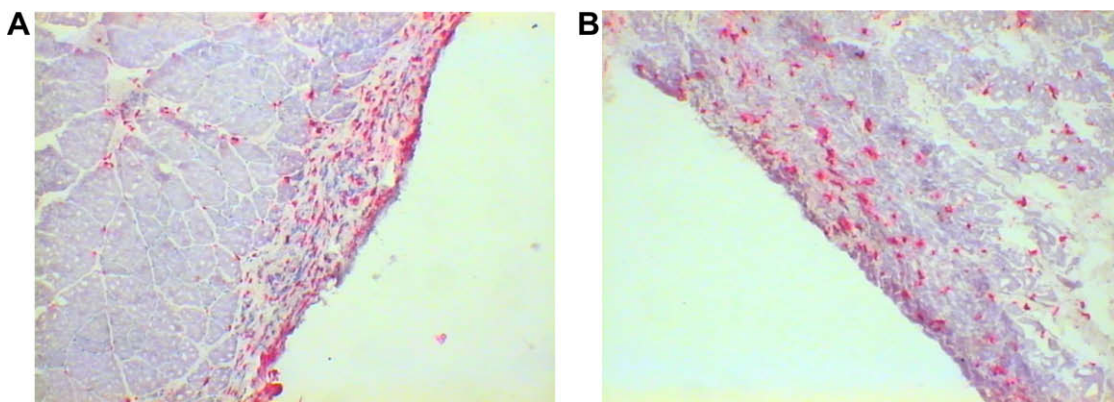


**Fig. 8.** Two exemplary images illustrating the immunohistochemical examination: (A) ED1 staining (total monocytes and macrophages) for a RM77AB implant sample on experiment day 14; (B) OX6 staining (MHC-class-II-positive cells) for a RM77AB implant sample on experiment day 56.

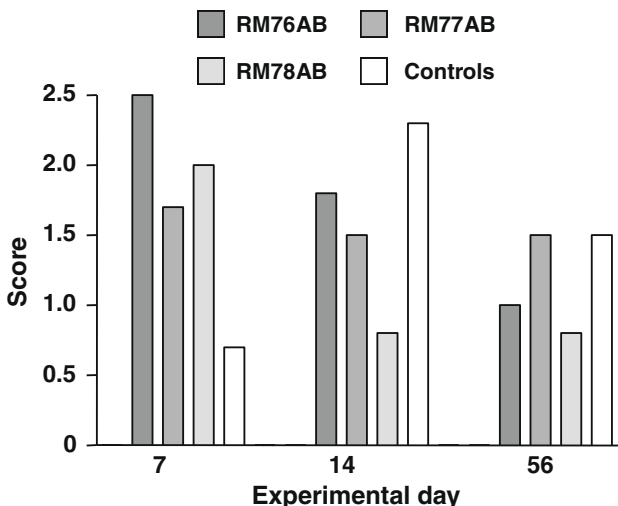


**Fig. 9.** Intensity of the cellular reaction as stained with HE in the peri-implant tissue of Lewis rats following i.m. implantation of titanium plates coated with different PPAAm layers (RM76AB, RM77AB and RM78AB; grey boxes) and uncoated titanium plates (white boxes) over a period of 56 days. The bars indicate the mean of the rating by two independent investigators on a scale of 0 (no reaction), 1 (low reaction), 2 (moderate reaction) to 3 (severe reaction).

of the study. A comparison between the number of macrophages and T-cells reveals that the macrophages are the dominant cell population in the context of the tissue response against all the implants. Consequently, the results from the histochemical HE staining mainly reflect the results for the ED1- and ED2-positive macrophages, especially regarding the differences on days 14 and 56 between the RM76AB and RM78AB samples, on the one hand, and the RM77AB and the control samples, on the other hand.

Taken together, it therefore seems that the PPAAm treatment has a favourable effect on the inflammatory reactions against these titanium plates. It is interesting to note the differences between the RM76AB and RM78AB samples, on the one hand, and the RM77AB samples, on the other hand. While the RM77AB samples were also comparable with the untreated control samples, only the RM76AB and the RM78AB samples demonstrated a lower macrophage reaction in comparison with the controls. Therefore, the different functionalization procedures for these three implant types probably influence their *in vivo* performance.

Indeed, an assessment of the physico-chemical thin film data leads to arguments supporting this conclusion. In principal, the XPS results demonstrate that these PPAAm films are comparable with each other as well as with similar PPAAm films which were used in earlier studies in which a more detailed XPS analysis as well as representative XPS spectrum data can be found [7,15]. This can be seen from the high nitrogen content, which is close to the monomer's nitrogen content N/C of 33% and accompanied by relatively low amino group retention in any case. Also oxygen content of the films is nearly identical at a low level. Hence, it is understandable that all implants exhibit similar and low local inflammatory response.

However, the surface analysis also demonstrated that low duty cycle conditions (RM77AB samples) result in films which exhibit differences compared with the other series. The most pronounced of these differences were seen for water stability. In addition, indications for slightly better structure retention in the case of lower duty cycle were found. These two observations are in accordance with the advanced understanding of plasma polymerization [18]. Reduction in duty cycle and shortening of pulse duration both lead to improved monomer structure retention in the polymer, which can be assigned in part to an increased incorporation of unreacted monomer molecules and of only loosely bound small oligomeric

fragments in the films. These low molecular weight components can be dissolved from the films [19]. Indeed, a higher loss of nitrogen due to sonication for the RM77AB low duty cycle samples was observed. Hence, it can be assumed that the observed higher inflammatory response caused by these samples may be a result of trace amounts of dissolved substances on top of the implant surface, which may act as an inflammation stimulus.

Another effect of duty cycle reduction can be a decrease in the density of reactive sites in the films, e.g., of carbon centred radicals which convert to peroxide radicals as a result of contact with air or water. The trend to lower oxygen uptake during sonication, as observed in the present study, can probably be attributed to this effect. In this context, the interesting question arises as to why the RM76AB and RM78AB samples, which exhibit a higher oxygen uptake during sonication, perform even better than the control samples concerning the inflammation response. A possible answer was found in the details of the FT-IR spectra, as described previously [20]. Obviously, all PPAAm samples possess a higher capability to take up water. A huge water absorption band was still found for all samples for several days after sonication. This effect was more pronounced for the RM76AB and RM78AB samples. Accordingly, it might be that a noticeable hydrogel-like character of the films exists which is slightly more developed for these samples. This effect could explain the lower inflammatory response against the RM76AB and RM78AB samples, since hydrogels are known to be very biocompatible due to only weak interaction with proteins [21]. This assumption is further supported by the observation that these samples exhibit lower capability of protein adhesion.

Considering the initial assumption that thin PPAAm coating of titanium, resulting from its beneficial effects on the interaction between the materials surface and the matrix substance hyaluronan, and thereby its positive influence on rapid cell–material contact and cell behaviour, could exhibit tissue-friendly behaviour *in vivo* too, the results of this study indicate that this is really possible. Regarding the inflammatory response, there seems to be an optimum quality of these films which is characterized by low water solubility. Even films with slightly enhanced solubility can increase the attachment of inflammatory cells.

Extending previous results from Kamath et al. which demonstrated that a plasma-based treatment with difference chemical groups had a distinct influence on the implant-mediated host tissue response [8], the results of this study indicate that even variations in the chemical composition for the same surface chemistry can affect local tissue reactions. While there are methodological differences between the work of Kamath et al. and the present study regarding the animal model (mice vs rat), the implant site (s.c. vs i.m.) as well as the implant shape and material (polypropylene microspheres vs Ti plates), their main finding regarding a pronounced myelocyte-related inflammatory response 14 days after implantation caused by surface-bound amino groups is consistent with results from the early study phase, especially regarding the T-cells and the MHC-class-II-positive cells. However, the results from experiment day 56 of the present study indicate that the host response improves in the long term. Using a similar experimental design to that of Kamath et al. (s.c. implantation of surface-modified polypropylene microspheres in mice), Nair et al. recently demonstrated that variations in the surface density of OH and COOH groups deposited by plasma treatment had only a relatively minor influence on the extent of the foreign body reaction [22]. As outlined above, the experimental model in the present study is different from that used by Nair et al. in a number of relevant aspects. Furthermore, the surfaces examined were functionalized with OH and COOH groups, while the focus of the present study was on NH<sub>2</sub> groups. Still, the conclusions of Nair et al. support the present results, as the differences which were observed in the present study between the *in vivo* results for the three different PPAAm im-

plants are mostly minor or moderate. As discussed by Nair et al., this might be due to a threshold density of a particular functional group for which further increasing the density beyond this threshold level has little or no effect on the body reactions. However, further studies are necessary to evaluate this hypothesis in more detail.

From the results of the present study, it can be concluded that the procedure as performed for the RM76AB and RM78AB samples warrants a more detailed examination of its *in vitro* and *in vivo* properties in further studies. Among other further clarification of inflammatory response and an examination of *in vivo* degradation of the films would be of interest. This is suggested by the tentative XPS investigations of explanted implants in this study, which demonstrated film erosion increasing with duration of implantation by increasing detection of titanium. Further, increased variations in measurements for long durations of implantation suggest that the films possibly become perforated. It would be of great interest to determine the mechanisms of this degradation. The present results suggest at least two candidate mechanisms: dissolution and biodegradation caused by inflammatory cells, e.g., phagocytosis. Dissolution is suggested by the fact that none of the films exhibited perfect water stability. Further studies should also include examination of the film-tissue interface. Compared with the as-grown PAAm films, the explant surfaces exhibit a strongly modified elemental composition. After 7 days of implantation, the nitrogen content is reduced by about half, and the oxygen content is increased threefold. With increasing duration of implantation, both effects strengthen and, in addition, small amounts of phosphorus accumulate. These changes might indicate the presence of cellular residues very strongly attached to the explant surface.

In addition to the examination of the degradation of the PAAm films and the underlying mechanisms, future studies should also involve a more detailed examination of short- and long-term inflammation. This is especially true for those implants which demonstrated a beneficial performance in the present study. In addition to the examination of the local tissue reaction as performed in this study, such a close examination of the inflammatory response should also include an analysis of the systemic release profile of pro- and anti-inflammatory cytokines.

## Acknowledgments

The authors are grateful to Kirsten Tornow and Urte Kellner for excellent technical support. The authors thank Marion Frant from iba Heiligenstadt, Germany, for the zeta-potential measurements. This study was supported by the Federal state of Mecklenburg-Vorpommern and the Helmholtz Association of German Research Centres (Grant No. VH-MV1) and by the Federal Ministry of Education and Research (Grant No. 13N9779, Campus PlasmaMed).

## Appendix A. Figures with essential colour discrimination

Certain figure in this article, particularly Figure 8, is difficult to interpret in black and white. The full colour images can be found in the on-line version, at doi: [10.1016/j.actbio.2009.09.003](https://doi.org/10.1016/j.actbio.2009.09.003).

## References

- [1] Esposito M. Titanium for dental applications. In: Brunette DM, Tengvall P, Textor M, Thomsen P, editors. Titanium in medicine. Berlin: Springer; 2001. p. 172–230.
- [2] Buser D, Broggini N, Wieland M, Schenk RK, Denzer AJ, Cochran DL, et al. Enhanced bone apposition to a chemically modified SLA titanium surface. *J Dent Res* 2004;83:529–33.
- [3] Schwarz F, Ferrari D, Herten M, Mihatovic I, Wieland M, Sager M, et al. Effects of hydrophilicity and microtopography on early stages of soft and hard tissue integration at non-submerged titanium implants: an immunohistochemical study in dogs. *J Periodontol* 2007;78:2171–84.
- [4] Zimmermann E, Geiger B, Addadi L. Initial stages of cell-matrix adhesion can be mediated and modulated by cell-surface hyaluronan. *Biophys J* 2002;82:1848–57.
- [5] Cohen M, Klein E, Geiger B, Addadi L. Organization and adhesive properties of the hyaluronan pericellular coat of chondrocytes and epithelial cells. *Biophys J* 2003;85:1996–2005.
- [6] Textor M, Sittig C, Frauchiger V, Tosatti S, Brunette DM. Properties and biological significance of natural oxide films on pure titanium. In: Brunette DM, Tengvall P, Textor M, Thomsen P, editors. Titanium in medicine. Berlin: Springer; 2001. p. 172–230.
- [7] Finke B, Lüthen F, Schröder K, Mueller PD, Bergemann C, Frant M, et al. Positively charged plasma polymerized titanium boosts osteoblastic focal contact formation in the initial adhesion phase. *Biomaterials* 2007;28:4521–34.
- [8] Kamath S, Bhattacharyya D, Padukudru C, Timmons RB, Tang L. Surface chemistry influences implant-mediated host tissue responses. *J Biomed Mater Res A* 2008;86:617–26.
- [9] Nebe JGB, Lüthen F. Integrin- and hyaluronan-mediated cell adhesion on titanium-hyaluronan-mediated adhesion. In: Breme J, Kirkpatrick CJ, Thull R, editors. Metallic biomaterial interactions. Weinheim: Wiley-VCH; 2008. p. 179–82.
- [10] Xia Z, Triffitt T. A review on macrophage responses to biomaterials. *Biomed Mater* 2006;1:R1–9.
- [11] Davis C, Fischer J, Ley K, Sarembock JJ. The role of inflammation in vascular injury and repair. *J Thromb Haemost* 2003;1:1699–709.
- [12] Rodriguez A, Voskerician G, Meyerson H, MacEwan SR, Anderson JM. T cell subset distributions following primary and secondary implantation at subcutaneous biomaterial implant sites. *J Biomed Mater Res A* 2008;85:556–65.
- [13] Goodman SB. Wear particles, periprosthetic osteolysis and the immune system. *Biomaterials* 2007;28:5044–8.
- [14] Walschus U, Hoene A, Neumann HG, Wilhelm L, Lucke S, Lüthen F, et al. Morphometric immunohistochemical examination of the inflammatory tissue reaction after implantation of calcium-phosphate-coated titanium-plates in rats. *Acta Biomater* 2009;5:776–84.
- [15] Nebe B, Lüthen F, Finke B, Bergemann C, Schröder K, Rychly J, et al. Improved initial osteoblast functions on amino-functionalized titanium surfaces. *Biomol Eng* 2007;24:447–54.
- [16] Schlosser M, Zippel R, Hoene A, Urban G, Ueberrueck T, Marusch F, et al. Antibody response to collagen after functional implantation of different polyester vascular prostheses in pigs. *J Biomed Mater Res A* 2005;72: 317–25.
- [17] Wilhelm L, Zippel R, von Woedtke T, Kenk H, Hoene A, Patryk M, et al. Immune response against polyester implants is influenced by the coating substances. *J Biomed Mater Res A* 2007;83:104–13.
- [18] Timmons RB, Griggs AJ. Pulsed plasma polymerizations. In: Biederman H, editor. Plasma polymer films. London: Imperial College Press; 2004. p. 217–45.
- [19] Siow KS, Britcher L, Kumar S, Griesser HJ. Plasma methods for the generation of chemically reactive surfaces for biomolecule immobilization and cell colonization – a review. *Plasma Process Polym* 2006;3:392–418.
- [20] Finke B, Schröder K, Ohl A. Structure retention and water stability of microwave plasma polymerized films from allylamine and acrylic acid. *Plasma Process Polym* 2009;6. doi:[10.1002/ppap.200930305](https://doi.org/10.1002/ppap.200930305).
- [21] Klee D, Höcker H. Polymers for biomedical applications: improvement of the interface compatibility. *Adv Polym Sci* 2000;149:1–57.
- [22] Nair A, Zou L, Bhattacharyya D, Timmons RB, Tang L. Species and density of implant surface chemistry affect the extent of foreign body reactions. *Langmuir* 2008;24:2015–24.

# Serum profile of pro- and anti-inflammatory cytokines in rats following implantation of low-temperature plasma-modified titanium plates

Uwe Walschus · Andreas Hoene · Maciej Patrzyk · Birgit Finke · Martin Polak · Silke Lucke · Barbara Nebe · Karsten Schroeder · Andreas Podbielski · Lutz Wilhelm · Michael Schlosser

Received: 11 October 2011 / Accepted: 20 February 2012 / Published online: 9 March 2012  
© Springer Science+Business Media, LLC 2012

**Abstract** Surface modification of Titanium (Ti) by low-temperature plasma influences cell-material interactions. Therefore, this study aimed at examining serum cytokine levels and associations after intramuscular implantation ( $n = 8$  rats/group) of Ti-plates with Plasma Polymerized Allyl Amine (Ti-PPAAm), Plasma Polymerized Acrylic Acid (Ti-PPAAC), and without such layers (Ti-Controls).

Uwe Walschus and Andreas Hoene contributed equally to this work.

U. Walschus · S. Lucke · M. Schlosser (✉)  
Department of Medical Biochemistry and Molecular Biology,  
Research Group of Predictive Diagnostics, Ernst Moritz Arndt  
University of Greifswald, Greifswalder Str. 11c, 17495  
Karlsruhe, Germany  
e-mail: schlosse@uni-greifswald.de

U. Walschus · M. Schlosser  
Institute of Pathophysiology, University of Greifswald,  
Karlsruhe, Germany

A. Hoene · M. Patrzyk  
Department of Surgery, University of Greifswald,  
Greifswald, Germany

B. Finke · M. Polak · K. Schroeder  
Leibniz Institute for Plasma Science and Technology (INP),  
Greifswald, Germany

B. Nebe  
Department of Internal Medicine, University of Rostock,  
Rostock, Germany

A. Podbielski  
Institute of Medical Microbiology, Virology and Hygiene,  
University of Rostock, Rostock, Germany

L. Wilhelm  
Department of Surgery, Hospital Demmin, Demmin, Germany

Pro-inflammatory (IL-2, IFN $\gamma$ , IL-6) and anti-inflammatory (IL-4, IL-10, IL-13) cytokines were measured weekly for 56 days. Ti-PPAAm caused increased IL-2 (d7-14, d35), increased IFN $\gamma$  (d35) and decreased IL-10 (d35, d49-56). Ti-PPAAC induced divergent anti-inflammatory cytokine changes with increased IL-4 (d28-56) and decreased IL-10 (d42-56). Ti-Controls elicited increased IL-2 (d42) and IFN $\gamma$  (d35-42, d56). IL-6 was not detected and IL-13 only in three samples, thus they do not influence the response against these Ti implants. Correlation analysis revealed surface-dependent associations between cytokines indicating the involvement of different inflammatory cell populations. Concluding, different plasma modifications induce specific serum cytokine profiles and associations indicating distinct inflammatory responses.

## 1 Introduction

Titanium (Ti) and Ti-based alloys are among the most widely used materials for bone replacement in reconstructive surgery and orthopaedics after loss or injury of bone. The main advantages of Ti are its excellent mechanical strength, its chemical stability including high resistance to corrosion and its well established biocompatibility, with a documented long-term performance of Ti implants for up to ten years after implantation and beyond [1]. From a clinical point of view, it is desirable to achieve an optimal level of implant ingrowth to balance the need for long-term stable anchoring of the implant in the host tissue with the possibility of implant removal in case of complications.

One possibility to modulate implant ingrowth is the use of surface modifications to influence tissue-material interactions. In previous in vitro studies, we examined several

treatments based on low-temperature plasma processes regarding their effects on cell behaviour on implant surfaces. Ti surfaces coated with Plasma Polymerized Allyl Amine films (Ti-PPAAm), resulting in an amino-group rich positively charged implant surface, had beneficial effects regarding rapid formation of osteoblastic focal adhesions of MG63 cells through the important focal contact proteins paxillin, vinculin and the phosphorylated focal adhesion kinase [2]. Ti-PPAAm also improved cell morphology and spreading, and no adverse effects on the in vitro cell characteristics were observed. A carboxyl-group rich negatively charged Ti surface based on a Plasma Polymerized Acrylic Acid film (Ti-PPAAC) stimulated mRNA expression of early bone differentiation markers like alkaline phosphatase, collagen 1 (COL) and runt-related transcription factor 2 (Runx2) under basal conditions as well as late bone differentiation markers like bone sialoprotein [3].

However, surface treatments not only affect cell attachment, differentiation and spreading but also influence the biocompatibility of the implants in the host environment. An important part of the in vivo biocompatibility is the inflammatory response caused by the biomaterial, consisting of an acute phase followed by a chronic phase which persists for the whole implantation period. Macrophages and other phagocytic cells were found to play a major role within these reactions [4] while T cells are also involved [5]. However, more studies are needed to elucidate their exact role [6, 7].

To examine the response of the body after implantation of biomaterials, the in vivo determination of different cytokines has recently been used in several studies [8–11]. Furthermore, a recent study which found that variations in the genes of cytokines including IL-2 and IL-6 influence the severity of osteolysis in patients with total hip arthroplasty demonstrates the potential relevance of cytokines for implant-associated complications [12]. Measuring cytokines in readily available body fluids like serum is a feasible approach to examine the inflammatory and immunological response of the body over an extended time period due to the diverse and distinct effects of cytokines within the immune system.

For example, the T cell derived pro-inflammatory cytokine IL-2 is essential for regulation of T cell function and proliferation especially for antigen-activated CD8+ T lymphocytes [13]. It also augments the production of other cytokines including IFN $\gamma$  typically released by various T cell populations. Furthermore, IL-2 is important for growth and differentiation of natural killer (NK) cells and has synergistic effects with a number of cytokines including IFN $\gamma$  and IL-12 [13].

IFN $\gamma$ , mainly produced by NK cells as well as CD4+ and CD8+ T cells, is another important pro-inflammatory cytokine. It is essential for regulation of antigen presentation to CD4+ T cells and for stimulation of NK cells and

macrophages, converting them from a resting to an activated state [14]. In recent models of different macrophage activation pathways, IFN $\gamma$  is the key regulator of the classic pathway leading to the pro-inflammatory M1 phenotype [15]. Furthermore, IFN $\gamma$  is a central link between the innate immune system and the T<sub>H</sub>1-mediated cellular part of the adaptive immune system and therefore represents one of the most important immune regulators [16].

IL-6, a pleiotropic cytokine with mainly pro-inflammatory functions, is predominantly produced by macrophages, fibroblasts, and endothelial cells but also by T and B lymphocytes, mast cells and some other cell types [17]. It stimulates the proliferation of B lymphocytes into antibody-producing cells and the production of immunoglobulins, and activates T lymphocytes by inducing the expression of the IL-2 receptor CD25 [17]. Furthermore, it induces acute-phase proteins like fibrinogen and C-reactive protein [17].

Another pleiotropic cytokine is IL-4 which is mainly secreted by mast cells. It stimulates proliferation of B cells, T cells and NK cells as well as the differentiation of CD4+ T cells into T<sub>H</sub>2 cells [18]. It has mostly anti-inflammatory effects including antagonizing the action of IFN $\gamma$ , enhancing the humoral immune response and switching macrophages to the anti-inflammatory M2 phenotype via an alternative activation pathway [15]. Comparable to the role of IFN $\gamma$ , it links the innate immune response with T<sub>H</sub>2-mediated humoral reactions of the adaptive immune system.

Among the T<sub>H</sub>2-associated anti-inflammatory cytokines, IL-10 is secreted by alternatively activated monocytes and macrophages but also by T and B lymphocytes [19, 20]. IL-10 production is enhanced by other cytokines like IL-4, IL-12, IFN $\alpha$  and IL-10 itself. It inhibits the expression of pro-inflammatory cytokines, shifts the immune response toward humoral functions and attenuates cellular immune reactions. For macrophages, it inhibits antigen presentation and maturation [20] and switches them to a deactivated state which is associated with immune suppression and tissue remodelling [21].

The anti-inflammatory cytokine IL-13 is mainly produced by T<sub>H</sub>2 cells, mast cells and NK cells. It has inhibitory effects on monocytes and macrophages by downregulating a number of pro-inflammatory cytokines [22]. The production of IL-13, together with IL-4, IL-6 and IL-10, was postulated as a characteristic feature in the cytokine release profile of mature T<sub>H</sub>2 cells [17]. It is structurally similar to IL-4 with which it shares many functions, with IL-4 playing the primary role in most situations [23].

Because of the important functions of IL-2, IFN $\gamma$ , IL-6, IL-4, IL-10 and IL-13 in the context of pro- and anti-inflammatory actions of the immune system, influencing

the innate and the adaptive response as key regulators of cellular and humoral reactions, the aim of the present study was the determination of the serum levels of these six cytokines following intramuscular implantation of Ti-PPAAm or Ti-PPAAC samples as well as control implants without such plasma-polymerized films over a period of 56 days as well as the examination of their associations by correlation analysis.

## 2 Materials and methods

### 2.1 Preparation of implants

Square Ti plates ( $5 \times 5 \times 1$  mm, DOT GmbH, Rostock, Germany) were cut from sheet of chemically pure titanium with a roughness of  $R_a = 0.28 \mu\text{m}$  on both sides and cleaned in an ultra sonic bath in isopropanol. For film deposition of Ti-PPAAm and Ti-PPAAC, a commercial microwave plasma reactor (2.45 GHz) was used which generates disc-like planar plasmas (Plasma Processor V55G, PlasmaFinish, Schwedt, Germany). Substrates were located in a downstream position with a distance of 9 cm to the microwave coupling window. Three implant series were prepared as follows:

#### 2.1.1 Ti-PPAAm implants

A Plasma Polymerized Allyl Amine (PPAAm) layer was created on both sides of the Ti plates by activation with a continuous mw oxygen-plasma (2.45 GHz, 500 W, 50 Pa, 100 sccm  $\text{O}_2$ /25 sccm Ar, 60 s) followed by a pulsed allylamine plasma (500 W, 50 Pa, 50 sccm allylamine/50 sccm Ar, 300 ms plasma on/1,700 ms plasma off, effective treatment duration 144 s). The resulting PPAAm film thickness was 50–100 nm.

#### 2.1.2 Ti-PPAAC implants

Using the same oxygen-plasma activation procedure as for the Ti-PPAAm series, a layer of Polymerized Acrylic Acid (PPAAC) was deposited on both sides of the Ti implants (700 W, 20 Pa, 50 sccm acrylic acid/20 sccm Ar, 50 ms on/50 ms off, effective treatment duration 60 s). The PPAAC film thickness was <50 nm.

#### 2.1.3 Ti-Controls implants

Ti plates which were treated on both sides with the oxygen-plasma activation procedure as described above served as controls.

The physico-chemical properties of the plasma-treated samples were examined by X-ray photoelectron

spectroscopy, Fourier transform spectroscopy, Zeta potential measurement and sonication for 10 min in ultrapure water as a test of film stability [3, 24].

## 2.2 Animal experiments

### 2.2.1 Laboratory animals

24 male Lewis rats (age 100d; Charles River Laboratories, Sulzfeld, Germany) were kept in our in-house facilities under conventional housing and feeding conditions and were randomized into three groups with  $n = 8$  animals per group according to their implant type (Ti-PPAAm, Ti-PPAAC, Ti-Controls).

### 2.2.2 Implantation procedure and serum sampling

Anesthesia of the animals was performed by i.p. application of a mixture of Rompun® (Bayer, Leverkusen, Germany) and Ketamin® (Sanofi-Ceva, Düsseldorf, Germany). For each animal, one implant of the respective implant series was implanted into a small pocket in the neck musculature and fixed with a nonresorbable synthetic polypropylene suture (PROLENE®, Ethicon Endo-Surgery, Inc., Hamburg, Germany). Blood was drawn from the retro-orbital sinus one day prior to operation (pre-OP) and in weekly post-operative (post-OP) intervals for a period of 56 days. After centrifugation, serum samples were immediately shock-frozen in liquid nitrogen and stored at  $-80^{\circ}\text{C}$  until cytokine determination.

All animal experiments were carried out in accordance with the animal protection law of the Federal Republic of Germany in its new version of 1 January 1987, with the principles of care for animals in laboratories (drawn up by the National Society for Medical Research) and with the Guidelines for Keeping and Using Laboratory Animals (NIH Publication No.80–23, revised 1985).

## 2.3 Cytokine determination

The serum levels of the rat cytokines IL-2, IFN $\gamma$ , IL-6, IL-4, IL-10 and IL-13 were measured using sandwich enzyme-linked immunosorbent assays (ELISA) based on matched monoclonal antibody pair kits (Cytoset®, Invitrogen GmbH, Karlsruhe, Germany) according to the manufacturers protocols. Briefly, rat sera were analyzed in 1/10 and 1/20 dilutions in phosphate-buffered saline (PBS, PAA Laboratories, Cölbe, Germany) supplemented with 0.01% (w/v) sodium azide, 1% (w/v) bovine serum albumin (BSA, Sigma-Aldrich, Taufkirchen, Germany) and 0.05% (v/v) Tween-20 (Serva, Heidelberg, Germany). Following incubation with the secondary biotinylated antibodies and

addition of streptavidin-horseradish-peroxidase, 3,3',5,5'-tetramethylbenzidine (TMB) was used as colorimetric substrate (Sigma-Aldrich, Taufkirchen, Germany). Optical density measurement was performed with a MRX Revelation microtiter plate reader (Dynatech laboratories, Inc., Chantilly, VA, USA) at dual wavelength of 450/630 nm.

#### 2.4 Statistical data analysis

Cytokine concentrations were determined as mean of two dilutions. Results are given as median and interquartile range (IQR) of eight individual rat values per implant group for each cytokine per day. The non-parametric Mann–Whitney test was used to compare the median values from post-OP days 7 to 56 versus the pre-OP values. To test for differences between the variances in the experimental groups on different experimental days, the non-parametric Levene's test was used. Non-parametric Spearman's correlation analysis was performed to evaluate interactions between the different cytokines of all animals in each group over all experimental days. For all statistical analysis, two-tailed *P* values of <0.05 were considered significant. Statistical analysis was performed using the software system GraphPad Prism version 4.02 (GraphPad Software, Inc., San Diego, CA, USA).

### 3 Results

#### 3.1 Ti-PPAAm group

In the Ti-PPAAm group, the IL-2 level was significantly increased up to twofold in the early phase on day 7 (median 361 pg/ml) and day 14 (median 225 pg/ml) and in the middle phase on day 35 (376 pg/ml) compared to the pre-OP values (162 pg/ml; Table 1). The IFN $\gamma$  concentration was significantly elevated on day 35 only (median 120 pg/ml) compared to the pre-OP values (82 pg/ml). The IL-4 serum concentration did not change significantly throughout the study. IL-6 was not found in any sample. The IL-10 levels were significantly decreased in the middle phase on day 35 (96 pg/ml) and in the late phase on day 49 (94 pg/ml) and day 56 (101 pg/ml) compared to the pre-OP values (154 pg/ml). Measurable, but low IL-13 concentrations were found in two animals on day 7 (both at 7 pg/ml) and in another animal on day 14 (9 pg/ml). Correlation analysis of cytokine concentrations in individual animals demonstrated a highly negative correlation of IL-2 with IL-10 ( $P < 0.0001$ ) and IL-4 ( $P = 0.001$ ) and a highly positive correlation of IL-10 with IL-4 ( $P < 0.0001$ ) and to a lesser extent with IFN $\gamma$  ( $P = 0.017$ ) while there was no correlation between IFN $\gamma$  and either IL-2 or IL-4 (Table 2).

#### 3.2 Ti-PPAAC group

In the Ti-PPAAC group, the serum concentrations of the pro-inflammatory cytokines IL-2 and IFN $\gamma$  remained constant throughout the study (Table 1). For the IL-4 level, a significant increase was observed in the middle phase on day 28 (median 10 pg/ml) and day 35 (19 pg/ml) as well as in the late phase on day 42 (32 pg/ml), day 49 (25 pg/ml) and day 56 (36 pg/ml) compared to the pre-OP values (3 pg/ml). Especially in the late phase from days 42 to 56, the IL-4 concentration was up to tenfold enhanced. Concurrently, the IL-10 concentration was significantly decreased during the middle phase on day 42 (105 pg/ml) and the late phase on day 49 (67 pg/ml) and day 56 (90 pg/ml) to about half of the pre-OP values (195 pg/ml). Furthermore, a tendency for a decreased IL-10 level was also observed already on day 35 (98 pg/ml) which was however not statistically significant. Throughout the study, neither IL-6 nor IL-13 were detected in any sample. For cytokine concentrations in the individual animals, IL-2 was negatively correlated with IL-4 ( $P = 0.008$ ) but positively correlated with IL-10 ( $P = 0.001$ ) while IL-10 was highly negatively correlated with IL-4 ( $P < 0.0001$ ) and IFN $\gamma$  ( $P < 0.0001$ ) whereas IFN $\gamma$  was positively correlated with IL-4 ( $P = 0.001$ ) and similar to the Ti-PPAAm group did not show a correlation with IL-2 (Table 2).

#### 3.3 Ti-Controls group

In the Ti-Controls group, a significant increase of the IL-2 level was found in the late phase on day 42 (median 207 pg/ml) compared to the pre-OP values (134 pg/ml; Table 1). Furthermore, the IFN $\gamma$  concentration was significantly increased in the middle phase on day 35 (50 pg/ml) as well as in the late phase on day 42 (52 pg/ml) and day 56 (54 pg/ml) to about twofold of the pre-OP values (28 pg/ml). The serum concentrations of IL-4 and IL-10 remained constant over the study course, and no measurable levels were found for IL-6 and IL-13 in any sample. Within this group, a highly significant negative correlation between IL-2 and IL-10 ( $P < 0.0001$ ) and a highly positive correlation between IL-4 and IL-10 ( $P = 0.004$ ), both comparable to the Ti-PPAAm group, as well as a positive correlation between IL-2 and IFN $\gamma$  ( $P = 0.033$ ) were found (Table 2).

#### 3.4 Comparison of variances between the experimental groups

For the pro-inflammatory cytokines IL-2 and IFN $\gamma$ , the respective variances were compared to assess the variability of the data before implantation (day 0) and on two exemplarily chosen post-OP days (day 35 and day 56). On day 0, no significant difference between the variances of

**Table 1** Serum concentrations of IL-2, IFN $\gamma$ , IL-4 and IL-10 in rats which received implants treated with plasma-polymerized allylamine (Ti-PPAAM group), with plasma-polymerized acrylic acid (Ti-PPAAC group), or without either treatment (Ti-Controls group)

|             |              | Experimental day |                     |                    |                  |                  |                    |                     |                   |                   |
|-------------|--------------|------------------|---------------------|--------------------|------------------|------------------|--------------------|---------------------|-------------------|-------------------|
|             |              | Pre-OP           | 7                   | 14                 | 21               | 28               | 35                 | 42                  | 49                | 56                |
| Ti-PPAAM    | IL-2         | 162<br>(108–212) | 361 **<br>(244–490) | 225 *<br>(222–234) | 233<br>(137–364) | 208<br>(155–456) | 376 *<br>(191–538) | 220<br>(154–435)    | 172<br>(137–203)  | 259<br>(124–421)  |
|             | IFN $\gamma$ | 82<br>(66–87)    | 72<br>(57–94)       | 79<br>(73–96)      | 68<br>(63–102)   | 83<br>(58–106)   | 120 *<br>(87–161)  | 80<br>(72–137)      | 88<br>(81–116)    | 86<br>(70–112)    |
|             | IL-4         | 9<br>(0–44)      | 10<br>(0–44)        | 14<br>(0–34)       | 11<br>(0–38)     | 9<br>(0–26)      | 10<br>(0–27)       | 9<br>(0–26)         | 8<br>(0–21)       | 9<br>(0–20)       |
|             | IL-10        | 154<br>(63–259)  | 107<br>(66–197)     | 159<br>(72–185)    | 153<br>(55–180)  | 125<br>(52–178)  | 96 *<br>(27–235)   | 98<br>(26–282)      | 94 *<br>(21–214)  | 101 *<br>(29–203) |
|             |              |                  |                     |                    |                  |                  |                    |                     |                   |                   |
| Ti-PPAAC    | IL-2         | 46<br>(13–61)    | 28<br>(15–71)       | 50<br>(7–193)      | 47<br>(14–109)   | 52<br>(6–99)     | 69<br>(6–189)      | 81<br>(6–114)       | 62<br>(12–140)    | 49<br>(3–112)     |
|             | IFN $\gamma$ | 120<br>(107–124) | 120<br>(95–125)     | 113<br>(102–121)   | 113<br>(94–124)  | 107<br>(95–116)  | 110<br>(100–121)   | 115<br>(112–124)    | 111<br>(96–132)   | 113<br>(100–121)  |
|             | IL-4         | 3<br>(1–8)       | 2<br>(0–7)          | 7<br>(2–13)        | 5<br>(0–9)       | 10 *<br>(5–19)   | 19 **<br>(10–28)   | 32 **<br>(19–72)    | 25 **<br>(23–46)  | 36 **<br>(17–48)  |
|             | IL-10        | 195<br>(81–291)  | 108<br>(37–174)     | 177<br>(104–260)   | 175<br>(120–215) | 182<br>(108–266) | 98<br>(16–159)     | 105 *<br>(9–149)    | 67 **<br>(13–130) | 90 **<br>(23–158) |
|             |              |                  |                     |                    |                  |                  |                    |                     |                   |                   |
| Ti-Controls | IL-2         | 134<br>(47–173)  | 133<br>(60–170)     | 125<br>(78–171)    | 126<br>(50–148)  | 167<br>(43–197)  | 153<br>(94–223)    | 207 **<br>(203–235) | 183<br>(98–229)   | 182<br>(115–215)  |
|             | IFN $\gamma$ | 28<br>(19–35)    | 31<br>(18–43)       | 25<br>(19–39)      | 33<br>(22–49)    | 33<br>(29–47)    | 50 *<br>(38–78)    | 52 **<br>(53–61)    | 42<br>(30–70)     | 54 *<br>(36–71)   |
|             | IL-4         | 0<br>(0–14)      | 0<br>(0–0)          | 0<br>(0–0)         | 0<br>(0–0)       | 0<br>(0–14)      | 0<br>(0–0)         | 0<br>(0–7)          | 0<br>(0–8)        | 0<br>(0–0)        |
|             | IL-10        | 23<br>(9–43)     | 33<br>(7–47)        | 14<br>(6–49)       | 8<br>(4–31)      | 19<br>(5–58)     | 24<br>(6–35)       | 15<br>(4–32)        | 21<br>(7–37)      | 23<br>(10–39)     |
|             |              |                  |                     |                    |                  |                  |                    |                     |                   |                   |

Data are given in pg/ml as median (interquartile range) for  $n = 8$  animals per group. IL-6 and IL-13 were not detectable in any group throughout the study except for IL-13 for two individual animals on day 7 and one animal on day 14

Asterisks indicate significant differences (Mann–Whitney test) compared to the pre-OP value of the respective group: \*  $-P \leq 0.05$ ; \*\*  $-P \leq 0.01$

the 3 groups for either IL-2 ( $P = 0.127$ ) or IFN $\gamma$  ( $P = 0.591$ ) were found. On day 35, the variances differed significantly between the three groups for IFN $\gamma$  ( $P = 0.006$ ) while the difference narrowly failed to be significant for IL-2 ( $P = 0.092$ ). On day 56, a significant difference was found for IL-2 ( $P < 0.0001$ ) but not for IFN $\gamma$  ( $P = 0.187$ ). A comparison of the respective implant series indicates that these differences can be attributed to higher variances in the Ti-PPAAM and Ti-PPAAC groups compared to the Ti-Controls group.

#### 4 Discussion

Titanium and its alloys are in wide use as implant materials due to their excellent mechanical strength, their chemical stability and their well established biocompatibility [1]. However, recurring complications frequently require

re-implantation. Therefore, chemical surface modifications might help to further improve the clinical performance of Ti implants. We have recently investigated Ti surfaces treated with different low-temperature plasma processes in a number of in vitro studies and found favourable results for an amino-group rich positively charged surface resulting from a Plasma Polymerized Allyl Amine treatment (PPAAM) regarding growth, morphology and spreading of MG63 osteoblasts [2]. Furthermore, a carboxyl-group rich negatively charged surface created by a Plasma Polymerized Acrylic Acid treatment (PPAAC) stimulated mRNA expression of early and late bone differentiation markers [3]. Based on these in vitro results, the in vivo performance regarding the acute and chronic inflammation against Ti samples modified with PPAAM and PPAAC was investigated in the present study by intramuscular implantation in Lewis rats and weekly determination of the systemic profile of the pro-inflammatory cytokines IL-2, IFN $\gamma$  and IL-6

**Table 2** Evaluation of interactions between different cytokines by correlation analysis

|                         | Ti-PPAAm                       | Ti-PPAAC                       | Ti-Controls                    |
|-------------------------|--------------------------------|--------------------------------|--------------------------------|
| IL-2 with IL-4          | $r_s = -0.369$<br>$P = 0.001$  | $r_s = -0.312$<br>$P = 0.008$  | $r_s = -0.226$<br>$P = 0.056$  |
| IL-2 with IL-10         | $r_s = -0.523$<br>$P < 0.0001$ | $r_s = 0.395$<br>$P = 0.001$   | $r_s = -0.532$<br>$P < 0.0001$ |
| IFN $\gamma$ with IL-4  | $r_s = 0.139$<br>$P = 0.243$   | $r_s = 0.391$<br>$P = 0.001$   | $r_s = 0.113$<br>$P = 0.345$   |
| IFN $\gamma$ with IL-10 | $r_s = 0.280$<br>$P = 0.017$   | $r_s = -0.421$<br>$P < 0.0001$ | $r_s = 0.187$<br>$P = 0.115$   |
| IL-2 with IFN $\gamma$  | $r_s = -0.098$<br>$P = 0.415$  | $r_s = -0.207$<br>$P = 0.081$  | $r_s = 0.252$<br>$P = 0.033$   |
| IL-4 with IL-10         | $r_s = 0.749$<br>$P < 0.0001$  | $r_s = -0.640$<br>$P < 0.0001$ | $r_s = 0.336$<br>$P = 0.004$   |

In each of the three experimental groups (Ti-PPAAm, Ti-PPAAC, Ti-Controls), the serum cytokine concentrations for all animals of the respective group on all experimental days were analyzed by non-parametric Spearman's correlation analysis to examine associations between the levels of IL-2, IL-4, IL-10 and IFN $\gamma$  with each other. IL-6 and IL-13 were not included in this analysis due to absence of measurable concentrations in serum. Data are given as Spearman's-Rho correlation coefficient  $r_s$  and  $P$ -value

as well as the anti-inflammatory cytokines IL-4, IL-10 and IL-13 for up to 56 days.

Overall, the results demonstrate a distinct pattern of systemic cytokine levels and associations depending on the surface treatment. This is generally in agreement with data previously reported by Schutte et al. [9] who examined the cytokine response in exudate from steel implant cages containing different polymer samples. Regarding the cytokines which were examined in the present study, they observed material-specific differences for IL-6 and IL-10 in the acute phase on day 1 as well as for IL-6 in the chronic phase on day 28. For IL-6 and IL-10, Schutte et al. reported concentrations up to 10,000 pg/ml while they found levels below 100 pg/ml for IL-4 as well as between 100 and 1,000 pg/ml in the acute phase and between 10 and 100 pg/ml in the chronic phase for IL-2. The magnitude and range of the results in the present study are comparable to these data for IL-4 while Schutte et al. found markedly higher levels for the other cytokines, especially in the very early acute phase. It has however to be kept in mind that they examined cytokine concentrations in exudate fluid drawn from the local vicinity of the implants as opposed to systemic serum levels as determined in the present study. Furthermore, day 1 after implantation for which Schutte et al. reported the highest concentrations was not included in the study period of the present study.

In the Ti-PPAAm group, IL-2 was elevated on days 7 and 14, indicating an increased acute inflammatory response. IL-2 is known to induce growth and proliferation

of T cells. Interestingly, in an earlier study we found a higher number of T cells in the peri-implant tissue of Ti-PPAAm samples compared to the controls especially on day 14 [25]. The IL-2 increase in the early phase in the present study might thus be associated with this higher T cell response. Another noteworthy observation in the Ti-PPAAm group was an additional distinct increase in the pro-inflammatory cytokine response as indicated by an increase of IL-2 and IFN $\gamma$  on day 35 which was followed by a slight but persistent reduction of IL-10 until the end of the study. It seems therefore that there is a transition around day 35 between two distinct phases of the systemic inflammatory reactions in the Ti-PPAAm group. In our earlier examination of local tissue reactions against different Ti-PPAAm implants series we also observed a number of changes for the physico-chemical properties of the surfaces. This included an increase of the O/C and the Ti/C ratios from day 7 to 56 [25] indicating that Ti became more visible to the surrounding tissue as the PPAAm layer was gradually degraded. However, due to study design the time points used in our earlier histological examination (days 7, 14 and 56) did not include day 35. Thus it's not possible from the data of both studies to establish a definitive link between the cytokine response on that day and corresponding changes in the implant surface properties. PPAAm film degradation could however be a plausible explanation for the two distinct phases of the systemic cytokine profile.

The Ti-PPAAC group differed from the Ti-PPAAm and Ti-Controls groups regarding the pro-inflammatory cytokines as both IL-2 and IFN $\gamma$  remained constant throughout the study. Furthermore, the Ti-PPAAC group was also the only with a significant IL-4 increase which was observed from day 28 to 56. In addition to the late phase IL-4 increase, the IL-10 level was moderately decreased from day 42 to 56. Such contrary changes for these two cytokines are noteworthy as they have similar effects on most aspects of the immune system [17, 19]. Interestingly, opposite or antagonistic effects of IL-4 and IL-10 were also reported in a number of studies regarding infection and tumor immunology [26–28]. As possible explanation, Marfaing-Koka et al. [26] discussed that IL-4 does not affect NF- $\kappa$ B activity in monocytes, resulting in IL-4 influencing the characteristics of an ongoing immune response rather than being a 'general deactivator' of cellular immunity like IL-10. Specht et al. [28] proposed a potential influence of IL-13 and IFN $\gamma$  but did not find support for a role of these two cytokines in additional experiments. From our results, there is also no indication for an involvement of these two cytokines regarding the antagonistic time course of IL-4 and IL-10 as IL-13 was not detected in any sample of the Ti-PPAAC group and IFN $\gamma$  did not change throughout the study in this group.

For the Ti-Controls group, a transient IL-2 increase on day 42 as well as a sustained IFN $\gamma$  increase from day 35 to 56 was observed while IL-4 and IL-10 remained unchanged. As these changes were moderate compared to the pre-OP level for IL-2 and IFN $\gamma$  it is unlikely that they reflect a strong pro-inflammatory response. For IL-2, these results are generally similar to other studies in which Ti did not elicit changes either in the IL-2 gene expression [29] or its secretion from stimulated splenic lymphocytes [30]. The lack of an IL-10 response after implantation of Ti was also observed by Suska et al. [31] who examined IL-10 in implant-interface exudate however only 12 and 48 h after implantation.

The analysis of correlations between IL-2, IFN $\gamma$ , IL-4 and IL-10 (Table 2) reveals a number of noticeable observations. First, there was a strong negative correlation between IL-4 and IL-2 in the Ti-PPAAm and Ti-PPAAC groups with a similar but narrowly not significant trend in the Ti-Controls group. This is consistent with the anti-inflammatory effects of IL-4 and with previous reports that IL-4 inhibits IL-2 secretion by dendritic cells [32] or by stimulated T cells [33]. Second, the known mutual antagonistic relationship between the anti-inflammatory IL-4 and the pro-inflammatory IFN $\gamma$  [14] is not reflected by the correlation analysis as there is no significant correlation between these two cytokines in the Ti-PPAAm and Ti-Controls group and a strong positive correlation in the Ti-PPAAC group. The observation in the Ti-PPAAC group is remarkable because IL-4 was previously found to induce IFN $\gamma$  production by NK cells while both inhibit each other's production by T cells [34]. Third, a highly significant negative correlation between IL-10 and IL-2 was found in the Ti-PPAAm and Ti-Controls groups, consistent with the fact that IL-10 was shown to inhibit IL-2 production by T cells [35]. However, deviating from these two groups a strong positive correlation between IL-10 and IL-2 was observed in the Ti-PPAAC group. Interestingly, NK cells were previously found to produce IL-10 following stimulation with IL-2 [36]. Fourth, IL-10 also demonstrated a divergent behaviour in the Ti-PPAAC group regarding its highly significant negative correlation with IFN $\gamma$ . While this is in line with the known opposite effects of both cytokines [14, 19], the fact that this antagonism is reflected by the correlation analysis only in the Ti-PPAAC group points to a possible IL-10-mediated inhibition of IFN $\gamma$  production by NK cells, as previously reported for in vitro experiments [37], specifically occurring in this group. Taken together, the results of the correlation analysis indicate a distinct role for NK cells in the Ti-PPAAC group which received implants with a carboxyl-rich negatively charged surface. This is of particular interest as a possible role of NK cells in implant-related inflammatory reactions has not been studied in much detail so far based on the

established knowledge about their functions in the immune system.

The nearly complete absence of IL-6 and IL-13 in all three groups throughout the study might be due to their serum concentrations being lower than the detection limits of the respective assays. Furthermore, a lack of a systemic IL-13 response was also reported by other authors for example for multiple sclerosis [38] or for clinical sepsis [39], indicating that the action of IL-13 is restricted to specific situations. For IL-6, an increase of its serum concentration following surgical trauma has been described previously [40], with a peak at 24 h after OP and no detectable levels 72 h after surgery. In another study, no IL-6 was found in serum from patients with different benign lung diseases [41]. Furthermore, in patients with a hip prosthesis IL-6 serum levels were very low for patients with and without osteolysis and did not differ from healthy controls without prosthesis [42]. On the other hand it was recently reported that carriers of a specific IL-6 gene SNP allele had a more than twofold risk for severe acetabular osteolysis following implantation of a hydroxyapatite-coated total hip prosthesis [12]. However, functional consequences of SNP polymorphisms are often unknown, thus an IL-6 gene polymorphism does not necessarily impact its expression levels. The results of the present study suggest that implantation-related inflammatory reactions against Ti implants do not involve a systemic release of IL-6 and IL-13. Further studies are however required as this probably depends on the examined time points and materials as demonstrated by the previously discussed results of Schutte et al. [9] for polymeric materials one day after implantation. Similarly, Brodbeck et al. [43] observed material-specific differences for IL-6 and IL-13 in adherent and exudate cells following implantation of surface-modified polyethylene terephthalate samples.

Overall, this study demonstrates distinct changes in the time course of the serum levels of pro- and anti-inflammatory cytokines after implantation of Ti samples chemically modified with different functional groups via low-temperature plasma processes. Interestingly, a similar finding of material-dependent changes of serum cytokine levels following subcutaneous implantation of four different materials (hydroxyapatite foam and granules, poly-e-caprolactone mesh, cross-linked type I collagen) in mice for 7, 14 and 28 days was also recently reported by Scaglione et al. [44] for FGF-2, IL-5, IL-12, MCP-1, and TNF $\alpha$ . The six cytokines included in the present study (IL-2, IFN $\gamma$ , IL-6, IL-4, IL-10, IL-13) did not change in that study which can be explained by a number of reasons. First, with the exception of the early IL-2 response in the Ti-PPAAm group most changes in the present study occurred after day 28, the end of the study period used by Scaglione et al., highlighting the relevance of long-term

observations. Second, different animal models (mice vs. rats), implantation sites (s.c. vs. i.m.) and materials (osteoconductive scaffolds vs. plasma-modified Ti plates) might also be responsible for the different observations. In addition to material-specific patterns in the serum profiles, distinct alterations in the associations between the different cytokines were observed in the different groups, possibly mediated by material-dependent interactions with certain immune cells. Furthermore, a large individual variability was found as indicated by significant differences between the groups of the variances for the pro-inflammatory cytokines IL-2 and IFN $\gamma$  on two exemplarily chosen post-OP days but not prior to implantation. Notably, the increased post-OP variability of the individual response was mainly observed in the Ti-PPAAm and Ti-PPAAC groups in contrast to the Ti-Controls group.

## 5 Conclusion

In summary, the findings of this study indicate that the systemic cytokine profile could be an additional parameter for in vivo examination of new or modified biomaterials as well as for in vivo monitoring or outcome prediction after implantation as recently demonstrated by Caruso et al. [45] for patients with left ventricular assist devices. Further studies including the analysis of different inflammatory cell populations at different time points could clarify the reasons for the observed differences between the materials regarding the time course of the cytokines and their correlations with each other as well as the possible associations of the serum cytokine levels with the local reactions at the implantation site. This could also help to understand the relationship between material properties, the systemic and local material-related inflammatory and immune reactions and the implant function, thereby elucidating the mediating role of cytokines within these interactions.

**Acknowledgments** We are grateful to Kirsten Tornow and Urte Kellner for excellent technical support. This study was supported by the Federal state of Mecklenburg-Vorpommern and the Helmholtz Association of German Research Centres (grant no. VH-MV1) and by the Federal Ministry of Education and Research (grant no. 13N9779, Campus PlasmaMed).

## References

1. Esposito M. Titanium for dental applications. In: Brunette DM, Tengvall P, Textor M, Thomsen P, editors. *Titanium in medicine*. Berlin: Springer; 2001. p. 172–230.
2. Finke B, Lüthen F, Schröder K, Mueller PD, Bergemann C, Frant M, Ohl A, Nebe BJ. Positively charged plasma polymerized titanium boosts osteoblastic focal contact formation in the initial adhesion phase. *Biomaterials*. 2007;28:4521–34.
3. Schröder K, Finke B, Ohl A, Lüthen F, Bergemann C, Nebe B, Rychly J, Walschus U, Schlosser M, Liefelth K, Neumann HG, Weltmann KD. Capability of differently charged plasma polymer coatings for control of tissue interactions with titanium surfaces. *J Adhes Sci Technol*. 2010;24:1191–205.
4. Xia Z, Triffitt T. A review on macrophage responses to biomaterials. *Biomed Mater*. 2006;1:R1–9.
5. Davis C, Fischer J, Ley K, Sarembock IJ. The role of inflammation in vascular injury and repair. *J Thromb Haemost*. 2003;1:1699–709.
6. Rodriguez A, Voskerician G, Meyerson H, MacEwan SR, Anderson JM. T cell subset distributions following primary and secondary implantation at subcutaneous biomaterial implant sites. *J Biomed Mater Res A*. 2008;85:556–65.
7. Goodman SB. Wear particles, periprosthetic osteolysis and the immune system. *Biomaterials*. 2007;28:5044–8.
8. Wang C, Lennartz MR, Loegering DJ, Stenken JA. Multiplexed cytokine detection of interstitial fluid collected from polymeric hollow tube implants—a feasibility study. *Cytokine*. 2008;43: 15–9.
9. Schutte RJ, Xie L, Klitzman B, Reichert WM. In vivo cytokine-associated responses to biomaterials. *Biomaterials*. 2009;30: 160–8.
10. Rodriguez A, Meyerson H, Anderson JM. Quantitative in vivo cytokine analysis at synthetic biomaterial implant sites. *J Biomed Mater Res A*. 2009;89:152–9.
11. Pereira-Lucena CG, Artigiani-Neto R, Lopes-Filho GJ, Frazao CV, Goldenberg A, Matos D, Linhares MM. Experimental study comparing meshes made of polypropylene, polypropylene + polyglactin and polypropylene + titanium: inflammatory cytokines, histological changes and morphometric analysis of collagen. *Hernia*. 2010;14:299–304.
12. Gallo J, Mrazek F, Petrek M. Variation in cytokine genes can contribute to severity of acetabular osteolysis and risk for revision in patients with ABG 1 total hip arthroplasty: a genetic association study. *BMC Med Genet*. 2009;10:109.
13. Smith KA. IL-2. In: Oppenheim JJ, Feldmann M, editors. *Cytokine reference: a compendium of cytokines and other mediators of host defense*. San Diego: Academic Press; 2001. p. 113–25.
14. Billiau A, Vandebroeck K. IFN $\gamma$ . In: Oppenheim JJ, Feldmann M, editors. *Cytokine reference: a compendium of cytokines and other mediators of host defense*. San Diego: Academic Press; 2001. p. 641–88.
15. Martinez FO, Helming L, Gordon S. Alternative activation of macrophages: an immunologic functional perspective. *Ann Rev Immunol*. 2009;27:451–83.
16. Billiau A, Matthys P. Interferon- $\gamma$ : a historical perspective. *Cytokine Growth Factor Rev*. 2009;20:97–113.
17. Matsuda T, Hirano T. IL-6. In: Oppenheim JJ, Feldmann M, editors. *Cytokine reference: a compendium of cytokines and other mediators of host defense*. San Diego: Academic Press; 2001. p. 537–63.
18. Keegan AD. IL-4. In: Oppenheim JJ, Feldmann M, editors. *Cytokine reference: a compendium of cytokines and other mediators of host defense*. San Diego: Academic Press; 2001. p. 127–35.
19. RdW Malefyt. IL-10. In: Oppenheim JJ, Feldmann M, editors. *Cytokine reference: a compendium of cytokines and other mediators of host defense*. San Diego: Academic Press; 2001. p. 165–85.
20. Mosser DM, Zhang X. Interleukin-10: new perspectives on an old cytokine. *Immunol Rev*. 2008;226:205–18.
21. Kou PM, Babensee JE. Macrophage and dendritic cell phenotypic diversity in the context of biomaterials. *J Biomed Mater Res A*. 2011;96:239–60.

22. McKenzie ANJ, Matthews DJ. IL-13. In: Oppenheim JJ, Feldmann M, editors. *Cytokine reference: a compendium of cytokines and other mediators of host defense*. San Diego: Academic Press; 2001. p. 203–11.
23. Wynn TA. IL-13 effector functions. *Annu Rev Immunol*. 2003;21:425–56.
24. Finke B, Schröder K, Ohl A. Structure retention and water stability of microwave plasma polymerized films from allylamine and acrylic acid. *Plasma Process Polym*. 2009;6:S70–4.
25. Hoene A, Walschus U, Patrzik M, Finke B, Lucke S, Nebe B, Schröder K, Ohl A, Schlosser M. In vivo examination of the inflammatory response against allylamine plasma polymer coated titanium implants in a rat model. *Acta Biomater*. 2010;6:676–83.
26. Marfaing-Koka A, Maravic M, Humbert M, Galanaud P, Emilie D. Contrasting effects of IL-4, IL-10 and corticosteroids on RANTES production by human monocytes. *Int Immunol*. 1996;8:1587–94.
27. Terres G, Coffman RL. The role of IL-4 and IL-10 cytokines in controlling an anti-tumor response in vivo. *Int Immunol*. 1998;10:823–32.
28. Specht S, Volkmann L, Wynn T, Hoerauf A. Interleukin-10 (IL-10) counterregulates IL-4-dependent effector mechanisms in Murine Filariasis. *Infect Immun*. 2004;72:6287–93.
29. Baldwin L, Hunt JA. Host inflammatory response to NiCr, CoCr and Ti in a soft tissue implantation model. *J Biomed Mater Res A*. 2006;79:574–81.
30. Wang JY, Wicklund BH, Gustilo RB, Tsukayama DT. Prosthetic metals impair murine immune response and cytokine release in vivo and in vitro. *J Orthop Res*. 1997;15:688–99.
31. Suska F, Gretzer C, Esposito M, Emanuelsen L, Wennerberg A, Tengvall P, Thomsen P. In vivo cytokine secretion and NF- $\kappa$ B activation around titanium and copper implants. *Biomaterials*. 2005;26:519–27.
32. Sauma D, Michea P, Lennon-Duménil AM, Fierro A, Morales J, Rosemblatt M, Bono MR. Interleukin-4 selectively inhibits interleukin-2 secretion by lipopolysaccharide-activated dendritic cells. *Scand J Immunol*. 2004;59:183–9.
33. Tanaka T, Hu-Li J, Seder RA, Fazekas de St Groth B, Paul WE. Interleukin 4 suppresses interleukin 2 and interferon gamma production by naive T cells stimulated by accessory cell-dependent receptor engagement. *Proc Natl Acad Sci USA*. 1993;90:5914–8.
34. Morris SC, Orekhova T, Meadows MJ, Heidorn SM, Yang J, Finkelman FD. IL-4 induces in vivo production of IFN-gamma by NK and NKT cells. *J Immunol*. 2006;176:5299–305.
35. Taga K, Tosato G. IL-10 inhibits human T cell proliferation and IL-2 production. *J Immunol*. 1992;148:1143–8.
36. Mehrotra PT, Donnelly RP, Wong S, Kanegae H, Geremew A, Mostowski HS, Furuke K, Siegel JP, Bloom ET. Production of IL-10 by human natural killer cells stimulated with IL-2 and/or IL-12. *J Immunol*. 1998;160:2637–44.
37. D'Andrea A, Aste-Amezaga M, Valiante NM, Ma X, Kubin M, Trinchieri G. Interleukin 10 (IL-10) inhibits human lymphocyte interferon gamma-production by suppressing natural killer cell stimulatory factor/IL-12 synthesis in accessory cells. *J Exp Med*. 1993;178:1041–8.
38. Nicoletti F, Marco RD, Patti F, Nicoletti A, Leonardi C, Reggio E, Meroni P, Reggio A. The antiinflammatory cytokine interleukin-13 is not detectable in the circulation of multiple sclerosis patients and is not inducible by interferon-beta1b treatment, that neither modifies its ex vivo secretion from peripheral blood mononuclear cells. *Autoimmunity*. 2000;32:265–70.
39. van der Poll T, de Waal Malefyt R, Coyle SM, Lowry SF. Antiinflammatory cytokine responses during clinical sepsis and experimental endotoxemia: sequential measurements of plasma soluble interleukin (IL)-1 receptor type II, IL-10, and IL-13. *J Infect Dis*. 1997;175:118–22.
40. Maruszynski M, Pojda Z. Interleukin 6 (IL-6) levels in the monitoring of surgical trauma. A comparison of serum IL-6 concentrations in patients treated by cholecystectomy via laparotomy or laparoscopy. *Surg Endosc*. 1995;9:882–5.
41. Yanagawa H, Sone S, Takahashi Y, Haku T, Yano S, Shinohara T, Ogura T. Serum levels of interleukin 6 in patients with lung cancer. *Br J Cancer*. 1995;71:1095–8.
42. Fiorito S, Magrini L, Goalard C. Pro-inflammatory and anti-inflammatory circulating cytokines and periprosthetic osteolysis. *J Bone Joint Surg Br*. 2003;85:1202–6.
43. Brodbeck WG, Voskerician G, Ziats NP, Nakayama Y, Matsuda T, Anderson JM. In vivo leukocyte cytokine mRNA responses to biomaterials are dependent on surface chemistry. *J Biomed Mater Res A*. 2003;64:320–9.
44. Scaglione S, Cilli M, Fiorini M, Quarto R, Pennesi G. Differences in chemical composition and internal structure influence systemic host response to implants of biomaterials. *Int J Artif Organs*. 2011;34:422–31.
45. Caruso R, Trunfio S, Milazzo F, Campolo J, De Maria R, Colombo T, Parolini M, Cannata A, Russo C, Paino R, Frigerio M, Martinelli L, Parodi O. Early expression of pro- and anti-inflammatory cytokines in left ventricular assist device recipients with multiple organ failure syndrome. *ASAIO J*. 2010;56:313–8.

# Application of Low-Temperature Plasma Processes for Biomaterials

Uwe Walschus<sup>1</sup>, Karsten Schröder<sup>2</sup>, Birgit Finke<sup>2</sup>,  
Barbara Nebe<sup>3</sup>, Jürgen Meichsner<sup>1</sup>, Rainer Hippler<sup>1</sup>,  
Rainer Bader<sup>3</sup>, Andreas Podbielski<sup>3</sup> and Michael Schlosser<sup>1</sup>

<sup>1</sup>*University of Greifswald, Greifswald*

<sup>2</sup>*Leibniz Institute for Plasma Science and Technology, Greifswald*

<sup>3</sup>*University of Rostock, Rostock  
Germany*

## 1. Introduction

Physical plasma is defined as a gas in which part of the particles that make up the matter are present in ionized form. This is achieved by heating a gas leading to dissociation of the molecular bonds and subsequently ionization of the free atoms. Thereby, plasma consists of positively and negatively charged ions and negatively charged electrons as well as radicals, neutral and excited atoms and molecules (Raizer, 1997; Conrads and Schmidt, 2000). On the one hand, plasma is a natural phenomenon as more than 90 % of the universe is in the plasma state, for example in fire, in the polar aurora borealis and perhaps most importantly in the nuclear fusion reactions of the sun. On the other hand, plasma can be created artificially and has found applications in technology like plasma screens or light sources. The use of high temperature plasma for energy production is still the focus of ongoing research.

For the modification of biomaterial surfaces, low temperature plasma which is sometimes also called cold plasma is used. It is characterized by a low degree of ionization at low or atmospheric pressure (Roth, 1995; Roth 2001; Hippler et al., 2008). To create low temperature plasmas, a compound is first transformed into a gas and then ionized by applying energy in the form of heat, direct or alternating electric current, radiation or laser light. Commonly used plasma gas sources are oxygen, nitrogen, hydrogen or argon. Two typical research plasma reactors for different applications are shown in Fig. 1. Depending on the nature and amount of energy, low temperature plasmas are characterized by a non-equilibrium between electron temperature and gas temperature. Thus the main parameters which define the characteristics of a plasma and thereby its applicability are its temperatures, types and densities of radicals and its level of ionization. In material science, possible applications of low-temperature plasmas include the modification of surface properties like electrochemical charge or amount of oxidation as well as attachment or modification of surface-bound chemical groups. Consequently, properties like hardness, resistance to chemical corrosion or physical abrasion, wettability, the water absorption capacity as well as the affinity toward

specific molecules can be modulated specifically and precisely by the use of low-temperature plasmas (Meichsner et al., 2011).

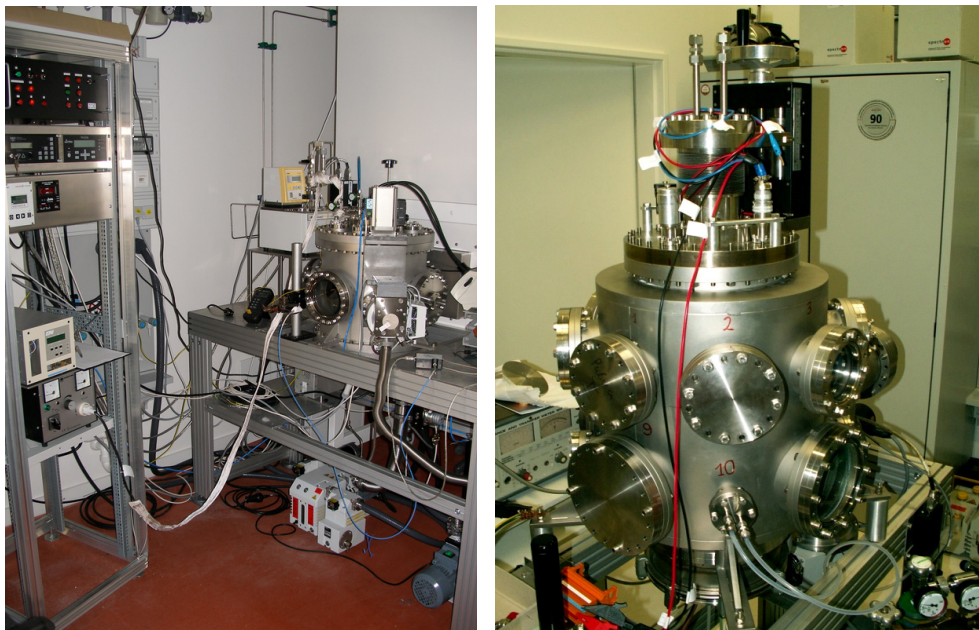


Fig. 1. Laboratory-size low-temperature plasma reactors for argon / ethylenediamine plasma (left) and pulsed magnetron sputtering (right)

Plasma treatments can be used to improve different aspects of the therapeutic characteristics of medical implants (Ohl & Schröder, 2008; Schröder et al., 2011). Possible applications include the incorporation of therapeutic agents into implants or the attachment of drug molecules onto the material surface. This includes for example plasma processes used for surface coupling of antibiotic substances or for integration of metal ions into biomaterial surfaces to create implants which exhibit long-lasting antibacterial properties after implantation. By creating such implants with antibacterial properties, the often devastating effects of implant-related infections could be markedly reduced. Therapeutic agents for other applications can be loaded onto implant surfaces via plasma treatment as well to achieve their controlled release over time. Possible applications are drug-eluting stents and vascular prostheses which release drugs to reduce blood coagulation and thrombosis as well as to prevent intima hyperplasia and restenosis.

Low-temperature plasma-modified surfaces were furthermore found to possess specific bioactive properties *in vitro* and *in vivo*. For example, such surfaces influence the attachment and growth of osteoblasts, fibroblasts and inflammatory cells which provides the possibility to enhance implant ingrowth and tissue regeneration as well as to reduce implant-related inflammation, thereby improving the biocompatibility. Another field of application is plasma sterilization of prosthetic materials which is a gentle approach that can be adapted for many different materials and which is especially advantageous over

conventional methods regarding the required time. From a process technology point of view, sterilization would also be a beneficial concomitant effect of other plasma treatments aimed at modulating specific material properties. The range of materials which can be treated with low-temperature plasma processes includes many materials with an established track record in regenerative medicine, for example ceramics like hydroxyapatite, polymeric materials like polyester, polypropylene, silicone and polytetrafluoroethylene, and metals like titanium, titanium-based alloys and steel. Consequently, the possible utilization of plasma treatments in the field of biomaterials includes a wide range of applications in cardiovascular and reconstructive surgery, orthopaedics and dentistry. Therefore, low-temperature plasma processes have great potential for improvement of medical implants. In the following, a concise overview of the respective applications and the underlying plasma processes is presented, putting an emphasis on recent developments. The main directions of research in this developing field are reviewed in terms of the respective aims, the relevant materials and the potential clinical applications.

## 2. Plasma-assisted creation of implants containing therapeutic compounds

The coating of implant surfaces with therapeutic agents is an interesting approach to improve the clinical outcome of implantation. In this field, the treatment with plasma can be used to either facilitate the surface attachment of the respective drug itself or to create a layer on top of a coating with a therapeutic compound to modulate the kinetics of its release. Among the multitude of possible applications, recent research activities are focused on two main directions: the equipment of implants with antibiotics and other compounds with antibacterial properties to prevent implant-related infections and the coating with anti-thrombogenic agents to prevent the formation of blood clots and thrombosis for implants with blood contact like vascular prostheses and stents. In principle, most of the plasma-based approaches used in these areas could also be applied with other drugs which have already been examined for drug-eluting implants, for example paclitaxel and everolimus (Butt et al., 2009), dexamethasone (Radke et al., 2004) or trapidil, probucol and cilostazol (Douglas, 2007) all aimed at reducing restenosis after implantation of vascular stents which is an emerging and clinically promising field for controlled drug release in biomaterials research.

### 2.1 Implant surfaces with antibacterial properties

The equipment of implants with antibacterial properties can be achieved either by attaching antibiotic substances or by creating surfaces which release metal ions which are known to have anti-infective effects. Polyvinylchloride, a polymer which is used for endotracheal tubes and catheters, was equipped with triclosan and bronopol, compounds with immediate and persistent broad-spectrum antimicrobial effects, after the surface was activated with oxygen plasma to produce more hydrophilic groups for effective coating (Zhang et al., 2006). Experiments using *Staphylococcus aureus* and *Escherichia coli* demonstrated the effectiveness of these surfaces. Similarly, polyvinylidenefluoride used for hernia meshes was modified by plasma-induced graft polymerization of acrylic acid with subsequent binding of the antibiotic gentamycin (Junge et al., 2005). In addition to the microbiological examination of the gentamycin-releasing material, the in vitro and in vivo biocompatibility was examined by cytotoxicity testing and implantation into Sprague-Dawley rats for up to 90 days, and no side effects on biocompatibility were observed. The fact that an implant

coating with a sustained release of gentamycin is effective against bacteria with no adverse effects on cellular proliferation was also confirmed by the evaluation of titanium implants with gentamycin grafted onto the surface of a plasma sprayed wollastonite coating (Li et al., 2008). Wollastonite was previously found to be a promising material for bone tissue repair due to its high bonding strength to titanium substrates, its mechanical properties and its bioactivity and biocompatibility (Liu et al., 2008).

Due to their well-known antibacterial effects, metals like silver, copper or tin are possible alternatives to classical antibiotic compounds as an effective and sustained release from coatings is possibly easier to achieve due to their small size. Similarly to gentamycin as mentioned before, silver has been used as a powder added to a plasma-sprayed wollastonite coating on titanium implants (Li et al., 2009). In comparison to a coating without silver, tests with *Escherichia coli* confirmed the antibacterial activity of the silver while an examination of osteoblast morphology revealed no obvious difference between both coatings. Furthermore, the release of silver was also examined for amino-hydrocarbon plasma polymer coatings (Lischer et al., 2011), after plasma immersion ion implantation into polyethylene (Zhang et al., 2008) and for silver nanoparticles bound to an allylamine plasma polymer thin film (Vasilev et al., 2010b). Similarly, the use of copper for antibacterial implant coatings has also been studied by plasma implantation into polyethylene (Zhang et al., 2007). The use of plasma immersion ion implantation is however not restricted to polymer materials as demonstrated by recent work on the application of this process for equipment of titanium surfaces with copper ions (Polak et al., 2010). Compared to controls, the implants created by this Plasma immersion ion implantation of copper reduced the number of methicillin-resistant *Staphylococcus aureus* cultivated on the respective surfaces (Schröder et al., 2010a). Ion implantation can also be used for non-metals like fluorine which is of particular relevance for dental applications. This was examined with titanium, stainless steel and polymethyl methacrylate for fluorine alone (Nurhaerani et al., 2006) or with stainless steel for a combination of fluorine with silver (Shinonaga & Arita, 2009).

## 2.2 Implant surfaces with reduced thrombogenicity

Another field of interest for plasma applications is the coating of implants with anti-thrombogenic agents. This is of special importance for vascular prostheses and stents which are in constant contact with blood. For these implants, thrombosis and blood clot formation are severe and potentially life-threatening complications. Classical anti-coagulants used for thrombosis prophylaxis and treatment include coumarin derivates like phenprocoumon for oral application as well as heparin which is physiologically found in the body and extracted for medicinal use from mucosal tissues of slaughtered meat animals and hirudin, originally from the European medical leech *Hirudo medicinalis*, for parenteral use. The Plasma-based attachment of heparin has for example been examined for stainless steel which is used in stents (Yang et al., 2010). For this application, a pulsed-plasma polymeric allylamine film with a high amino group density was created to subsequently immobilize heparin via its carboxylic groups and established coupling chemistry using 1-Ethyl-3-(3-dimethylaminopropyl) carbodiimide and N-Hydroxysuccinimide. In a similar way, a heparin coating of polystyrene surfaces was achieved by preadsorption with undecylenic acid, a FDA-approved natural fungicide for skin disorders, followed by treatment with argon plasma and covalent immobilization of an albumin-heparin conjugate (van Delden et

al., 1997). Another example is the heparinization of polyurethane by low temperature plasma and grafting of poly(acrylic acid), water-soluble chitosan and heparin (Lin et al., 2005). In addition to well-established anti-coagulants, the endothelial membrane protein thrombomodulin, a co-factor in the thrombin-activated anticoagulant pathway, has also been examined regarding plasma-based attachment on biomaterial surfaces. This application was studied for polytetrafluoroethylene, a common material for vascular prostheses, via CO<sub>2</sub> plasma activation and subsequent vapour phase graft polymerization of acrylic acid (Vasilets et al., 1997; Sperling et al., 1997). Another surface modification which was examined for reduced thrombogenicity was plasma-induced graft polymerization of 2-methacryloyloxyethyl phosphorylcholine on titanium alloy surfaces which resulted in reduced deposition and activation of platelets in subsequent in vitro experiments with ovine blood (Ye et al., 2009).

### 2.3 Regulation of drug release by barrier layers

In addition to plasma-assisted surface attachment of therapeutic compounds, plasma processes can also be used to create an over-coating which acts as a barrier to regulate the drug release. This application has for example been examined using daunomycin, an antibiotic substance, and rapamycin, a compound with immunosuppressive and anti-proliferative effects which is used for example in stents to prevent excessive tissue growth, in combination with a plasma polymerized tetramethylcyclo-tetrasiloxane coating (Osaki et al., 2011). Changing the deposition time length resulted in different coating thickness which, like the molecular weight of the drug, was found to influence the drug-release rate. A comparable approach was used on polyetherurethane onto which a plasma-deposited poly(butyl methacrylate) membrane with controlled porosity was applied to control the release of ciprofloxacin (Hendricks et al., 2000). Adhesion and colonization of *Pseudomonas aeruginosa* was evaluated to assess the antimicrobial effectiveness.

Furthermore, an over-coating can also be applied to surfaces which release metal ions. For instance, the antibacterial surfaces created by plasma immersion ion implantation of copper as mentioned before were also treated with an additional layer of plasma-polymerized allylamine to regulate the Cu release and to modulate cellular adhesion and spreading. This combination reduced the antibacterial effects of the surface to some extent but did not completely disable it (Schröder et al., 2010a). On the other hand, the combined treatment also led to lower local inflammatory reactions after implantation into rats (Schlosser, unpublished data), highlighting the need to find an optimal balance between in vivo biocompatibility and sufficient antibacterial effects. Another study demonstrated that creation of thin films by plasma polymerization for controlled release of silver ions and traditional antibiotics is applicable to the surface of many different medical devices (Vasilev et al., 2010a).

The use of an over-coating to regulate the release rate is not only possible for antibiotics but also for antithrombogenic agents. This has for example been studied for hirudin for which an additional layer of 2-hydroxyethyl methacrylate created by glow discharge plasma deposition on drug-loaded polyurethane matrices served as a diffusional barrier controlling the hirudin release kinetics depending on the plasma coating conditions (Kim et al., 1998).

Of more general interest for the field of drug-releasing implants is a recent study which describes the use of liposomes, artificial vesicles enclosed by a lipid bilayer. Liposomes can

be used as drug containers by encapsulation of therapeutic compounds, in some cases additionally targeted to their site of action by antibodies, and potentially offer a wide range of applications. Covalent coating of liposomes onto stainless steel was achieved via radiofrequency glow plasma assisted creation of a thin film of acrylic acid characterized by surface carboxylic groups to which the liposomes were attached via formation of amide bonds (Mourtas et al., 2011). While the study was considered by the authors to be a proof of principle, the presented method seems to be a versatile approach due to possible changes of process parameters for the liposome immobilization procedure as well as regarding the choice of different drugs for encapsulation.

### 3. Plasma-based surface functionalization

Medical implants interact with their surrounding tissue in a complex manner. For example, a so called neointima layer is formed over time at the inner surface of vascular prostheses. Bone implants based on calcium phosphate possess osteoconductive and osteoinductive properties. Most importantly, all biomaterials are foreign to the body and the aim of acute and chronic inflammatory reactions which can persist for as long as the implant remains in the body. While short-term temporary implants which are removed some time after implantation should rather be inert, long-term implants intended for permanent presence in the recipient's body should ideally possess bioactive properties to facilitate proper tissue integration. A multitude of different approaches has been examined with the aim to influence the interactions between biomaterials and the host tissue, for example by regulation of protein and cell attachment to improve the implant ingrowth and to reduce implant-related inflammation. Possible methods include for example the coating with different proteins, with biomembrane-derived phospholipids, with diamond-like carbon or ceramics or the attachment of chemical groups to create surfaces with a specific electric charge. Low-temperature plasmas have extensively been examined in vitro and in vivo for these applications.

#### 3.1 Creation of bioactive surfaces

The cell-material and tissue-material interactions can be influenced by modifying the surface charge via chemical groups. For example, an enhanced osteoblast growth in vitro was observed for surfaces modified with plasma-polymerized 1-aminoheptane (Zhao et al., 2011). The plasma-based deposition of acetaldehyde and allylamine polymer coatings on silicon and perfluorinated poly(ethylene-co-propylene) was found to influence the outgrowth of bovine corneal epithelial tissue for up to 21 days (Thissen et al., 2006). A treatment of Titanium samples with a comparable process called plasma-polymerized allylamine, based on the polymerization of allylamine after activation with a continuous wave oxygen-plasma, creates a positively charged amino group rich surface aimed at improving attachment of the negatively charged matrix substance hyaluronan. This coating was found to be advantageous concerning initial osteoblast adhesion and spreading (Nebe et al., 2007) and to have beneficial effects in vitro on the formation of focal adhesions as well as on cell morphology and spreading (Finke et al., 2007) and vinculin mobility (Rebl et al., 2010) of osteoblasts. An in vivo examination in rats revealed no negative influence on the number of total and tissue macrophages, T cells and MHC class II antigen-presenting cells in the peri-implant tissue (Hoene et al., 2010). Furthermore, it was demonstrated that the

plasma parameters influence the surface properties and thereby the host response. Samples with a lower plasma duty cycle (ratio of plasma on-time  $t_{on}$  divided by the overall pulse duration  $t_{on} + t_{off}$ ) resulted in a higher layer thickness and protein absorption as well as a lower oxygen uptake due to sonication in distilled water. Consequently, the hydrogel-like character of the plasma-polymerized allylamine films was probably more developed for the high duty cycle samples, resulting in an overall lower inflammatory response *in vivo* than for the implants created with a low duty cycle (Hoene et al., 2010). Similar results regarding enhanced cell adhesion were also obtained for a plasma consisting of a mixture of argon and ethylenediamine (Finke et al., 2011). A treatment of a hip prosthesis with this plasma process is exemplarily shown in Fig. 2.

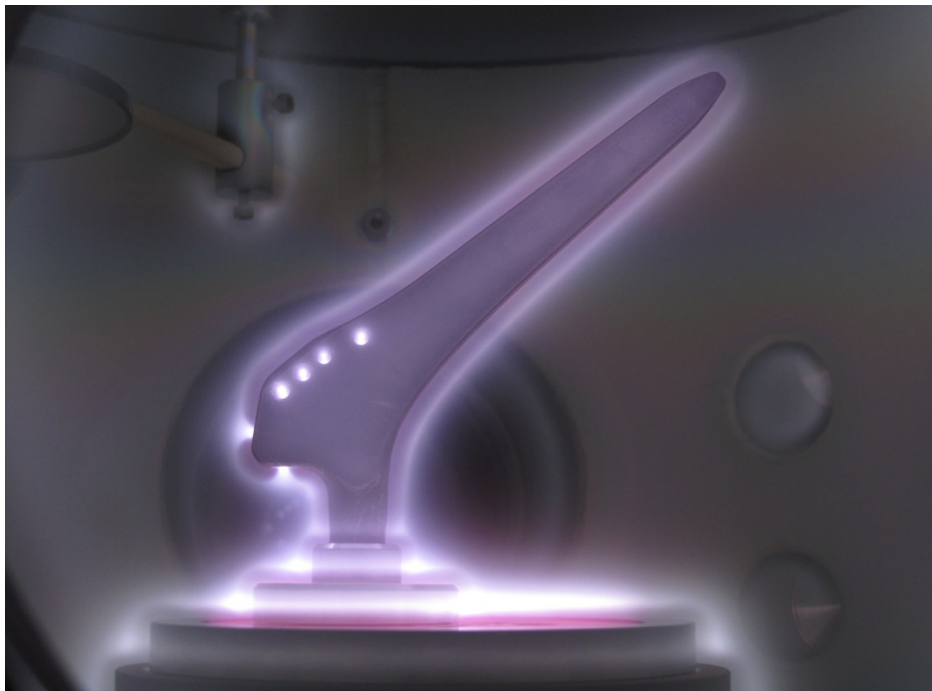


Fig. 2. Hip joint implant in low pressure plasma using a mixture of argon and ethylenediamine for cell adhesive coating

In contrast to these positively charged  $\text{NH}_2$  films, a coating of Titanium implants with acrylic acid after similar plasma activation, called plasma-polymerized acrylic acid, results in a negatively charged COOH-group rich surface which was found to facilitate osteogenic differentiation by stimulation of mRNA expression of early (ALP, COL, Runx2) as well as late (BSP, OCN) bone differentiation markers (Schröder et al., 2010b). However, the long-term inflammatory response *in vivo* caused by this coating were increased compared to uncoated controls (Schröder et al., 2010b), highlighting the difficult balance that improving one specific aspect of implant characteristics is often accompanied by adverse changes in other parameters. Furthermore, it illustrates the problem that the results of *in vitro* experiments on the one hand and *in vivo* studies on the other are often inconsistent due to

the complex nature of reactions in a living organism which can only partially and often inadequately be modelled using *in vitro* approaches.

Similar to metals and metal alloys, cell attachment on polymers can also be modulated by plasma treatment. The application of glow-discharge plasma of mixed ammonia and oxygen on polytetrafluoroethylene surfaces reduced the hydrophobicity and increased the attachment of aorta endothelial cells (Chen et al., 2003). Furthermore, an oxygen plasma has been shown to improve surface attachment of mouse fibroblasts L-929 on thermoplastic polyetherurethane used for gastric implants (Schlicht et al., 2010).

Low-temperature plasma can also be used to achieve immobilization of bioactive molecules. This was demonstrated for example by an oxygen plasma treatment to enhance the immobilization of simvastatin, which stimulates bone formation, onto Ti surfaces (Yoshinari et al., 2006). The deposition of thin film from ethylene plasma on Ti surfaces allows the chemical attachment of hydroxyethylmethacrylate onto Ti to improve the *in vitro* adhesion of mouse fibroblasts L-929 (Morra & Cassinelli, 1997). Albumin nanoparticles conjugated with a truncated fragment of fibronectin were directly patterned onto polymers to elicit adhesion and spreading of human mesenchymal stem cells and fibroblasts (Rossi et al., 2010). Stable coating of collagen type I onto two different metal alloys (Ti6Al4V, X2CrNiMo18) was achieved using a argon-hydrogen plasma and found to increase the viability and attachment of human osteoblast-like osteosarcoma cells SAOS-2 (Hauser et al., 2010), and coating of collagen onto silicone performed with an argon-oxygen plasma led to increased adhesion and viability of mouse fibroblasts 3T3 (Hauser et al., 2009). Poly(lactide-co-glycolide), a biodegradable polymer widely used as scaffold material for tissue engineering, was modified by oxygen plasma treatment followed by anchorage of cationized gelatine for improved attachment and growth of mouse fibroblasts 3T3 (Shen et al, 2007).

A popular material for bioactive coatings on implants for bone replacement is calcium phosphate which is the main natural component in the bone matrix where it accounts for more than half of the bone weight. It exists in a variety of different chemical preparations differing in their atomic and ionic lattice configuration, their Ca:P ratio, the number and size of pores, and their surface area. One calcium phosphate preparation commonly used for biomaterials is hydroxyapatite ( $\text{Ca}_{10}(\text{PO}_4)_6(\text{OH})_2$ ) which is generally considered to be osteoconductive and osteoinductive (Walschus et al., 2009). Using a process called plasma spraying, it is possible to deposit thin and dense layers of hydroxyapatite onto metal implant surfaces (de Groot et al., 1987). Due to the well-established bioactive properties and good biocompatibility of hydroxyapatite, these coatings have been clinically used in dentistry and orthopedics since the mid 1980s (Tang et al., 2010). Furthermore, plasma spraying can also be used to create other layers like Ca-Si-Ti-based sphene ceramics (Wu et al., 2009), hydroxyapatite/ silica ceramics (Morks 2008), zirconia (Morks & Kobayashi 2008; Wang et al., 2010), yttria-stabilized zirconia (Wang et al., 2009) or hydroxyapatite/ yttria/ zirconia composites (Chang et al., 1997; Gu et al., 2004). One important advantage of plasma-sprayed coatings for biomaterials is the ability to precisely modify the microstructure by modulating the parameters of the plasma process (Khor et al., 2004; Huang et al., 2010) to study and improve microstructure-related tissue growth stimulation.

### **3.2 Plasma-assisted vapour deposition of inert diamond-like carbon layers**

Another field of increasing interest which should be mentioned briefly in this chapter is the plasma-based coating of implants with diamond-like carbon for which plasma-assisted chemical vapour deposition is the most commonly used deposition method. Diamond-like

carbon layers can exhibit the typical diamond crystalline structure, an amorphous structure or a mixture of both (Schlosser & Ziegler, 1997). Furthermore, depending on the coating procedure, they can consist of pure carbon or contain other elements. Overall, diamond-like carbon films are characterized by an excellent mechanical stability and hardness, a high corrosion resistance as well as reduced tissue-material interactions and no detectable cytotoxicity (Schlosser & Ziegler, 1997). Particularly for implants where inertness of the surface is required, they are therefore an attractive option for coating of medical implants in a number of applications in reconstructive surgery and dentistry (Roy & Lee, 2007). Diamond-like carbon coatings have for example been examined for ureteral stents (Laube et al., 2007), orthodontic archwires (Kobayashi et al., 2007), joint implants (Thorwarth et al., 2010) or cardiovascular stents (De Scheerder et al., 2000).

#### 4. Plasma sterilization

Sterilization as the elimination of living microorganisms like bacteria, viruses and fungi, especially pathogenic agents, is an important aspect in biomaterials applications to prevent implant-related infections. Commonly used methods to achieve sterility include the treatment with heat, chemicals and irradiation. Each of those methods has its specific disadvantages and not all are equally usable for the sterilization of medical implants. For example, a heat treatment can lead to irreversible modifications of heat-labile materials and to denaturation of protein coatings. Irradiation with UV or gamma rays requires cost-intensive equipment with high safety requirements and can also cause irreversible modifications of proteins such as albumin and collagen used as sealing impregnation of vascular prostheses, as well as biomaterials like polymers. Chemical sterilization using for example ethylene oxide could result in residuals on the treated surface. Therefore, the application of low-temperature plasma processes as an alternative sterilization technique which is a gentle process from a physico-chemical point of view has been the focus of ongoing research since several years. It is known that exposure to plasma effectively and irreversibly damages cells from different bacteria species like for example *Escherichia coli*, *Staphylococcus aureus*, *Pseudomonas aeruginosa*, *Bacillus cereus* or *Bacillus subtilis* (Bazaka et al., 2011). Especially for modified or functionalized biomaterials, sterilization with low-temperature plasma would therefore be an attractive option as it could be achieved as a secondary effect of plasma treatment aimed at other surface modification purposes (Bazaka et al., 2011).

The application of plasma sterilization of heat-sensitive silicone implants has recently been demonstrated (Hauser et al., 2011). Similarly, sterilization of poly-L-lactide electrospun microfibers which can be used to repair tissue defects can effectively be achieved by hydrogen peroxide gas plasma which ensures sterility of the scaffolds and does not affect their chemical and morphological features (Rainer et al., 2010). Biodegradable polyester three-dimensional tissue engineering scaffolds which are particularly prone to morphological degeneration by high temperature and pressure were successfully sterilized with an argon-based radio-frequency glow discharge plasma (Holy et al., 2001), demonstrating the usefulness of plasma sterilization for damageable materials. Similar results were also obtained for starch based biomaterials for which a recent study found that treatment with oxygen plasma resulted in more hydrophilic surfaces compared to UV-irradiation (Pashkuleva et al., 2010). Furthermore, both methods gave comparable results regarding osteoblast adherence, from which the authors concluded that plasma sterilization

as well as UV-irradiation improved the biocompatibility and can be used as cost-effective methods for sterilization.

For metal implants, it was found that rapid and efficient sterilization of different alloys like X2CrNiMo18-15-3, Ti6Al7Nb und Ti6Al4V is possible with plasmas based on different gas mixtures such as argon/oxygen, argon/hydrogen and argon/nitrogen (Hauser et al., 2008). Sterilization of non-woven polyethylene terephthalate fiber structures for vascular grafts with either ethylene oxide or low temperature plasma resulted in comparable fibroblastic viability but a significantly higher TNF- $\alpha$  release, indicating activation of macrophages, for macrophages incubated on the fibres which were treated with ethylene oxide (Dimitrievska et al., 2011). Subcutaneous implantation into mice demonstrated inflammation accompanied by a foreign body reaction with no difference after 30 days between the samples treated with the two sterilization methods. A comparison of the effects of sterilization with gamma irradiation, ethylene oxide treatment, electron beam irradiation and plasma sterilization on the in vitro behaviour of polylactide fibres revealed that sterilization with both gamma and electron beam irradiation caused a decrease of the intrinsic viscosity while treatment with ethylene oxide and plasma sterilization had no pronounced effects on the sample properties (Nuutinen et al., 2002). These results also highlight the potential of plasma sterilization as a gentle alternative to other commonly used sterilization methods. However, it is not equally suitable for all materials as it might have adverse effects on relevant material properties. For example, demineralized bone matrix which was sterilized with low-temperature gas-plasma sterilization lost its osteoinductive capacity (Ferreira et al., 2001).

Another application related to sterilization is the removal of surface contaminations. This is particularly important for residues like prion proteins which have contagious and pathogenic properties. The usefulness of plasma treatment for molecular-level removal of proteinaceous contamination was recently demonstrated for silicon and surgical stainless steel surfaces (Banerjee et al., 2010).

## 5. Conclusions and outlook

Low temperature plasmas offer a wide range of applications in biomaterials research to improve the clinical performance of medical implants by modifying their surface characteristics. In many cases, the use of plasmas facilitates modifications which are difficult or unable to achieve by conventional physical or chemical methods, like for example the stable attachment of molecules onto noble metal surfaces. The concise overview presented in this chapter demonstrates the potential of low temperature plasma processes for the precise modification of specific implant surface properties while retaining the overall characteristics of the material. The main aims of research in this field are to reduce implant-related complications like infections, thrombus formation and inflammation as well as to modulate the cell-material and tissue-material interactions for improved implant ingrowth. Another equally important area of research is the use of plasmas for sterilization. The studies which were presented here indicate that plasma processes are applicable for practically all commonly used biomaterials including metals, polymers, ceramics and composites, offering a wide range of clinical applications in all fields of reconstructive medicine.

Given the versatility of low temperature plasma processes and the diverse nature of materials and clinical applications, it is difficult to predict future developments in this field. If there is any specific trend, then it is an increase in the number of studies which deal with biodegradable materials, reflecting an overall surge of interest in biomaterials research for this kind of materials. Another development is the use of increasingly sophisticated methods for surface analysis, making it possible to draw precise conclusions regarding relationships

between process parameters, surface characteristics and the biological response. Two important aspects in need of more research are on the one hand the aging-related surface changes of plasma-modified biomaterials and on the other hand their *in vivo* behaviour. Most of the studies discussed here used only *in vitro* methods to assess the biocompatibility. However, for the step from the lab into clinical practice it is essential to examine the *in vivo* biocompatibility by using appropriate animal models. There are several aspects of biocompatibility, both short- and long-term, which can not be adequately examined with *in vitro* methods like cell culture techniques. More detailed *in vivo* testing together with a better understanding of the influence of the plasma parameters on the physico-chemical material properties and on the response of cells, tissues and living organisms will ultimately turn currently promising research projects into clinical applications for improved implants. The increasing interest in the application of low-temperature plasmas in biomaterials science is illustrated by the formation of long-term and large-scale research projects, scientific centers and institutional networks in recent years, for example the Plasma Physics and Radiation Technology Cluster at the Eindhoven University of Technology in the Netherlands, the Center for Advanced Plasma Surface Technology (CAPST) in Korea, and the Campus PlasmaMed at the Leibniz Institute of Plasma Science and Technology Greifswald, the University of Greifswald and the University of Rostock in Germany.

## 6. References

- Banerjee K.K., Kumar S., Bremmell K.E. & Griesser H.J. (2010). Molecular-level removal of proteinaceous contamination from model surfaces and biomedical device materials by air plasma treatment. *Journal of Hospital Infection*, Vol. 76, No. 3, pp. 234-242.
- Bazaka K., Jacob M.V., Crawford R.J. & Ivanova E.P. (2011). Plasma-assisted surface modification of organic biopolymers to prevent bacterial attachment. *Acta Biomaterialia*, Vol. 7, No. 5, pp. 2015-2028.
- Butt M., Connolly D. & Lip G.Y. (2009). Drug-eluting stents: a comprehensive appraisal. *Future Cardiology*, Vol. 5, No. 2, pp. 141-157.
- Chang E., Chang W.J., Wang B.C. & Yang C.Y. (1997). Plasma spraying of zirconia-reinforced hydroxyapatite composite coatings on titanium. Part I: phase, microstructure and bonding strength. *Journal of Materials Science: Materials in Medicine*, Vol. 8, No. 4, pp. 193-200.
- Chen M., Zamora P.O., Som P., Peña L.A. & Osaki S. (2003). Cell attachment and biocompatibility of polytetrafluoroethylene (PTFE) treated with glow-discharge plasma of mixed ammonia and oxygen. *Journal of Biomaterials Science: Polymer Edition*, Vol. 14, No. 9, pp. 917-935.
- Conrads H. & Schmidt M. (2000). Plasma generation and plasma sources. *Plasma Sources Science and Technology*, Vol. 9, No. 4, pp. 441-454.
- de Groot K., Geesink R., Klein C.P. & Serekan P. (1987). Plasma sprayed coatings of hydroxylapatite. *Journal of Biomedical Materials Research*, Vol. 21, No. 12, pp. 1375-1381.
- De Scheerder I., Szilard M., Yanming H., Ping X.B., Verbeken E., Neerinck D., Demeyere E., Coppens W. & Van de Werf F. (2000). Evaluation of the biocompatibility of two new diamond-like stent coatings (Dylyn) in a porcine coronary stent model. *Journal of Invasive Cardiology*, Vol. 12, No. 8, pp. 389-394.

- Dimitrievska S., Petit A., Doillon C.J., Epure L., Ajji A., Yahia L. & Bureau M.N. (2011). Effect of sterilization on non-woven polyethylene terephthalate fiber structures for vascular grafts. *Macromolecular Bioscience*, Vol. 11, No. 1, pp. 13-21.
- Douglas J.S. Jr. (2007). Pharmacologic approaches to restenosis prevention. *American Journal of Cardiology*, Vol. 100, No. 5 Suppl. 1, pp. S10-S16.
- Ferreira S.D., Dernell W.S., Powers B.E., Schochet R.A., Kuntz C.A., Withrow S.J. & Wilkins R.M. (2001). Effect of gas-plasma sterilization on the osteoinductive capacity of demineralized bone matrix. *Clinical Orthopaedics and Related Research*, Vol. 388, pp. 233-239.
- Finke B., Lüthen F., Schröder K., Mueller P.D., Bergemann C., Frant M., Ohl A. & Nebe B.J. (2007). The effect of positively charged plasma polymerization on initial osteoblastic focal adhesion on titanium surfaces. *Biomaterials*, Vol. 28, No. 30, pp. 4521-4534.
- Finke B., Hempel F., Testrich H., Artemenko A., Rebl H., Kylian O., Meichsner J., Biederman H., Nebe B., Weltmann K.-D., Schröder K. (2011). Plasma processes for cell-adhesive titanium surfaces based on nitrogen-containing coatings. *Surface & Coatings Technology*, Vol. 205, Suppl. 2, pp. S520-S524.
- Gu Y.W., Khor K.A., Pan D. & Cheang P. (2004). Activity of plasma sprayed yttria stabilized zirconia reinforced hydroxyapatite/Ti-6Al-4V composite coatings in simulated body fluid. *Biomaterials*, Vol. 25, No. 16, pp. 3177-3185.
- Hauser J., Halfmann H., Awakowicz P., Köller M. & Esenwein S.A. (2008). A double inductively coupled low-pressure plasma for sterilization of medical implant materials. *Biomedical Engineering*, Vol. 53, No. 4, pp. 199-203.
- Hauser J., Zietlow J., Köller M., Esenwein S.A., Halfmann H., Awakowicz P. & Steinau H.U. (2009). Enhanced cell adhesion to silicone implant material through plasma surface modification. *Journal of Materials Science: Materials in Medicine*, Vol. 20, No. 12, pp. 2541-2548.
- Hauser J., Köller M., Bensch S., Halfmann H., Awakowicz P., Steinau H.U. & Esenwein S. (2010). Plasma mediated collagen-I-coating of metal implant materials to improve biocompatibility. *Journal of Biomedical Materials Research Part A*, Vol. 94, No. 1, pp. 19-26.
- Hauser J., Esenwein S.A., Awakowicz P., Steinau H.U., Köller M. & Halfmann H. (2011). Sterilization of heat-sensitive silicone implant material by low-pressure gas plasma. *Biomedical Instrumentation & Technology*, Vol. 45, No. 1, pp. 75-79.
- Hendricks S.K., Kwok C., Shen M., Horbett T.A., Ratner B.D. & Bryers J.D. (2000). Plasma-deposited membranes for controlled release of antibiotic to prevent bacterial adhesion and biofilm formation. *Journal of Biomedical Materials Research*, Vol. 50, No. 2, pp. 160-170.
- Hippner R., Kersten H., Schmidt M. & Schoenbach K.H. (2008). Low temperature plasma physics: Fundamental aspects and applications. Wiley-VCH, Weinheim, Germany.
- Hoene A., Walschus U., Patrzyk M., Finke B., Lucke S., Nebe B., Schröder K., Ohl A. & Schlosser M. (2010). In vivo investigation of the inflammatory response against allylamine plasma polymer coated titanium implants in a rat model. *Acta Biomaterialia*, Vol. 6, No. 2, pp. 676-683.
- Holy C.E., Cheng C., Davies J.E. & Shoichet M.S. (2001). Optimizing the sterilization of PLGA scaffolds for use in tissue engineering. *Biomaterials*, Vol. 22, No. 1, pp. 25-31.

- Huang Y., Song L., Liu X., Xiao Y., Wu Y., Chen J., Wu F. & Gu Z. (2010). Hydroxyapatite coatings deposited by liquid precursor plasma spraying: controlled dense and porous microstructures and osteoblastic cell responses. *Biofabrication*, Vol. 2, No. 2, paper 045003.
- Junge K., Rosch R., Klinge U., Krones C., Klosterhalfen B., Mertens P.R., Lynen P., Kunz D., Preiss A., Peltroche-Llacsahuanga H. & Schumpelick V. (2005). Gentamicin supplementation of polyvinylidenefluoride mesh materials for infection prophylaxis. *Biomaterials*, Vol. 26, No. 7, pp. 787-793.
- Khor K.A., Gu Y.W., Pan D. & Cheang P. (2004). Microstructure and mechanical properties of plasma sprayed HA/YSZ/Ti-6Al-4V composite coatings. *Biomaterials*, Vol. 25, No. 18, pp. 4009-4017.
- Kim D.D., Takeno M.M., Ratner B.D. & Horbett T.A. (1998). Glow discharge plasma deposition (GDPD) technique for the local controlled delivery of hirudin from biomaterials. *Pharmaceutical Research*, Vol. 15, No. 5, pp. 783-786.
- Kobayashi S., Ohgoe Y., Ozeki K., Hirakuri K. & Aoki H. (2007). Dissolution effect and cytotoxicity of diamond-like carbon coatings on orthodontic archwires. *Journal of Materials Science: Materials in Medicine*, Vol. 18, No. 12, pp. 2263-2268.
- Laube N., Kleinen L., Bradenahl J. & Meissner A. (2007). Diamond-like carbon coatings on ureteral stents--a new strategy for decreasing the formation of crystalline bacterial biofilms? *Journal of Urology*, Vol. 177, No. 5, pp. 1923-1927.
- Li B., Liu X., Cao C., Dong Y., Wang Z. & Ding C. (2008). Biological and antibacterial properties of plasma sprayed wollastonite coatings grafting gentamicin loaded collagen. *Journal of Biomedical Materials Research Part A*, Vol. 87, No. 1, pp. 84-90.
- Li B., Liu X., Cao C., Dong Y. & Ding C. (2009). Biological and antibacterial properties of plasma sprayed wollastonite/silver coatings. *Journal of Biomedical Materials Research Part B: Applied Biomaterials*, Vol. 91, No. 2, pp. 596-603.
- Lin W.C., Tseng C.H. & Yang M.C. (2005). In-vitro hemocompatibility evaluation of a thermoplastic polyurethane membrane with surface-immobilized water-soluble chitosan and heparin. *Macromolecular Bioscience*, Vol. 5, No. 10, pp. 1013-1021.
- Lischer S., Körner E., Balazs D.J., Shen D., Wick P., Grieder K., Haas D., Heuberger M. & Hegemann D. (2011). Antibacterial burst-release from minimal Ag-containing plasma polymer coatings. *Journal of the Royal Society Interface*, Vol. 8, No. 60, pp. 1019-1030.
- Liu X., Morra M., Carpi A. & Li B. (2008). Bioactive calcium silicate ceramics and coatings. *Biomedicine & Pharmacotherapy*, Vol. 62, No. 8, pp. 526-529.
- Meichsner J., Schmidt M., Wagner H.E. (2011). Non-thermal Plasma Chemistry and Physics. Taylor & Francis, London, UK.
- Morks M.F. (2008). Fabrication and characterization of plasma-sprayed HA/SiO<sub>2</sub> coatings for biomedical application. *Journal of the Mechanical Behavior of Biomedical Materials*, Vol. 1, No. 1, pp. 105-111.
- Morks M.F. & Kobayashi A. (2008). Development of ZrO<sub>2</sub>/SiO<sub>2</sub> bioinert ceramic coatings for biomedical application. *Journal of the Mechanical Behavior of Biomedical Materials*, Vol. 1, No. 2, pp. 165-171.
- Morra M. & Cassinelli C. (1997). Organic surface chemistry on titanium surfaces via thin film deposition. *Journal of Biomedical Materials Research*, Vol. 37, No. 2, pp. 198-206.

- Mourtas S., Kastellorizios M., Klepetsanis P., Farsari E., Amanatides E., Mataras D., Pistillo B.R., Favia P., Sardella E., d'Agostino R. & Antimisiaris S.G. (2011). Covalent immobilization of liposomes on plasma functionalized metallic surfaces. *Colloids and Surfaces B: Biointerfaces*, Vol. 84, No. 1, pp. 214-220.
- Nebe B., Finke B., Lüthen F., Bergemann C., Schröder K., Rychly J., Liefelth K. & Ohl A. (2007). Improved initial osteoblast functions on amino-functionalized titanium surfaces. *Biomolecular Engineering*, Vol. 24, No. 5, pp. 447-54.
- Nurhaerani, Arita K., Shinonaga Y. & Nishino M. (2006). Plasma-based fluorine ion implantation into dental materials for inhibition of bacterial adhesion. *Dental Materials Journal*, Vol. 25, No. 4, pp. 684-692.
- Nuutinen J.P., Clerc C., Virta T. & Törmälä P. (2002). Effect of gamma, ethylene oxide, electron beam, and plasma sterilization on the behaviour of SR-PLLA fibres in vitro. *Journal of Biomaterials Science: Polymer Edition*, Vol. 13, No. 12, pp. 1325-1336.
- Ohl A., Schröder K. (2008). Plasma assisted surface modification of biointerfaces. In: Hippler R., Kersten H., Schmidt M. & Schoenbach K.H. Low temperature plasma physics: Fundamental aspects and applications. Wiley-VCH, Weinheim, Germany, pp. 803-819.
- Osaki S.G., Chen M. & Zamora P.O. (2011). Controlled Drug Release through a Plasma Polymerized Tetramethylcyclo-tetrasiloxane Coating Barrier. *Journal of Biomaterials Science: Polymer Edition*, published online before print January 28, 2011, doi: 10.1163/092050610X552753.
- Pashkuleva I., Marques A.P., Vaz F. & Reis R.L. (2010). Surface modification of starch based biomaterials by oxygen plasma or UV-irradiation. *Journal of Materials Science: Materials in Medicine*, Vol. 21, No. 1, pp. 21-32.
- Polak M., Ohl A., Quaas M., Lukowski G., Lüthen F., Weltmann K.-D. & Schröder K. (2010). Oxygen and Water Plasma-Immersion Ion Implantation of Copper into Titanium for Antibacterial Surfaces of Medical Implants. *Advanced Engineering Materials*, Vol. 12, No. 9, pp. B511-B518.
- Radke P.W., Weber C., Kaiser A., Schober A. & Hoffmann R. (2004). Dexamethasone and restenosis after coronary stent implantation: new indication for an old drug? *Current Pharmaceutical Design*, Vol. 10, No. 4, pp. 349-355.
- Rainer A., Centola M., Spadaccio C., Gherardi G., Genovese J.A., Licoccia S. & Trombetta M. (2010). Comparative study of different techniques for the sterilization of poly-L-lactide electrospun microfibers: effectiveness vs. material degradation. *International Journal of Artificial Organs*, Vol. 33, No. 2, pp. 76-85.
- Raizer Y.P. (1997). Gas Discharge Physics. Springer, Berlin, Germany.
- Rebl H., Finke B., Ihrke R., Rothe H., Rychly J., Schröder K. & Nebe B.J. (2010). Positively Charged Material Surfaces Generated by Plasma Polymerized Allylamine Enhance Vinculin Mobility in Vital Human Osteoblasts. *Advanced Engineering Materials*, Vol. 12, No. 8, pp. B356-B364.
- Rossi M.P., Xu J., Schwarzbauer J. & Moghe P.V. (2010). Plasma-micropatterning of albumin nanoparticles: Substrates for enhanced cell-interactive display of ligands. *Biointerphases*, Vol. 5, No. 4, pp. 105-113.
- Roth J.R. (1995). Industrial Plasma Engineering. Volume 1: Principles. Institute of Physics Publishing, Bristol, UK.
- Roth J.R. (2001). Industrial Plasma Engineering. Volume 2: Applications to Nonthermal Plasma Processing. Institute of Physics Publishing, Bristol, UK.

- Roy R.K. & Lee K.R. (2007). Biomedical applications of diamond-like carbon coatings: a review. *Journal of Biomedical Materials Research Part B: Applied Biomaterials*, Vol. 83, No. 1, pp. 72-84.
- Schlicht H., Haugen H.J., Sabetrakeh R. & Wintermantel E. (2010). Fibroblastic response and surface characterization of O<sub>2</sub>(2)-plasma-treated thermoplastic polyetherurethane. *Biomedical Materials*, Vol. 5, No. 2, paper 25002
- Schlosser M. & Ziegler M. (1997). Biocompatibility of Active Implantable Devices. In: Fraser, D.M. (Ed.). *Biosensors in the Body. Continuous In Vivo Monitoring*. John Wiley & Sons, Chichester, UK, pp. 140-170.
- Schröder K., Finke B., Polak M., Lüthen F., Nebe J.B., Rychly J., Bader R., Lukowski G., Walschus U., Schlosser M., Ohl A. & Weltmann K.-D. (2010a). Gas-Discharge Plasma-Assisted Functionalization of Titanium Implant Surfaces. *Materials Science Forum*, Vols. 638-642, pp. 700-705.
- Schröder K., Finke B., Ohl A., Lüthen F., Bergemann C., Nebe B., Rychly J., Walschus U., Schlosser M., Liefeth K., Neumann H.-G. & Weltmann K.-D. (2010b). Capability of Differently Charged Plasma Polymer Coatings for Control of Tissue Interactions with Titanium Surfaces. *Journal of Adhesion Science and Technology*, Vol. 24, No. 7, pp. 1191-1205.
- Schröder K., Foest R., Ohl A. (2011). Biomedical applications of plasmachemical surface functionalization. In: Meichsner J., Schmidt M., Wagner H.E. *Non-thermal Plasma Chemistry and Physics*. Taylor & Francis, London, UK, in press
- Shen H., Hu X., Yang F., Bei J. & Wang S. (2007). Combining oxygen plasma treatment with anchorage of cationized gelatin for enhancing cell affinity of poly(lactide-co-glycolide). *Biomaterials*, Vol. 28, No. 29, pp. 4219-4230.
- Shinonaga Y. & Arita K. (2009). Surface modification of stainless steel by plasma-based fluorine and silver dual ion implantation and deposition. *Dental Materials Journal*, Vol. 28, No. 6, pp. 735-742.
- Sperling C., König U., Hermel G., Werner C., Müller M., Simon F., Grundke K., Jacobasch H.J., Vasilets V.N. & Ikada Y. (1997). Immobilization of human thrombomodulin onto PTFE. *Journal of Materials Science: Materials in Medicine*, Vol. 8, No. 12, pp. 789-791.
- Tang Q., Brooks R., Rushton N. & Best S. (2010). Production and characterization of HA and SiHA coatings. *Journal of Materials Science: Materials in Medicine*, Vol. 21, No. 1, pp. 173-181.
- Thissen H., Johnson G., Hartley P.G., Kingshott P. & Griesser H.J. (2006). Two-dimensional patterning of thin coatings for the control of tissue outgrowth. *Biomaterials*, Vol. 27, No. 1, pp. 35-43.
- Thorwarth G., Falub C.V., Müller U., Weisse B., Voisard C., Tobler M. & Hauert R. (2010). Tribological behavior of DLC-coated articulating joint implants. *Acta Biomaterialia*, Vol. 6, No. 6, pp. 2335-2341.
- van Delden C.J., Lens J.P., Kooyman R.P., Engbers G.H. & Feijen J. (1997). Heparinization of gas plasma-modified polystyrene surfaces and the interactions of these surfaces with proteins studied with surface plasmon resonance. *Biomaterials*, Vol. 18, No. 12, pp. 845-852.
- Vasilets V.N., Hermel G., König U., Werner C., Müller M., Simon F., Grundke K., Ikada Y. & Jacobasch H.J. (1997). Microwave CO<sub>2</sub> plasma-initiated vapour phase graft

- polymerization of acrylic acid onto polytetrafluoroethylene for immobilization of human thrombomodulin. *Biomaterials*, Vol. 18, No. 17, pp. 1139-1145.
- Vasilev K., Simovic S., Losic D., Griesser H.J., Griesser S., Anselme K. & Ploux L. (2010a). Platforms for controlled release of antibacterial agents facilitated by plasma polymerization. *Conference Proceedings of the IEEE Engineering in Medicine and Biology Society*, pp. 811-814.
- Vasilev K., Sah V.R., Goreham R.V., Ndi C., Short R.D. & Griesser H.J. (2010). Antibacterial surfaces by adsorptive binding of polyvinyl-sulphonate-stabilized silver nanoparticles. *Nanotechnology*, Vol. 21, No. 21, paper 215102.
- Walschus U., Hoene A., Neumann H.-G., Wilhelm L., Lucke S., Lüthen F., Rychly J. & Schlosser M. (2009). Morphometric immunohistochemical examination of the inflammatory tissue reaction after implantation of calcium phosphate-coated titanium plates in rats. *Acta Biomaterialia*, Vol. 5, No. 2, pp. 776-784.
- Wang G., Liu X., Gao J. & Ding C. (2009). In vitro bioactivity and phase stability of plasma-sprayed nanostructured 3Y-TZP coatings. *Acta Biomaterialia*, Vol. 5, No. 6, pp. 2270-2278.
- Wang G., Meng F., Ding C., Chu P.K. & Liu X. (2010). Microstructure, bioactivity and osteoblast behavior of monoclinic zirconia coating with nanostructured surface. *Acta Biomaterialia*, Vol. 6, No. 3, pp. 990-1000.
- Wu C., Ramaswamy Y., Liu X., Wang G. & Zreiqat H. (2009). Plasma-sprayed CaTiSiO<sub>5</sub> ceramic coating on Ti-6Al-4V with excellent bonding strength, stability and cellular bioactivity. *Journal of the Royal Society Interface*, Vol. 6, No. 31, pp. 159-168.
- Yang Z., Wang J., Luo R., Maitz M.F., Jing F., Sun H. & Huang N. (2010). The covalent immobilization of heparin to pulsed-plasma polymeric allylamine films on 316L stainless steel and the resulting effects on hemocompatibility. *Biomaterials*, Vol. 31, No. 8, pp. 2072-2083.
- Ye S.H., Johnson C.A. Jr., Woolley J.R., Oh H.I., Gamble L.J., Ishihara K. & Wagner W.R. (2009). Surface modification of a titanium alloy with a phospholipid polymer prepared by a plasma-induced grafting technique to improve surface thromboresistance. *Colloids and Surfaces B: Biointerfaces*, Vol. 74, No. 1, pp. 96-102.
- Yoshinari M., Hayakawa T., Matsuzaka K., Inoue T., Oda Y., Shimono M., Ide T. & Tanaka T. (2006). Oxygen plasma surface modification enhances immobilization of simvastatin acid. *Biomedical Research*, Vol. 27, No. 1, pp. 29-36.
- Zhang W., Chu P.K., Ji J., Zhang Y., Liu X., Fu R.K., Ha P.C. & Yan Q. (2006). Plasma surface modification of poly vinyl chloride for improvement of antibacterial properties. *Biomaterials*, Vol. 27, No. 1, pp. 44-51.
- Zhang W., Zhang Y., Ji J., Yan Q., Huang A. & Chu PK. (2007). Antimicrobial polyethylene with controlled copper release. *Journal of Biomedical Materials Research Part A*, Vol. 83, No. 3, pp. 838-844.
- Zhang W., Luo Y., Wang H., Jiang J., Pu S. & Chu PK. (2008). Ag and Ag/N<sub>2</sub> plasma modification of polyethylene for the enhancement of antibacterial properties and cell growth/proliferation. *Acta Biomaterialia*, Vol. 4, No. 6, pp. 2028-2036.
- Zhao J.H., Michalski W.P., Williams C., Li L., Xu H.S., Lamb P.R., Jones S., Zhou Y.M. & Dai X.J. (2011). Controlling cell growth on titanium by surface functionalization of heptylamine using a novel combined plasma polymerization mode. *Journal of Biomedical Materials Research Part A*, Vol. 87, No. 2, pp. 127-134.